POLITECNICO DI TORINO

Collegio di Ingegneria Chimica e dei Materiali

Corso di Laurea Magistrale
in Ingegneria Chimica e dei Processi Sostenibili

Tesi di Laurea Magistrale

Vacuum Induced Surface Freezing (VISF) and surface treatment of containers

Relatore

prof. Roberto Pisano

Candidato

Francesco Regis

Ottobre 2020

Table of contents

Riassunto esteso in italiano

1. Introduzione

La liofilizzazione è un processo utilizzato nell'industria farmaceutica, ma non solo, per rimuovere il solvente (acqua o altro) da un farmaco senza danneggiare la struttura molecolare della sostanza attiva, lavorando quindi a bassa temperatura e pressione. Allo stato solido si riesce a garantire una durata di conservazione sufficientemente lunga delle proteine poiché le reazioni di degradazione vengono inibite o sufficientemente rallentate. Il processo di liofilizzazione si compone di tre fasi: congelamento, essiccazione primaria ed essiccazione secondaria.

Partendo da acqua a temperatura ambiente la si può raffreddare fino a temperature inferiori a quella di equilibrio termodinamico (0°C) senza che essa congeli. Questo fenomeno è chiamato sottoraffreddamento. La differenza tra la temperatura di equilibrio termodinamico e la temperatura di nucleazione è il grado di sottoraffreddamento; esso dipende dal grado di purezza dell'acqua e dalle condizioni di congelamento. Il profilo di temperatura di una soluzione farmaceutica durante il congelamento è mostrato nella Figura 1.1.

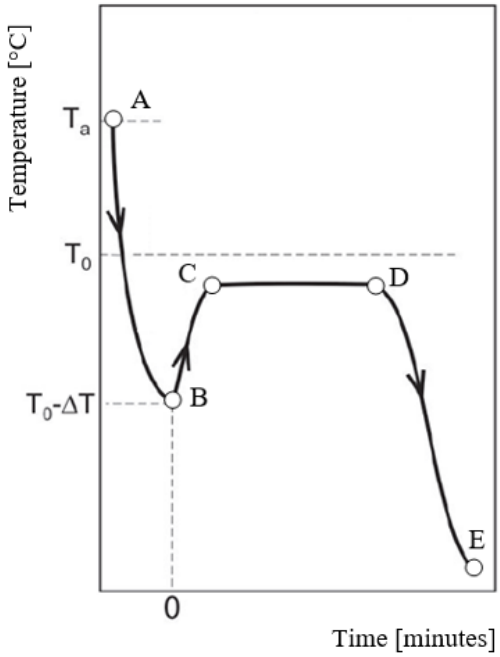

Figura 1.1: Profilo di temperatura di una soluzione farmaceutica durante il congelamento. Il processo di raffreddamento inizia dalla temperatura ambiente T_a e prosegue fino alla temperatura di cristallizzazione T_0-ΔT quando per via del processo esotermico di solidificazione la temperatura si alza fino a quasi la temperatura di congelamento di equilibrio T0. A seguire si ha un ulteriore raffreddamento. Figura tratta da Fan *et al*., 2018 con modifiche.

Nella prima fase AB la soluzione viene raffreddata fino alla sua nucleazione in B. La nucleazione è un fenomeno stocastico che porta alla formazione di nuclei di cristalli stabili su scala nanometrica. Questo processo è legato al moto Browniano nell'acqua sottoraffreddata: a causa di fluttuazioni di densità, le molecole d'acqua possono formare ammassi caratterizzati da forti legami a idrogeno ed organizzarsi in una struttura simile a quella del ghiaccio (Matsumoto *et al*., 2002). Il fenomeno di nucleazione è esotermico e ciò comporta un aumento della temperatura nella fase BC. I cristalli di ghiaccio formati iniziano quindi a crescere (CD), a una temperatura quasi costante grazie alla rimozione del calore tramite il raffreddamento. La

crescita dei cristalli avviene grazie all'addizione di ulteriori molecole d'acqua della soluzione, sempre più concentrata, all'interfaccia dei nuclei formati. Quando la solidificazione è completa (D) la soluzione viene ulteriormente raffreddata (DE). A circa -40 °C il campione di acqua pura conterrà almeno un nucleo di acqua dal quale spontaneamente può iniziare la crescita dei cristalli di ghiaccio (Kasper e Friess, 2011). Tuttavia, affinché avvenga tale nucleazione, non devono esserci impurità nella soluzione, il che è molto difficile. La nucleazione può essere distinta in primaria e secondaria. La nucleazione primaria si verifica in sistemi in cui i cristalli di soluzione non sono già presenti; può essere omogenea o eterogenea se indotta da particelle estranee. La nucleazione secondaria è solo di tipo eterogeneo e si verifica quando cristalli come quelli che si formeranno sono già presenti nella soluzione.

Il numero di cristalli di ghiaccio, la loro dimensione e la velocità di crescita del ghiaccio dipendono dal processo di congelamento, più in particolare dalla temperatura di nucleazione e dalla velocità di raffreddamento. Una bassa velocità di raffreddamento e/o un'elevata temperatura di nucleazione favoriscono la formazione di pochi nuclei che creeranno quindi grandi cristalli di ghiaccio. Al contrario, un'elevata velocità di raffreddamento e/o una bassa temperatura di nucleazione favoriscono la formazione di molti nuclei e di conseguenza di piccoli cristalli di ghiaccio. Il numero di cristalli formati e la loro dimensione determineranno a loro volta la porosità della torta liofilizzata (Rambhatla *et al*., 2004). La fase di congelamento è quindi molto importante perché è responsabile sia della variabilità all'interno del lotto che all'interno del prodotto.

L'effetto di sottoraffreddamento ottenuto sul campione dipende dai metodi di congelamento adottati. Ad esempio, il congelamento può essere effettuato mediante azoto liquido, caricamento di flaconi su ripiani preraffreddati o il mediamente una rampa su ripiani a temperatura controllata (congelamento convenzionale). La prima fase di un ciclo di liofilizzazione convenzionale consiste nell'inserire nei contenitori un determinato volume di soluzione, tapparli parzialmente e posizionarli sui ripiani a temperatura controllata del liofilizzatore. Temperature e tempi del processo di raffreddamento sono tali da ottenere la completa solidificazione della soluzione. La temperatura finale deve essere inferiore a T_g' se gli eccipienti sono non cristallini o inferiore a T_{eu} se sono cristallini. Monitorando la velocità di raffreddamento si controlla la morfologia del ghiaccio che influenza la successiva fase di essiccazione. Un valore di compromesso consigliato per la velocità di raffreddamento è di circa 1 °C min^{-1} (Tang e Pikal, 2004).

Mentre la maggior parte dei protocolli di congelamento convenzionali consentono il controllo della velocità di raffreddamento, la natura dell'evento di nucleazione è stocastica: l'istante e la temperatura alla quale la nucleazione si verifica sono casuali (Oddone *et al*., 2014). Questo è considerato un demerito perché porta a una grande variabilità da flacone a flacone e da lotto a lotto ed è in contrasto con i severi requisiti dell'industria farmaceutica in termini di controllo del processo e qualità del prodotto (Pisano *et al*., 2019). Nello specifico, la temperatura di nucleazione definisce le dimensioni, il numero e la morfologia dei cristalli di ghiaccio e quindi il comportamento di essiccazione da cui dipende la stabilità del prodotto (Oddone *et al*., 2020). Non è attualmente possibile controllare la nucleazione; tuttavia, si cerca di renderle questo fenomeno il più uniforme possibile forzandolo da avvenire ad una data temperatura per tutti i campioni del lotto (Barresi e Pisano, 2018). Sono stati proposti diversi metodi per controllare la nucleazione, quali agenti nucleanti, electro-freezing, ultrasuoni, depressurizzazione, tecnica dell'Ice Fog e Vacuum-Induced Surface Freezing (VISF).

Il modo più semplice ed economico per controllare con precisione la temperatura di nucleazione è la VISF perché non sono necessari hardware e attrezzature aggiuntive (Barresi e Pisano, 2018). Inoltre, i problemi di sterilità sono legati solo alla sterilizzazione di grandi

valvole necessarie per la depressurizzazione (Arsiccio *et al*., 2018a). Secondo questa tecnica, i flaconi vengono caricati sugli scaffali a temperatura ambiente e pressione atmosferica. Quindi la soluzione contenuta nei flaconi viene raffreddata alla temperatura del fluido T_n che deve essere superiore alla temperatura di nucleazione spontanea. Quando la temperatura della soluzione si porta a uno stazionario si decrementa la pressione all'interno della camera fino ad un valore basso (~ 1 mbar) per un breve periodo, generalmente inferiore a 1 min, finché non viene indotta la nucleazione in tutti i flaconi. Questa riduzione della pressione provoca una parziale evaporazione dell'acqua e, quindi, una rapida riduzione della temperatura del prodotto, favorendo la nucleazione. Rispetto all'approccio originale di Kramer *et al*., Oddone *et al*. ha proposto l'isolamento della camera di essiccazione dal condensatore una volta raggiunto il valore di vuoto desiderato. Questa modifica mira a ridurre i fenomeni di blow-up, facendo aumentare la pressione all'interno della camera di congelamento grazie all'evaporazione del solvente. Il risultato è un miglioramento nell'eleganza del prodotto finale. Non appena la nucleazione è avvenuta in tutti i campioni del batch la pressione atmosferica viene ripristinata e il prodotto viene raffreddato ad una temperatura compresa tra -40 ° C e -50 ° C, seguendo una rampa, per completare la fase di congelamento.

Durante il congelamento la maggior parte dell'acqua viene convertita in ghiaccio ed è quindi disponibile per la sublimazione durante l'essiccazione primaria (Oddone *et al*., 2017). La fase di essiccazione primaria rappresenta la maggior parte del ciclo di liofilizzazione. La forza motrice della sublimazione è la differenza tra la pressione di vapore di equilibrio del ghiaccio alla temperatura del materiale congelato e la pressione parziale dell'acqua all'interno della camera. Quando il ghiaccio sublima, l'interfaccia di sublimazione si ritira dall'esterno verso l'interno, formando un guscio poroso di materiale essiccato. Il vapore acqueo prodotto dalla sublimazione viene trasportato per convezione e diffusione attraverso la torta, entra nella camera a vuoto e infine si raccoglie sulla piastra del condensatore. Dall'equazione 1.1 si può vedere che la velocità di rimozione del vapore acqueo dipende dalla resistenza del prodotto, che a sua volta riflette il modo in cui la soluzione iniziale è stata congelata. Come si può vedere in Figura 1.5 il tempo di essicazione primaria diminuisce con l'aumentare della dimensione media dei pori fino ad un valore limite del diametro dei pori, oltre il quale non varia più. Poiché la curva raggiunge l'asintoto, la morfologia del prodotto non influenza più il tempo di essiccazione, quindi l'essiccazione primaria non sarà più controllata dal trasferimento di massa ma dal trasferimento di calore. Il plateau indica infatti il punto in cui la tensione di vapore del ghiaccio eguaglia la pressione parziale dell'acqua all'interno della camera annullando la forza motrice della sublimazione (Franks e Auffret, 2007, Pisano *et al*., 2011). Per ottimizzare la fase di essiccazione primaria, evitando il collasso della struttura porosa secca, la temperatura di sublimazione deve essere prossima alla temperatura di collasso T_c (es. temperatura di transizione vetrosa per un prodotto amorfo), ma sempre inferiore (Johnson, 2011). Il collasso del prodotto influirebbe negativamente sulle caratteristiche estetiche e chimico-fisiche del prodotto essiccato. Durante l'essiccazione primaria, il tasso di sublimazione è diminuito con l'aumento della pressione della camera ed aumentato con l'incremento della temperatura del ripiano su cui sono posti i flaconi (Patel e Pikal, 2011). La fase di essiccazione primaria termina quando non è più presente uno strato congelato (Liapis e Bruttini, 1994).

La restante acqua non congelata (acqua assorbita o legata), solitamente il 15-20% in peso/ peso di soluto (Rambhatla *et al*., 2004), richiede una fase di essiccazione secondaria (fase di desorbimento) per la sua rimozione. L'essiccazione secondaria viene eseguita sottovuoto a temperature dei ripiani superiori a quelle che si hanno durante l'essiccazione primaria. Il vapore desorbito viene trasportato attraverso i pori del materiale essiccato (Liapis e Bruttini, 1994). L'umidità residua diminuisce fino a raggiungere un livello di plateau. Questo valore dipende

dalla formulazione e dalla temperatura di essiccazione secondaria, mentre non varia con il protocollo di congelamento utilizzato (Oddone *et al*., 2017).

La morfologia del prodotto dipende dalla velocità di raffreddamento e dalla temperatura di nucleazione. Più alto è il grado di sottoraffreddamento, più si formano cristalli di ghiaccio di piccole dimensioni (Pikal *et al*., 2002; Pisano e Capozzi, 2017). Se la velocità di raffreddamento è bassa, la dimensione dei cristalli di ghiaccio è determinata dalla temperatura di nucleazione (Morris *et al*., 2004). I metodi di congelamento controllato inducono la nucleazione a temperatura più alta rispetto al congelamento convenzionale, producendo cristalli di ghiaccio più grandi che, da un lato, accelerano l'essiccazione primaria grazie alla minore resistenza al flusso di vapore e, dall'altro, riducono la superficie specifica del prodotto liofilizzato rallentando la fase di desorbimento durante l'essicazione secondaria (Rambhatla *et al*., 2004). Oddone *et al*. ha osservato che la VISF segue questa tendenza, ma nel complesso promuove una sostanziale riduzione del tempo di essicazione totale e una migliore omogeneità da flacone a flacone in termini di umidità residua finale. La variabilità tra i flaconi causa un comportamento eterogeneo durante l'essiccazione per via delle differenze nella velocità di trasferimento del calore e nella resistenza al trasporto del vapore nello strato essiccato (Searles *et al*., 2011). Queste considerazioni sono vere sia per i soluti cristallini che per quelli amorfi, ma per i primi il desorbimento è molto più veloce nell'essiccazione secondaria (Oddone *et al*., 2017).

La corretta scelta del packaging primario è di grande importanza sia per il processo di liofilizzazione del prodotto sia per la sua stabilità e integrità durante lo stoccaggio. Ad oggi i flaconi costituiscono il 50-55% del packaging volto a produrre sostanze iniettabili, le siringhe il 25-30%, mentre il resto è dato da ampolle e tubofiale (Sacha *et al*., 2010). Sono disponibili flaconi di diverse dimensioni e qualità. Nonostante il rischio di rottura, il basso coefficiente di scambio termico e la possibilità di interazioni con il prodotto, il vetro è il materiale più utilizzato grazie alla sua durata chimica, pulizia, bassa permeabilità ai gas, possibilità di sterilizzazione terminale e trasparenza (Schaut *et al*., 2014). I flaconi di plastica, visualmente identici a quelli in vetro, incontrano difficoltà a essere maneggiati dal sistema di riempimento a causa del basso peso e potenzialmente possono interagire con il prodotto farmaceutico (assorbimento, adsorbimento, migrazione) (Sacha *et al*., 2010).

Per contenere farmaci parenterali generalmente viene utilizzato il vetro borosilicato di Tipo I che è principalmente composto da biossido di silicio (~ 81%) e ossido borico (~ 13%), con bassi livelli di ossidi che non prendono parte a network, quali ossidi di sodio e alluminio. È un vetro chimicamente resistente (bassa lisciviabilità) avente, anche, un basso coefficiente di espansione termica (Sacha *et al*., 2010). La sua composizione gli conferisce elevata resistenza idrolitica che si manifesta nella resistenza del vetro al rilascio di sostanze minerali idrosolubili nella soluzione farmaceutica.

Gli ossidi che non possono entrare nella rete strutturale del vetro sono relativamente liberi di migrare dal contenitore alla soluzione. Il processo di lisciviazione è un processo di scambio ionico controllato dalla diffusione che coinvolge i protoni di una soluzione acquosa e gli ioni alcalini presenti nel vetro (ad esempio Li^{+}, Na^{+}, K^{+}, Mg^{++}, Ca^{++} e Mg^{+++}). Questa perdita di ioni idronio durante la lisciviazione porta all'aumento del pH della soluzione del prodotto e alla potenziale instabilità delle biomolecole (Sacha *et al*., 2010; Ennis *et al*., 2001). Durante lo stoccaggio la superficie del vetro a contatto con la soluzione può essere soggetta a delaminazione (Ditter *et al*., 2018a), ossia alla formazione di fiocchi e particelle generalmente inaccettabili (Cailleteau *et al*., 2008; Iacocca e Allgeier, 2007). Per ovviare a questo problema i contenitori possono essere rivestiti internamente. Se la tensione superficiale della soluzione è inferiore all'energia superficiale del contenitore, la soluzione diffonde sulla parete interna di

quest'ultimo. Il risultato sono striature, macchie o anche strati sottili uniformi di prodotto depositati sulla superficie interna del contenitore sopra la cake (Langer *et al*., 2020). Il fenomeno, identificato con il nome di fogging si trasforma da difetto estetico a critico se compromette l'integrità della chiusura del contenitore (Huang *et al*., 2019). I fattori che portano al fogging sono inversamente proporzionali all'angolo di contatto della superficie interna del flacone, pertanto questo fenomeno può essere limitato o eliminato con rivestimenti idrofobici (Langer *et al*., 2020). Infine, il vetro può adsorbire quantità significative di proteine dalla soluzione (Grohganz *et al*., 2004). Per garantire un dosaggio accurato è possibile incrementare volume di riempimento e/o concentrazione, ma questo provoca un aumento dei costi (Hoger *et al*., 2015). Altre soluzioni possono essere l'aggiunta di eccipienti (Duncan *et al*., 1995; Wendorf *et al*., 2004) o l'uso di contenitori in grado di limitare la perdita di attività proteica (Kondo e Mihara, 1996).

Nella scelta di un flacone per una data operazione spesso il rispetto della classe idrolitica I non è sufficiente, pertanto, si possono trattare o rivestire le superfici interne dei contenitori al fine di migliorarne la qualità e ridurre al minimo le interazioni con la formulazione (Ditter *et al*., 2018b). Per questo motivo, oltre ai flaconi non trattati in vetro borosilicato di Tipo I (S-) nel presente lavoro sono anche stati testati flaconi solfatati (ST), siliconati (S +) e TopLyo® (TL). Tutti i flaconi utilizzati sono conformi alla norma ISO 8362-1 e di dimensione 2R.

I flaconi solfatati sono costituiti da vetro di Tipo I a cui è stato applicato un trattamento di solforazione con sale di solfato di ammonio. Il trattamento consiste nel portare il solfato di ammonio ad alte temperature (> 490 ° C) in modo che si decomponga. Questo vapore reagisce con gli alcali superficiali (metalli cationici) per formare sali di sodio e potassio solubili in acqua e scalza il calcio tramite l'idrogeno. Dopo il lavaggio si forma uno strato arricchito di silice che funge da barriera per l'ulteriore eluizione di alcali (Preston e Anderson, 1985; Sacha *et al*., 2010). Pertanto, il trattamento di solforazione riduce l'alcalinità superficiale (Iacocca *et al*., 2010) e sopprime la formazione di particelle (Ogawa *et al*., 2013). Questo trattamento del vetro riduce anche la potenziale lisciviazione, ma può danneggiare la superficie del flacone favorendo la delaminazione (Ennis *et al*., 2001; Sacha *et al*., 2010). I costi del trattamento sono contenuti.

Il trattamento di siliconatura consiste nell'applicare ad un vetro di Tipo I un'emulsione non ionica di olio di dimeticone in acqua al 35%. Questi flaconi sono prodotti direttamente da GSK Vaccines. Il film ottenuto dopo l'applicazione dell'emulsione offre ottime proprietà idrorepellenti, antiaderenti e termoresistenti. I flaconi siliconati contengono quantità minori di Na e B e maggiori di Si e C di quelli non trattati (Huang *et al*., 2019). Il rivestimento in silicone inibisce il legame idrogeno tra acqua, silanolo e gruppi silossanici sulla superficie del vetro (Kawano *et al*., 2017). Inoltre, l'interazione tra le varie fasi data dalla forza di Van der Waals è minore in caso di vetro rivestito (Kawano *et al*., 2017). L'energia libera superficiale inferiore rispetto a quella di un vetro non trattato provoca una riduzione dell'energia adesiva (Kawano *et al*., 2017). I vantaggi della siliconatura della superficie interna di contenitori utilizzati per la liofilizzazione sono molteplici:

- Il rivestimento sopprime il contatto tra la soluzione e il vetro dei flaconi che è ricco di cationi (Ogawa *et al*., 2013) fungendo quindi da barriera contro l'eluizione di alcali dal vetro (White *et al*., 2008; Iacocca *et al*., 2010);
- Il rivestimento evita la delaminazione dalla superficie del vetro (White *et al*., 2008; Ogawa *et al*., 2016);
- Il rivestimento riduce la lisciviazione di ioni dalla superficie del vetro a livelli accettabili;

- Il rivestimento si traduce in una superficie idrofobica che resiste a legami non specifici riducendo le perdite di campione causate da questo tipo di interazioni con il contenitore. L'assorbimento di proteine sulla superficie è ridotto e la stabilità durante la conservazione aumentata;
- Le superfici, grazie ai rivestimenti idrofobici, risultano molto omogenee impedendo l'adesione delle sostanze liofilizzate alle pareti interne dei flaconi. Le conseguenze sono una perfetta trasparenza del flacone (il fogging è limitato) e un drenaggio quasi completo del prodotto che consente un miglior dosaggio;
- La morfologia del prodotto è migliore.

Tuttavia, il potenziale di aggregazione proteica è maggiore in presenza di olio di silicone nel rivestimento della superficie interna (Jones *et al*., 2005) e il film SiO2 non sopprime la formazione di particelle nella soluzione (Ogawa *et al*., 2013).

I flaconi TopLyo® sono costituiti da vetro di Tipo I combinato con uno strato Si-O-C-H trasparente e non poroso. Grazie al rivestimento idrofobo applicato mediate PICVD (Plasma-Impulse Chemical Vapor Deposition) sono particolarmente consigliati per la liofilizzazione. La composizione superficiale di questi flaconi è dominata da C, Si e O (Huang *et al*., 2019). Nella Tabelle 2.2 e 2.3 sono presentate le proprietà fisiche e chimiche del rivestimento ultrasottile dei TopLyo®. Le caratteristiche dei TopLyo® sono simili a quelle dei flaconi siliconati prodotti da GSK Vaccines, ma il trattamento di qualità superiore li rende più idrofobici. Questi flaconi possono, quindi, vantare tutti i vantaggi per la liofilizzazione dei flaconi siliconati.

Le formulazioni testate sono state: acqua demineralizzata (DW), acqua demineralizzata + 0,02% w/v Tween 80 (DW+TW80), 5% w/w saccarosio (Suc), 5% w/w saccarosio + 0,02% w/v Tween 80 (Suc+TW80), 5% w/w mannitolo (MAN) e 5% w/w mannitolo + 0,02% w/v Tween 80 (MAN+TW80).

Il saccarosio è lo zucchero più utilizzato nella liofilizzazione dei biofarmaci (Fissore *et al*., 2019). È un disaccaride amorfo dato dal glucosio e dal fruttosio legati tramite un legame glicosidico. Può agire sia come crioprotettore che come lioprotettore. Grazie alla Tg 'di -32 ° C e alla Tg di 74 ° C il saccarosio aumenta anche la stabilità durante lo stoccaggio (Heljo, 2013).

Il mannitolo è un polialcol che può essere utilizzato come eccipiente per la liofilizzazione delle proteine. La capacità del mannitolo di stabilizzare le proteine è limitata alla sua forma amorfa, purtroppo ha una bassa Tg 'di -32 ° C e -25 ° C e una bassissima Tg di 12,6 ° C e quindi cristallizza facilmente (Cavatur *et al*., 2002; Yu *et al*., 1998). Il mannitolo può formare polimorfi ed emiidrati diversi a seconda della temperatura e della velocità di cristallizzazione (Hawe e Friess, 2006).

Il polisorbato 80, noto anche come Tween 80, è un tensioattivo non ionico sintetico composto dall'unione del sorbitolo con l'ossido di etilene esterificato con acidi grassi. I tensioattivi non ionici possono proteggere le proteine da aggregazione, adsorbimento superficiale e precipitazione derivati da stress legati ad agitazione, congelamento ed essiccazione (Kiese *et al*., 2008; Hillgren *et al*., 2002; Wang, 2005). Il polisorbato 80 può essere utilizzato in campo farmaceutico come solubilizzante, stabilizzante o emulsionante (Schwartzberg e Navari, 2018; Khan *et al*., 2015). Il Tween 80 è una molecola anfifilica con componenti idrofobiche e idrofile (Kerwin, 2008; Khan *et al*., 2015). Le molecole di polisorbato 80 orientano le loro porzioni idrofobiche all'interfaccia aria-acqua o solido-acqua, e per concentrazioni superiori alla concentrazione micellare critica (0,01% w/v) si assemblano come micelle in soluzione.

1.1 Obiettivi della tesi

Gli scopi del presente lavoro di ricerca sono stati:

- valutare l'effetto sul prodotto ottenuto mediate nucleazione controllata (VISF) dei diversi trattamenti superficiali dei flaconi e delle soluzioni con cui sono stati riempiti;
- trovare la miglior combinazione di tipo di flaconi e soluzioni per eseguire la VISF;
- implementare la VISF attraverso una modalità automatica.

Tali argomenti non sono stati trovati in alcuna trattazione all'interno della letteratura.

Il punto di partenza è stato la comprensione dei principi del congelamento, delle tecniche per controllare la temperatura di nucleazione, delle fasi di essiccazione e dell'effetto delle proprietà del contenitore sul prodotto finale.

2. Metodi

Sono stati eseguiti una serie di esperimenti in GSK Vaccines, a Rixensart (Belgio).

2.1 Determinazione di P_{first} e P_{last} (Esperimento 1)

L'obiettivo del primo esperimento è stato quello di rilevare il range di pressione nel quale avviene la nucleazione in un batch di flaconi applicando la VISF. Per ispezione visiva sono stati rilevati ed annotati i valori di pressione P_{first} e P_{last}, che corrispondono rispettivamente al valore di pressione a cui è stata osservata per la prima volta la nucleazione in alcuni flaconi e al valore di pressione a cui l'ultimo flacone è nucleato. Al momento dell'inizio del raffreddamento la soluzione è trasparente e limpida, mentre a seguito della nucleazione la soluzione diventa opaca a causa della presenza di cristalli di ghiaccio. Le soluzioni e i flaconi testati sono quelli sopra presentati; i dettagli dei cicli sono riportati in Tabella 2.5.

Cycle details							
S-		ST		S+		TL	
Solution	T_n[°C]	Solution	T_n[°C]	Solution	T_n[°C]	Solution	T_n[°C]
DW	-5,0	DW	-5,0	DW	-5,0	DW	-5,0
DW	-10,0	DW	-10,0	DW	-10,0	DW	-10,0
DW+TW80	-5,0	DW+TW80	-5,0	DW+TW80	-5,0	DW+TW80	-5,0
DW+TW80	-10,0	DW+TW80	-10,0	DW+TW80	-10,0	DW+TW80	-10,0
Suc	-5,0	Suc	-5,0	Suc	-5,0	Suc	-5,0
Suc	-10,0	Suc	-10,0	Suc	-10,0	Suc	-10,0
Suc+TW80	-5,0	Suc+TW80	-5,0	Suc+TW80	-5,0	Suc+TW80	-5,0
Suc+TW80	-10,0	Suc+TW80	-10,0	Suc+TW80	-10,0	Suc+TW80	-10,0
MAN	-5,0	MAN	-5,0	MAN	-5,0	MAN	-5,0
MAN	-10,0	MAN	-10,0	MAN	-10,0	MAN	-10,0
MAN+TW80	-5,0	MAN + TW80	-5,0	MAN+TW80	-5,0	MAN+TW80	-5,0
MAN+TW80	-10,0	MAN + TW80	-10,0	MAN+TW80	-10,0	MAN+TW80	-10,0

Tabella 2.5: Dettagli dei cicli per gli esperimenti 1 e 2.

Venti flaconi sono stati riempiti con 0,5ml di soluzione e parzialmente tappati con tappi igloo (tipo Helvoet FM 460) per permettere la comunicazione dello spazio di testa dei flaconi con la camera del liofilizzatore. I flaconi sono stati quindi posizionati sul ripiano centrale della camera del liofilizzatore HETO DW 8030 in modo sfalsato ad una distanza di 4 centimetri dal bordo anteriore del ripiano. Tre sonde del sensore Tempris sono state inserire in 3 flaconi nelle posizioni indicate in Figura 3.8 per monitorare la temperatura della soluzione. Durante il caricamento, la temperatura del ripiano è stata impostata a 4 ° C ed una volta terminato la soluzione nei flaconi è stata equilibrata a T_n = -5 °C o T_n = -10 °C e pressione atmosferica, come spiegato nella sezione 2.2.2.2. Ad equilibrio raggiunto la pompa a vuoto è stata accesa diminuendo la pressione nella camera. A seguito della nucleazione dell'ultimo campione la pressione atmosferica è stata ristabilita.

2.2 Determinazione di t_n (Esperimento 2)

Un secondo esperimento è stato condotto per rilevare, per una data soluzione e un dato tipo di flacone, il valore di pressione P_n per cui almeno il 70% dei flaconi nucleano e il tempo t_n necessario per la nucleazione a questa pressione. La nucleazione è stata rilevata mediante ispezione visiva, allo stesso modo dell'esperimento 1. Anche le soluzioni e i flaconi testati sono i medesimi dell'esperimento 1; i dettagli dei cicli sono riportati nella tabella 2.5. Venti flaconi sono stati riempiti con 0,5ml di soluzione e parzialmente tappati con tappi igloo (tipo Helvoet FM 460) per consentire la comunicazione dello spazio di testa dei flaconi con la camera del liofilizzatore. I flaconi sono stati quindi posizionati sul ripiano centrale della camera a vuoto del liofilizzatore HETO DW 8030 in modo sfalsato ad una distanza di 4 centimetri dal bordo anteriore del ripiano. Tre sonde del sensore Tempris sono state inserite in 3 flaconi nelle posizioni indicate in Figura 3.8 per monitorare la temperatura della soluzione. Durante il caricamento, la temperatura del ripiano è stata impostata a 4 ° C ed una volta terminato la soluzione nei flaconi è stata equilibrata a T_n = -5 ° C o T_n = -10 ° C e pressione atmosferica, come spiegato nella sezione 2.2.2.2. Al raggiungimento di T_n la pompa del vuoto è stata accesa diminuendo la pressione in camera al valore P_n ottenuto mediante l'equazione empirica 2.1:

$$P_n = P_{first} - \frac{P_{first} - P_{last}}{c} \tag{2.1}$$

Dove c è un coefficiente assunto uguale a 3, P_{first} e P_{last} sono valori di pressione ottenuti nell'esperimento 1 corrispondente. Raggiunto il valore di P_n, la valvola tra il condensatore e la camera del liofilizzatore è stata chiusa isolando così quest'ultima. La camera è stata mantenuta isolata fino a quando non è stata osservata la nucleazione in tutti i flaconi e a seguire è stata ristabilita la pressione atmosferica. Il tempo t_n richiesto per indurre la nucleazione è stato annotato. Se meno del 70% dei campioni sono nucleati in un tempo massimo di 5 minuti l'esperimento è stato ripetuto diminuendo il valore di c di una unità o mezza unità.

2.3 Determinazione dell'influenza del processo di degassificazione

È stata, quindi, eseguita una serie di test per indagare, per una data soluzione in un flacone TopLyo®, l'influenza del processo di degassaggio sui fenomeni di bubbling ed ebollizione. La scelta del tipo di flacone è ricaduta sui TopLyo® perché il caso più critico in termini di fenomeni di bubbling ed ebollizione. Le formulazioni testate sono state: acqua demineralizzata, acqua demineralizzata + 0,02% w/v Tween 80, 5% w/w saccarosio + 0,02% w/v Tween 80 e 5% w/w mannitolo+ 0,02% w/v Tween 80. Un gruppo di dieci flaconi TopLyo® è stato riempito con 0,5 ml della soluzione scelta, mentre un altro gruppo di dieci flaconi TopLyo® è stato riempito con 0,6 ml della stessa soluzione. Per tener conto dell'evaporazione della soluzione durante la

degassificazione i flaconi destinati a questo processo sono stati riempiti 0,1 ml in più degli altri. Una sonda del sensore Tempris è stata inserita in ogni gruppo di flaconi per monitorare la temperatura, come mostrato nella Figura 2.10. I flaconi sono stati parzialmente tappati con tappi igloo (tipo Helvoet FM 460) per mettere in comunicazione lo spazio di testa del flacone con la camera a vuoto.

Il gruppo di flaconi con volume di riempimento pari a 0,6 ml è stato posto, in modo sfalsato, sulla parte sinistra del ripiano centrale della camera del liofilizzatore HETO DW 8030 ad una distanza di 4 centimetri dal bordo anteriore del ripiano. Questi flaconi sono stati equilibrati a una temperatura di 10 °C a pressione atmosferica e degassati. La soluzione è stata degassata direttamente all'interno dei flaconi per evitare successivi spostamenti che avrebbero potuto annullare l'efficacia del trattamento. La procedura di degassaggio cambia se il Tween 80 è presente o meno nella soluzione. Se il Tween 80 non è presente per evitare la nucleazione causata dall'ebollizione le soluzioni sono degassate a pressione più elevata.

In assenza di Tween 80:

1. si abbassa la pressione all'interno della camera del liofilizzatore a 10 mbar e la si mantiene a questo valore per 10 minuti;
2. si abbassa la pressione all'interno della camera del liofilizzatore a 7 mbar e la si mantiene a questo valore per 20 minuti.

In presenza di Tween 80:

1. si abbassa la pressione all'interno della camera del liofilizzatore a 10 mbar e la si mantiene a questo valore per 5 minuti;
2. si abbassa la pressione all'interno della camera del liofilizzatore a 7 mbar e la si mantiene a questo valore per 10 minuti;
3. si abbassa la pressione all'interno della camera del liofilizzatore a 4 mbar e la si mantiene a questo valore per 15 minuti.

Terminata la degassificazione la pressione nella camera del liofilizzatore è stata riportata a quella atmosferica e il secondo gruppo di flaconi, riempiti 0,5 ml, è stato caricato nella parte destra dello stesso ripiano. Durante il caricamento la temperatura del ripiano è stata mantenuta a 4°C, mentre terminata questa fase la soluzione nei flaconi è stata equilibrata ad una T_n = -5 °C e pressione atmosferica. Al raggiungimento di T_n la pompa a vuoto è stata accesa diminuendo la pressione nella camera. I fenomeni di ebollizione/bubbling sono stati monitorati nei diversi gruppi di flaconi e a nucleazione avvenuta la pressione atmosferica è stata ristabilita.

2.4 Analisi del prodotto liofilizzato

Infine, tre test identificati con le lettere A, B e C sono stati svolti per investigare la morfologia del prodotto liofilizzato. Per i loro vantaggi, presentati nell'introduzione, i flaconi utilizzati in questi esperimenti sono stati quelli siliconati mentre quelli non trattati sono stati utilizzati come confronto. Le soluzioni testate sono state quelle a base di saccarosio (5% w/w saccarosio and 5% w/w saccarosio + 0,02% w/v Tween 80) perché la sua presenza garantisce un residuo solido finale e permette di avere P_n superiori al mannitolo, come visto dai risultati dell'esperimento 2. La scelta della T_n tra -5 °C e -10 °C è pressoché indifferente. Negli esperimenti seguenti è stato utilizzato T_n = -5 °C, tuttavia un T_n = -10 °C potrebbe consentire di utilizzare P_n leggermente superiore riducendo la probabilità di blow up delle cakes.

Nell'esperimento A un vassoio composto da 378 flaconi non trattati riempiti con 0,5 ml di 5% w/w di saccarosio e un vassoio di 378 flaconi siliconati riempiti con 0,5 ml della stessa

soluzione sono stati caricati sui ripiani della camera del liofilizzatore HETO DW 8030. Tre sonde del sensore Tempris sono state inserite in tre flaconi siliconati nella posizione mostrata nella Figura 2.11 per monitorare la temperatura. I flaconi sono stati parzialmente tappati con tappi igloo (tipo Helvoet FM 460) per mettere in comunicazione lo spazio di testa del flacone con la camera del liofilizzatore. Il vassoio di flaconi siliconati è stato posto sul ripiano centrale della camera del liofilizzatore, mentre quello di flaconi non trattati è stato posto sul ripiano sovrastante. Il caricamento è stato effettuato ad una temperatura del ripiano di 4 °C e a seguire la soluzione nei flaconi è stata equilibrata a una temperatura T_n = -5 °C e pressione atmosferica. Raggiunta questa condizione la pompa a vuoto è stata accesa diminuendo la pressione in camera al valore P_n. Quindi, a tale valore di pressione, la valvola tra il condensatore e la camera del liofilizzatore è stata chiusa, isolando così quest'ultima. Dopo un tempo pari a t_n la pressione atmosferica è stata ristabilita nella camera del liofilizzatore. Il valore di P_n scelto è il minore tra i valori di P_n corrispondenti a flaconi non trattati e siliconati trovati nell'esperimento 2 per la soluzione scelta equlibrata a T_n = -5. Il valore di t_n è il corrispondente a P_n. Quindi dalla Tabella 2.6 si può notare che il valore inferiore di P_n è 0,9 mbar a cui corrisponde un t_n di 7 s. Per ottenere il prodotto finale i flaconi sono stati quindi sottoposti a congelamento, essiccazione primaria ed essiccazione secondaria i cui dettagli sono riportati nelle Tabelle 2.7, 2.8 e 2.9. Una volta completata l'essiccazione secondaria, il liofilizzatore ha chiuso automaticamente i flaconi isolando il loro spazio di testa dalla camera per evitare un'umidificazione del prodotto nella fase di scarico.

La metodologia con la quale è stato eseguito l'esperimento B è uguale a quella dell'esperimento A, l'unica differenza consiste nell'utilizzare una soluzione di 5% w/w saccarosio + 0,02% w/v Tween 80 invece di solo 5% w/w saccarosio. Quindi, dalla Tabella 2.10 si può notare che il valore inferiore di P_n è 0,9 mbar a cui corrisponde un t_n di 1 s.

Nell'esperimento C un vassoio composto da 378 campioni siliconati riempiti con 5% w/w saccarosio + 0,02% w/v Tween 80 è stato caricato sul ripiano centrale della camera del liofilizzatore HETO DW 8030. I flaconi sono stati riempiti con 0,6 ml di soluzione, invece che con un volume pari a 0,5 ml come negli esperimenti A e B per tenere conto dell'evaporazione della soluzione durante la degassificazione. Tre sonde del sensore Tempris sono state inserite in tre flaconi siliconati nella posizione mostrata nella Figura 2.11 per monitorare la temperatura. I flaconi sono stati parzialmente tappati con tappi igloo (tipo Helvoet FM 460) per mettere in comunicazione lo spazio di testa del flacone con la camera del liofilizzatore. Questi flaconi sono stati equilibrati a una temperatura T_n = 10 °C e degassati secondo la procedura presentata nella sezione 2.2.5.2 in presenza di Tween 80. La soluzione è stata degassata direttamente all'interno dei flaconi per evitare successivi spostamenti che avrebbero potuto annullare l'efficacia del trattamento. Al termine della degassificazione la pressione nella camera da vuoto è stata riportata a quella atmosferica e i flaconi sono stati equilibrati ad una temperatura T_n = -5 °C. Quando la soluzione nei flaconi ha raggiunto T_n, la pompa a vuoto è stata accesa diminuendo la pressione in camera al valore P_n. Raggiunto il valore P_n, la valvola tra il condensatore e la camera da vuoto è stata chiusa, isolando così quest'ultima. Dopo un tempo pari a t_n la pressione atmosferica è stata ristabilita nella camera a vuoto. I valori di P_n e t_n sono quelli che sono stati trovati nell'esperimento 2 per un flacone siliconato riempito con 5% w/w saccarosio + 0,02% w/v Tween 80 ed equilibrato a T_n = -5 e, quindi, coincidono con quelli dell'esperimento B. Per ottenere il prodotto finale i flaconi sono stati quindi sottoposti a congelamento, essiccazione primaria ed essiccazione secondaria i cui dettagli sono riportati nelle Tabelle 2.7, 2.8 e 2.9. Una volta completata l'essiccazione secondaria, il liofilizzatore ha chiuso automaticamente i flaconi isolando il loro spazio di testa dalla camera per evitare un'umidificazione del prodotto nella fase di scarico.

3. Risultati

3.1 Determinazione di P_{first} e P_{last} (Esperimento 1)

I risultati dell'esperimento 1 sono riportati nelle tabelle 3.2, 3.3, 3.4 e 3.5. Nella determinazione di P_{first} sono stati scartati valori di pressione superiori a quelli scelti perché isolati a causa della natura stocastica della nucleazione e/o della possibile presenza di impurità nei flaconi. Valori di pressioni corrispondenti a flaconi contenenti le sonde del sensore Tempris non sono stati considerati attendibili per la nucleazione perché quest'ultime hanno agito da agenti nucleanti favorendo la nucleazione. A conferma di ciò nel caso di T_n = -10 ° C la nucleazione dei flaconi contenenti le sonde è avvenuta frequentemente prima di raggiungere T_n e quindi a pressione atmosferica. Sempre a causa della natura stocastica della nucleazione ripetendo gli esperimenti è possibile avere piccole variazioni dei risultati. Attraverso la Tabella 3.6 si può avere una visione complessiva di esperimenti fatti con differenti T_n, soluzioni e flaconi.

		S-		ST		S+		TL	
Solution	T_n **[°C]**	P_{first} **[mbar]**	P_{last} **[mbar]**	P_{first} **[mbar]**	P_{last} **[mbar]**	P_{first} **[mbar]**	P_{last} **[mbar]**	P_{first} **[mbar]**	P_{last} **[mbar]**
DW	-5,0	1,3	0,7	1,2	0,9	1,2	0,8	1,3	1,2
DW	-10,0	1,3	0,8	1,3	0,9	1,2	0,9	1,2	0,9
DW+TW80	-5,0	1,2	0,8	1,2	0,9	1,2	0,9	1,3	0,7
DW+TW80	-10,0	1,3	0,8	1,3	0,8	1,1	0,8	1,2	0,8
Suc	-5,0	1,2	0,8	1,1	0,8	1,1	0,8	1,2	0,9
Suc	-10,0	1,2	0,8	1,1	0,8	1,0	0,8	1,1	0,8
Suc+TW80	-5,0	1,2	1,0	1,2	0,9	1,2	0,8	1,1	0,7
Suc+TW80	-10,0	1,2	0,9	1,3	0,9	1,1	0,9	1,2	0,8
MAN	-5,0	1,2	0,7	1,2	0,6	1,1	0,6	1,1	0,8
MAN	-10,0	1,0	0,7	1,3	0,7	1,2	0,8	1,2	0,8
MAN+TW80	-5,0	1,1	0,7	1,2	0,7	1,1	0,8	0,9	0,7
MAN+TW80	-10,0	1,1	0,7	1,2	0,7	1,2	0,8	1,1	0,7

Tabella 3.6: Rappresentazione schematica dei risultati dell'esperimento 1.

Seguendo le linee orizzontali nella Tabella 3.6, si può vedere che a parità di soluzione non c'è un'influenza marcata del tipo di flacone su P_{first} e P_{last}. Mentre, analizzando le linee verticali della Tabella 3.6, si può notare che a parità di T_n e tipo di flacone, i valori di P_{first} e P_{last} sono leggermente inferiori se si aggiunge un soluto (saccarosio o mannitolo) al solvente (acqua). In particolare, le soluzioni contenenti mannitolo sono quelle con i valori di pressione di nucleazione inferiori. Aggiungendo un soluto non volatile a un solvente, la nucleazione avviene a temperature inferiori (depressione del punto di congelamento) rispetto al caso di un solvente puro. Ciò è causato da una diminuzione del potenziale chimico o, in modo equivalente, da una diminuzione della tensione di vapore. Per raggiungere una temperatura più bassa della soluzione nei flaconi è, pertanto, necessaria una maggiore evaporazione che si ottiene a pressioni inferiori nella camera del liofilizzatore. L'evaporazione è un processo endotermico che abbassa la temperatura della soluzione favorendo la nucleazione del ghiaccio. Analogamente, mantenendo costanti la soluzione e il tipo di fiala, nel caso di T_n = -10 ° C poiché quando si inizia ad abbassare la pressione si è ad una temperatura inferiore rispetto a T_n=-5°C sarà necessaria una minor evaporazione che è raggiunta a valori di pressione maggiori.

In alcuni tipi di flaconi, con determinate soluzioni, sono stati osservati fenomeni di ebollizione e /o bubbling durante l'abbassamento della pressione nella camera del liofilizzatore. La diminuzione della pressione nella camera favorisce il degassamento della soluzione nei flaconi. Per pressioni inferiori a 50 mbar, si formano piccole bolle tra la superficie interna dei flaconi e la soluzione, come si può vedere nella Figura 3.2. Queste bolle continuano a crescere al diminuire della pressione fino a quando a partire dai 10 mbar iniziano a risalire la bottiglia scoppiando, come si può vedere nella Figura 3.3. Questo fenomeno, identificato con il nome di bubbling, cessa raggiunti i 2-3 mbar. L'altro fenomeno osservabile nella soluzione all'interno dei flaconi diminuendo la pressione è l'ebollizione. Quando un liquido raggiunge il punto di ebollizione si formano bolle di aeriforme all'interno della sua massa. Il punto di ebollizione è la temperatura alla quale la tensione di vapore del liquido è uguale alla pressione esercitata sul liquido dall'atmosfera circostante. Diminuendo la pressione, dai 35-40 mbar, iniziano a formarsi bolle molto piccole sul fondo dei flaconi come si può vedere nella Figura 3.4. Queste bolle crescono e a partire dai 10 mbar fino a fine nucleazione salgono in superficie ed esplodono nell'aria, come si può vedere nella Figura 3.5. Sia il bubbling che l'ebollizione possono influenzare la morfologia della torta. Essendo entrambi fenomeni tumultuosi possono portare alla nucleazione della soluzione, questo è particolarmente evidente nel caso dell'ebollizione. In Figura 3.6 sono riportate una serie di flaconi contenenti cake irregolari a causa dell'ebollizione.

La presenza e l'intensità dei fenomeni di bubbling e boiling è stata riportata, per i casi analizzati dall'esperimento 1, nelle tabelle 3.7, 3.8, 3.9, 3.10. Dalle tabelle 3.6 e 3.7 si nota che l'ebollizione non è mai presente nei flaconi non trattati e in quelli solfatati grazie alle forti interazioni tra la superficie interna dei flaconi e le soluzioni in esse contenute. Invece, il bubbling in questi flaconi è sempre presente ad eccezione li si riempia con acqua demineralizzata oppure, solo per i flaconi solfatati, con 5% w/w mannitolo. I casi in cui il bubbling è più intenso sono quelli delle soluzioni contenenti Tween 80 perché i tensioattivi abbassano la tensione superficiale del liquido facilitando la formazione di schiuma e prevengono la rottura delle bolle grazie alla loro natura anfifilica. Anche, il saccarosio può essere correlato al bubbling. Il saccarosio inibisce la coalescenza delle bolle in un intervallo di concentrazione 0,01-0,3 M (Henry e Craig, 2009): la concentrazione di saccarosio nelle soluzioni testate è di circa 0,15 M e quindi è compresa nell'intervallo. Henry e Craig hanno suggerito che l'inibizione della coalescenza della bolla può essere correlata al comportamento degli osmoliti all'interfaccia aria-acqua, mentre non vi è alcuna correlazione con l'aumento del gradiente di tensione superficiale o con meccanismi elettrostatici. Per quanto riguarda il mannitolo, in letteratura non sono stati trovati articoli che lo colleghino al bubbling e nessuna chiara relazione tra questo eccipiente e la formazione di bolle può essere derivata dagli esperimenti effettuati. Il bubbling è generalmente più debole per T_n = -10 °C che per T_n = -5 °C poiché ad una temperatura inferiore si può disciogliere più aria nella soluzione e quindi ne viene rilasciata meno. Infine, si può osservare che il bubbling è leggermente meno diffuso ed intenso nei flaconi solfatati rispetto a quelli non trattati. Per quanto riguarda i flaconi siliconati e TopLyo®, i cui risultati sono riportati nelle tabelle 3.6 e 3.7, il bubbling è sempre presente ad eccezione che li si riempia con acqua demineralizzata oppure, solo per i flaconi solfatati, con 5% w/w mannitolo. Anche per questi tipi di flaconi il bubbling è più intenso per le soluzioni contenenti Tween 80 ed è generalmente un poco più debole per T_n = -10 °C che per T_n = -5 °C. In assenza di Tween 80 si verifica sempre l'ebollizione della soluzione decrementando la pressione. Il Tween 80 elimina il l'ebollizione migliorando la bagnabilità della superficie interna dei flaconi grazie alle sue proprietà anfifiliche. L'ebollizione è più diffusa e più intensa nei flaconi TopLyo® che in quelli siliconati. Ciò è dovuto al maggior angolo di contatto e quindi alla maggiore idrofobicità dei primi che minimizzano le interazioni tra la soluzione e il contenitore facilitando l'ebollizione. L'aggiunta di un soluto non volatile, come il mannitolo o il saccarosio, al solvente provoca un incremento del punto di ebollizione. Ciò è dovuto a una

diminuzione del potenziale chimico o, in modo equivalente, a una diminuzione della tensione di vapore. Di conseguenza, a parità di T_n, l'ebollizione avviene per valori di pressione inferiori. A pressione atmosferica, per una soluzione al 5% w/w di saccarosio l'elevazione del punto di ebollizione è di un ordine di grandezza inferiore al grado centigrado (Holven, 1936; Tressler *et al*., 1941). Inoltre, a parità di concentrazione di soluto, l'aumento del punto di ebollizione diminuisce al diminuire della pressione (Crapiste e Lozano, 1988). Pertanto, le variazioni del punto di ebollizione tra le soluzioni utilizzate sono trascurabili.

Un altro fenomeno osservato nell'esperimento 1 in flaconi non trattati, e in misura maggiore in quelli solfatati è stato il fogging. I flaconi riempiti con soluzioni contenenti mannitolo sono stati quellii caratterizzati da una maggior intensità del fenomeno. Il fogging non è dipende dal bubbling, poiché si è verificato anche in assenza di quest'ultimo, ma dagli angoli di contatto delle superfici interne dei flaconi. Il fogging è rilevante per bassi angoli di contatto, infatti è assente nei flaconi siliconati e TopLyo® che per via del loro trattamento hanno superfici idrofobiche. La Figura 3.9 presenta a sinistra flaconi solfatati e a destra flaconi TopLyo® entrambi contenenti una soluzione 5% w/w di mannitolo appena nucleata; osservando la diversa trasparenza dei flaconi, è chiaro che quelli solfatati presentano un appannamento assente nei TopLyo®.

3.2 Determinazione di t_n (Esperimento 2)

I risultati dell'esperimento 2 sono presentati nelle Tabelle 3.10, 3.11, 3.12 e 3.13 dalle quali, per motivi di spazio, sono state omesse le informazioni relative ai fenomeni di bubbling ed ebollizione che sono avvenuti con la stessa diffusività e intensità dell'esperimento 1. Nei conteggi del numero di flaconi nucleati non sono stati tenuti in conto quelli contenenti sonde del sensore Tempris perché queste agiscono come agenti nucleanti favorendo la nucleazione. Nel caso non sia stato ottenuto il 100% di nucleazione dei flaconi sono stati attesi 300 secondi prima della fine dell'esperimento 2. Le tabelle riportano, per ogni caso, il valore di t_n corrispondente al tempo che intercorre tra l'isolamento della camera e la nucleazione dell'ultimo flacone. In genere t_n non varia molto e la media dei valori ottenuti per le varie combinazioni di flaconi e soluzioni è 9 sec, come mostrato in Figura 3.10. Il valore ottimale di t_n è inferiore a 1 min perché un tempo più lungo può portare a blow up della cake (Oddone *et al*., 2020). Se tutti i flaconi sono già nucleati al momento dell'isolamento della camera del liofilizzatore t_n è zero e quindi la camera avrebbe potuto essere isolata qualche istante prima. La percentuale di flaconi nucleati non è sempre del 100% in parte perché i valori di P_n sono quasi sempre superiori a quelli di P_{last} riscontrati dall'esperimento 1, in parte perché la pressione all'interno della camera isolata tende ad aumentare nel tempo per l'evaporazione della soluzione. Se la nucleazione del 100% dei flaconi si ottiene ad una pressione P_n superiore a P_{last} è perché mantenendo la pressione a valori prossimi a P_n l'evaporazione continua e con essa la diminuzione della temperatura nella soluzione favorendo la nucleazione. Il valore P_n è generalmente compreso tra P_{first} e P_{last}, da cui viene calcolato utilizzando la Formula 2.1. Tuttavia, in un caso, per ottenere almeno il 70% dei campioni nucleati è stato necessario ricorrere a pressioni inferiori a P_{last} confermando la natura stocastica della nucleazione che può avvenire a pressioni diverse ripetendo l'esperimento. Come mostrato dalla Figura 3.11 per flaconi non trattati, la nucleazione avviene per valori di P_n più vicini a P_{first} che a P_{last}, mentre per gli altri tipi di flaconi analizzati P_n è circa la metà tra P_{first} e P_{last} (c = 1,5).

Attraverso la Tabella 3.14 risulta più immediato un confronto tra i valori di P_n ottenuti con differenti T_n, soluzioni e flaconi. Seguendo le linee orizzontali si può vedere che non c'è una marcata influenza del tipo di flaconi su P_n a parità di soluzione utilizzata. Mentre, analizzando le linee verticali della Tabella 3.14, si può notare che a parità di T_n e tipologia di

fiala, i valori di P_n sono simili per le diverse soluzioni, solo quelli delle soluzioni contenenti mannitolo sono leggermente inferiori agli altri. La ragione di ciò è la depressione del punto di congelamento a seguito dell'aggiunta di un soluto non volatile a un solvente.

A causa dei bassi valori di P_n è possibile che la cake si sollevi all'interno del flacone secondo il fenomeno del blow up o "flying cake", come mostrato in Figura 3.12. In caso di blow up di cake contenenti Tween 80, resti di soluzione non ancora solidificati possono formare bolle sotto la cake che solidificano con questa morfologia, come mostrato in Figura 3.13. Il blow up della cake va evitato perché porta ad un prodotto inaccettabile. Le tabelle 3.15 e 3.16 mostrano la presenza di blow up per le combinazioni di soluzioni e le tipologie di flaconi testati nell'esperimento 2. Confrontandole è possibile notare che il blow up è correlato al tipo di flacone: per flaconi non trattati o solfatati non sono generalmente presenti flying cakes, che invece si trovano in flaconi siliconati e TopLyo®. Questo perché le ultime due tipologie di flaconi, grazie ai rivestimenti idrofobici, hanno una superficie interna molto omogenea che riduce l'attrito tra la cake e le pareti dei contenitori. Quindi, a parità di P_n in un flacone con rivestimento in silicone, può verificarsi blow up delle cakes, che invece non è presente negli altri tipi di flaconi indagati.

		S-	ST	S+	TL
Solution	***T_n* [°C]**	***P_n* [mbar]**	***P_n* [mbar]**	***P_n* [mbar]**	***P_n* [mbar]**
DW	-5,0	1,1	1,0	1,0	1,2
DW	-10,0	1,1	1,1	1,1	1,0
DW+TW80	-5,0	1,1	1,0	0,9	0,9
DW+TW80	-10,0	1,0	1,0	0,9	0,9
Suc	-5,0	1,0	0,9	0,9	1,0
Suc	-10,0	1,0	0,9	0,9	0,9
Suc + TW80	-5,0	1,0	1,0	0,9	0,8
Suc + TW80	-10,0	1,0	1,0	1,0	0,9
MAN	-5,0	0,9	0,8	1,0	0,9
MAN	-10,0	0,8	0,9	1,0	1,0
MAN + TW80	-5,0	0,9	0,8	0,7	0,7
MAN + TW80	-10,0	0,9	0,8	0,9	0,8

Tabella 3.14: Rappresentazione schematica dei valori di P_n ottenuti dall'esperimento 2.

3.3 Determinazione dell'influenza del processo di degassificazione

Per quanto riguarda i test di degassificazione, durante l'applicazione di questa procedura all'acqua demineralizzata in flaconi TopLyo® è stato osservato il fenomeno dell'ebollizione, ma non quello del bubbling. Ciò è in accordo con i risultati dell'esperimento 1, infatti durante il degassamento la pressione nella camera dal liofilizzatore è stata portata a 7 mbar e l'ebollizione è evidente sotto i 10 mbar. Abbassando la pressione nella camera per avere la nucleazione dell'acqua, il fenomeno dell'ebollizione è stato ugualmente diffuso per il gruppo di campioni sottoposti a degassaggio e quelli non, mentre l'intensità dell'ebollizione è stata leggermente inferiore per i flaconi degassati. Questo può essere osservato nella Figura 3.16 dove a sinistra della linea rossa sono presenti i campioni che sono stati soggetti a degassaggio mentre a destra quelli non. L'intensità leggermente maggiore dell'ebollizione nei flaconi non degassati può essere dovuta all'aria disciolta nell'acqua che in caso di degassaggio è già stata rilasciata abbassando la pressione la prima volta. Come si può vedere nella Figura 3.17, la

morfologia della torta ottenuta dopo la nucleazione non è accettabile, anche per campioni che sono stati degassati, a causa dell'ebollizione.

Durante il degassaggio nei flaconi TopLyo® contenenti soluzioni di acqua demineralizzata + 0,02% w/v Tween 80, 5% w/w saccarosio + 0,02% w/v Tween 80 e 5% w/w mannitolo + 0,02% w/v Tween 80 si è verificato il fenomeno del bubbling ma non quello dell'ebollizione grazie alla presenza del Tween 80. Ciò è in accordo con i risultati dell'esperimento 1, infatti durante il degassamento la pressione nella camera dal liofilizzatore è stata portata a 4 mbar e il bubbling è evidente sotto i 10 mbar. Abbassando la pressione nella camera per avere la nucleazione della soluzione, il fenomeno del bubbling è risultato essere presente solo nei campioni che non sono stati sottoposti a degassamento. Questo per le soluzioni di acqua demineralizzata + 0,02% w/v Tween 80, 5% w/w saccarosio + 0,02% w/v Tween 80 e 5% w/w mannitolo + 0,02% w/v Tween 80 si può osservare rispettivamente nelle Figure 3.18, 3.20 e 3.22 dove a sinistra della linea rossa sono presenti i campioni che sono stati sottoposti a degassaggio mentre a destra quelli non. È quindi evidente che la presenza di Tween 80 elimina il fenomeno dell'ebollizione, grazie ad un miglioramento della bagnabilità della superficie interna dei flaconi. A sua volta il bubbling causato dal Tween 80 può essere eliminato con un processo di degassificazione. A seguito del degassaggio dei campioni, è importante evitare di trasferimento della soluzione in altri contenitori con pipette perché ciò annullerebbe il processo appena concluso. Per questo motivo il degassaggio è stato effettuato direttamente nei flaconi tenendo conto dell'evaporazione nei 30 minuti in cui le soluzioni sono a bassa pressione con un piccolo aumento del volume di riempimento. Come si può vedere in Figura 3.19, la morfologia della cake ottenuta dopo la nucleazione di acqua demineralizzata + 0,02% w/v Tween 80 è accettabile per i campioni che sono stati sottoposti a degassaggio, mentre gli altri hanno presentato piccoli difetti dovuti al bubbling. Come si osserva nelle Figure 3.21 e 3.23, rispettivamente per 5% w/w saccarosio + 0,02% w/v Tween 80 e 5% w/w mannitolo + 0,02% w/v Tween 80, a seguito della nucleazione si ha il blow up della cake anche per campioni che sono stati degassati. Probabilmente questo avrebbe potuto essere evitato isolando la camera del liofilizzatore per un dato valore di P_n, come fatto nell'esperimento 2, invece di terminare l'esperimento con la nucleazione dell'ultimo campione. In entrambi i casi la morfologia della torta ottenuta dopo la nucleazione è accettabile per i campioni sottoposti a degassaggio, mentre per gli altri le cakes presentano piccoli difetti dovuti al bubbling. Inoltre, solo nel caso di campioni che non sono stati degassati, sono presenti bolle sotto la torta dovute al Tween 80.

3.4 Analisi del prodotto liofilizzato

Negli esperimenti A, B e C seguendo la procedura necessaria per la nucleazione con P_n e t_n ottenuti dall'esperimento 2, sono nucleati tutti i flaconi nonostante la percentuale di campioni nucleati in tali condizioni, riportata in Tabella 3.12, sia dell'88%. Questo è dovuto al tempo necessario per abbassare la pressione nella camera che con 378, e ancor di più con 756 flaconi, è di almeno un ordine di grandezza superiore a quella con i 20 flaconi dell'esperimento 2. Più tempo a valori di pressione prossimi a P_n, prima di isolare la camera, ha permesso una maggiore evaporazione della soluzione abbassando ulteriormente la temperatura nei flaconi e quindi aumentando la percentuale di campioni nucleati a P_n rispetto all'esperimento 2. Se alcuni flaconi non sono nucleati mediante la VISF lo hanno fatto in modo incontrollato con il successivo congelamento a -52 °C.

Nell'esperimento A nel caso di flaconi non trattati, le cakes liofilizzate si trovano tutte sul fondo e hanno una morfologia abbastanza buona. L'assenza di blow up è una conferma dei risultati dell'esperimento 2, presentati nella Tabella 3.15. C'è qualche piccolo difetto superficiale dovuto al debole bubbling, osservato nelle stesse condizioni nell'esperimento 1. A

causa delle buone interazioni tra vetro e soluzione vi è la presenza di prodotto adeso alla superficie laterale del flacone e la curvatura della superficie della cake è convessa, come si può vedere nella Figura 3.23. Il vetro dei flaconi non presenta macchie di soluzione ed i tappi sono puliti, nonostante il bubbling. Sempre nell'esperimento A nel caso di flaconi siliconati, solo il 4,5% delle cakes si trova sul fondo, mentre il restante 95,5% sono flying cakes. Nel conteggio dei flaconi per il calcolo delle percentuali sono esclusi quelli contenenti termocoppie che potrebbero aver distorto i risultati. La presenza del blow up è una conferma dei risultati dell'esperimento 2, presentati nella Tabella 3.16. La superficie delle cakes ha molti difetti dovuti a bubbling e boiling, osservati nelle stesse condizioni anche nell'esperimento 1, che la rendono non è accettabile. Il rivestimento siliconico risulta in una superficie idrofobica resistente a legami aspecifici, quindi sono ridotte le perdite di campione causate da questo tipo di interazioni con il contenitore. Il prodotto non è aderente alle superfici laterali dei flaconi e la superficie delle cakes ha una curvatura concava, come si può vedere in Figura 3.24. Nel caso di flying cakes, sotto di esse si possono trovare residui di prodotto aderente al vetro. I tappi dei flaconi sono puliti, nonostante il bubbling. Sia per flaconi non trattati che siliconati tra il fondo delle cakes e quello dei flaconi non vi sono tracce di bolle. Ciò è in accordo con quanto visto nella sezione 3.3, in cui la presenza di queste bolle è attribuita al Tween 80 assente nell'esperimento A.

Nell'esperimento B nel caso di flaconi non trattati il 60,6% delle cakes si trova sul fondo dei flaconi, mentre il restante 39,4% sono flying cakes. Nel conteggio dei flaconi, per il calcolo delle percentuali, sono escluse quelle contenenti termocoppie che potrebbero aver distorto i risultati. A causa delle buone interazioni tra vetro e soluzione vi è la presenza di prodotto adeso alla superficie laterale del flacone e la curvatura della superficie della cake è convessa, come si può vedere nella Figura 3.25. Il vetro dei flaconi presenta alcune macchie di prodotto, mentre i tappi sono puliti, nonostante le bolle. Sempre nell'esperimento B nel caso di flaconi siliconati solo il 27,6% delle cakes si trova sul fondo dei flaconi, mentre il restante 72,4% sono flying cakes. Il rivestimento siliconico risulta in una superficie idrofobica resistente a legami aspecifici, quindi sono ridotte le perdite di campione causate da questo tipo di interazioni con il contenitore. Il prodotto non è aderente alle superfici laterali dei flaconi e la superficie delle cakes ha una curvatura concava, come si può vedere in Figura 3.26. Sempre per merito del rivestimento siliconico non sono presenti residui di prodotto aderenti al vetro. I tappi dei flaconi sono puliti, nonostante il bubbling. In entrambi i tipi di flaconi la superficie delle cakes presenta piccoli difetti dati dal bubbling, che è stato osservato nelle stesse condizioni anche nell'esperimento 1. Tuttavia, cosa rende inaccettabili i prodotti è l'alta percentuale di flying cakes e la presenza tra il fondo delle cakes quello dei flaconi di bolle. Ciò è in accordo con quanto visto al paragrafo 3.3, in cui la presenza di queste bolle è stata attribuita al Tween 80. Per i flaconi siliconati la percentuale di flying cakes supera il 70%, mentre per i flaconi non trattati questa è inferiore al 40% perché i rivestimenti idrofobici riducono l'attrito tra la cake e la superficie interna del contenitore. Da un lato quindi la presenza del Tween 80 elimina il fenomeno dell'ebollizione, grazie ad un miglioramento della bagnabilità della superficie interna dei flaconi; mentre dall'altro il Tween 80 aumenta il fenomeno del bubbling perché abbassa la tensione superficiale del liquido facilitando la formazione di schiuma e previene la rottura delle bolle grazie alla sua natura anfifilica.

Nell'esperimento C le cakes hanno una buona morfologia grazie all'assenza di fenomeni di bubbling ed ebollizione prima della nucleazione. La presenza di Tween 80 elimina il fenomeno dell'ebollizione, grazie ad un miglioramento della bagnabilità della superficie interna dei flaconi, e a sua volta il bubbling derivato dal Tween 80 viene eliminato dal processo di degasaggio. Contrariamente alle previsioni che avrebbero potuto essere fatte dai risultati dell'esperimento 2 la superficie interna dei flaconi è siliconata, ma tutte le cakes sono

perfettamente aderenti al fondo del contenitore. La ragione di ciò potrebbe risiedere nel fatto che, grazie all'elevato numero di flaconi e l'elevato volume di vapore che ne consegue, la diminuzione della pressione nella camera del liofilizzatore durante la VISF è stata più lenta. Il rivestimento siliconico risulta in una superficie idrofobica resistente a legami aspecifici, quindi sono ridotte le perdite di campione causate da questo tipo di interazioni con il contenitore. Il prodotto non è aderente alle superfici laterali dei flaconi e la superficie delle cakes ha una curvatura concava, come si può vedere in Figura 3.27. Sempre per merito del rivestimento siliconico non sono presenti residui di prodotto aderenti al vetro ad eccezione di due casi isolati in cui sono presenti schizzi di prodotto sui flaconi dovuti al bubbling nella fase di degassaggio. I tappi dei flaconi non presentano tracce di prodotto, nonostante il bubbling nel processo di degassificazione.

4. Conclusioni

Questo progetto di tesi magistrale è stato mirato a un'indagine approfondita dell'effetto dei trattamenti superficiali dei flaconi sulla fattibilità della nucleazione controllata mediante tecnica VISF. Una ricerca bibliografica approfondita e numerosi esperimenti sono stati effettuati presso GSK Vaccines (Rixensart).

Nell'esperimento 1, dato un tipo di contenitori e una soluzione, per flaconi in equilibrio a un dato T_n è stato identificato l'intervallo di pressione nel quale si ha la nucleazione di tutti i campioni. Il fatto che la nucleazione non avvenga contemporaneamente in tutti i flaconi conferma la sua natura stocastica. Confrontando, a parità di soluzione utilizzata, i flaconi non trattati, quelli solfatati, i siliconati e i TopLyo® non è stata identificata un'influenza marcata del tipo di flacone su P_{first} e P_{last}. Variando il tipo di soluzione, l'esperimento 1 ha dimostrato che aggiungendo un soluto non volatile a un solvente, la nucleazione avviene a temperature inferiori (depressione del punto di congelamento). Se il valore di T_n è -5 °C invece di -10 °C, per la nucleazione è necessaria una maggiore evaporazione che è ottenuta abbassando leggermente di più la pressione nella camera del liofilizzatore.

Il bubbling è stato osservato per tutte le combinazioni testate, ad eccezione dell'acqua demineralizzata e del 5% w/w di mannitolo solo nei flaconi solfatati. Questo fenomeno è più intenso e diffuso nei casi in cui Tween 80 è presente nella soluzione. Questo perché i tensioattivi sono composti che abbassano la tensione superficiale del liquido facilitando la formazione di schiuma e prevengono la rottura delle bolle grazie alla loro natura anfifilica. Anche il saccarosio può essere correlato al bubbling. Il saccarosio inibisce la coalescenza delle bolle in un intervallo di concentrazione 0,01-0,3 M (Henry e Craig, 2009): la concentrazione di saccarosio nelle soluzioni testate è di circa 0,15 M e quindi è compresa nell'intervallo. Henry e Craig hanno suggerito che l'inibizione della coalescenza della bolla può essere correlata al comportamento degli osmoliti all'interfaccia aria-acqua, mentre non vi è alcuna correlazione con l'aumento del gradiente di tensione superficiale o con meccanismi elettrostatici. Per quanto riguarda il mannitolo, in letteratura non sono stati trovati articoli che lo colleghino al bubbling e nessuna chiara relazione tra questo eccipiente e la formazione di bolle può essere derivata dagli esperimenti effettuati. Il fenomeno dell'ebollizione è presente in tutti i flaconi con rivestimenti siliconici interni, ma è inibito dalla presenza di Tween 80 nella soluzione che migliora la bagnabilità della superficie interna dei contenitori grazie alle sue proprietà anfifiliche. L'ebollizione è più diffusa e più intensa nei flaconi TopLyo® che in quelli siliconati. Ciò è dovuto al maggior angolo di contatto e quindi alla maggior idrofobicità dei primi che sono più efficienti nel minimizzare le interazioni tra la soluzione e il contenitore, facilitando l'ebollizione. Sia il bubbling che l'ebollizione portano ad ottenere prodotti con una morfologia inaccettabile.

Il fenomeno del fogging è stato osservato in flaconi non trattati e, in maggior misura, in flaconi solfatati. Il fogging è importante per bassi angoli di contatto; lo dimostra il fatto che questo fenomeno non è stato rilevato per flaconi siliconati e TopLyo® che hanno superfici interne idrofobiche. I flaconi solfatati hanno quindi dato risultati molto simili a quelli non trattati, solo il bubbling è stato leggermente meno intenso, ma in compenso l'appannamento è stato più evidente.

Nell'esperimento 2, per ogni combinazione di soluzione e trattamento superficiale dei flaconi, è stato determinato un valore di pressione P_n a cui isolare la camera del liofilizzatore per un tempo t_n al fine di ottenere la nucleazione dei campioni precedentemente in equilibrio a T_n e pressione atmosferica. I valori di P_n sono simili per le diverse soluzioni, solo quelli delle soluzioni contenenti mannitolo sono leggermente inferiori agli altri. In genere, t_n è inferiore ai 10 secondi. La durata ottimale per il mantenimento della pressione al valore di P_n è inferiore a 1 min perché un tempo più lungo può portare al blow up delle cakes (Oddone *et al*., 2020). L'aumento della pressione ottenuto isolando la camera del liofilizzatore dal condensatore ha lo scopo di ridurre i fenomeni di blow up grazie a P_n superiori agenti sul campione. Tuttavia, flaconi siliconati e TopLyo® hanno presentato comunque flying cakes perché i rivestimenti idrofobici riducono l'attrito fra la cake e la superficie interna del contenitore. In caso di blow up e presenza di Tween 80 resti di soluzione non ancora solidificati possono formare bolle sotto la cake che solidificano con questa morfologia. Il blow up della cake va evitato perché porta ad un prodotto inaccettabile. Le considerazioni sul bubbling e sull'ebollizione ottenute nell'esperimento 1 sono state confermate dall' esperimento 2.

L'influenza del processo di degassaggio sui fenomeni di bubbling ed ebollizione è stata studiata per varie soluzioni in flaconi TopLyo® nei quali si hanno i casi più critici. Degassando l'acqua demineralizzata il successivo fenomeno dell'ebollizione nella fase di nucleazione è risultato leggermente meno intenso in quanto l'aria disciolta nell'acqua è stata rilasciata abbassando la pressione la prima volta. Poiché la riduzione dell'ebollizione non è stata sostanziale, il degassaggio è stato applicato a soluzioni contenenti Tween 80 che causa forte bubbling ma elimina l'ebollizione. Le soluzioni contenenti Tween 80 degassate non hanno presentato né bubbling né ebollizione durante la VISF e di conseguenza la morfologia delle cakes è risultata buona. Il degassaggio consente quindi di applicare la tecnica di nucleazione controllata VISF anche a soluzioni contenute in flaconi con rivestimento interno in silicone.

Sono state, quindi, effettuate una serie di prove per trovare una combinazione di tipo di flacone e soluzione in grado di dare, tramite nucleazione controllata con il metodo VISF e successiva liofilizzazione, un prodotto con una morfologia accettabile. In questi esperimenti, grazie ai valori di P_n e t_n determinati nell'esperimento 2, per ogni combinazione di soluzione e flacone, è stato possibile implementare la tecnica VISF attraverso una modalità automatica, senza necessità di regolazioni manuali della pressione mediante ispezione visiva dei campioni.

Per i loro vantaggi, presentati nell'introduzione, i flaconi di interesse in questi esperimenti sono stati quelli siliconati. Tra quelle testate, la soluzione che ha portato ai risultati migliori è stata 5% w/w saccarosio + 0,02% w/v Tween 80 perché è caratterizzata da P_n superiori al mannitolo, come visto dai risultati dell'esperimento 2. A differenza del mannitolo, il saccarosio rimane amorfo durante la liofilizzazione e quindi è stata necessaria una fase di essiccazione secondaria per ottenere il prodotto liofilizzato. Infatti, nei soluti amorfi, circa il 20% dell'acqua non congelata è associata alla soluzione solida e deve essere rimossa mediante un processo di diffusione durante l'essiccazione secondaria, mentre nel materiale cristallino quasi tutta l'acqua è congelata e può essere facilmente rimossa durante l'essiccazione primaria (Nail *et al*., 2002). Un processo con un soluto cristallino potrebbe essere più efficiente perché le temperature di fusione eutettica sono solitamente superiori alle temperature di transizione vetrosa, consentendo

una temperatura del prodotto più elevata durante l'essiccazione primaria senza lo scioglimento/collasso della torta (Kasper e Friess, 2011). La scelta della T_n tra -5 °C e -10 °C è pressoché indifferente. Una T_n = -10 °C potrebbe consentire di utilizzare una P_n leggermente superiore, come visto dai risultati dell'esperimento 2, riducendo il rischio di blow up. Inducendo la nucleazione a temperature più elevate, si producono cristalli di ghiaccio più grandi che, da un lato, accelerano l'essiccazione primaria per la minore resistenza al flusso di vapore e, dall'altro, riducono l'area specifica del prodotto liofilizzato causando un rallentamento della fase di desorbimento (Oddone *et al*., 2017).

Nella Figura 4.1, da sinistra a destra, sono presentati i prodotti ottenuti dalla liofilizzazione di 5% w/w saccarosio in flaconi non trattati, 5% w/w di saccarosio in flaconi siliconati e 5% w/w di saccarosio + 0,02% w/v Tween 80 degassato in flaconi siliconati. I prodotti ottenuti da soluzioni non degassate hanno mostrato difetti sulla superficie della cake dovuti a bubbling e/o ebollizione. Nei flaconi non trattati, a causa delle buone interazioni tra vetro e soluzione vi è la presenza di prodotto adeso alla superficie laterale del flacone e la curvatura della superficie della cake è convessa. Nei flaconi siliconati il rivestimento interno idrofobico è resistente a legami aspecifici, quindi sono ridotte le perdite di campione causate da questo tipo di interazioni con il contenitore. Il prodotto ottenuto da flaconi siliconati non è aderente alle superfici laterali del contenitore e la superficie delle cakes ha una curvatura concava. Il fenomeno del blow up è assente nei flaconi non trattati grazie al buon attrito tra la cake e le pareti del flacone, mentre è presente in quelli siliconati in assenza di degassificazione. L'eliminazione del bubbling, grazie al degassaggio, unitamente al lento abbassamento della pressione nella camera del liofilizzatore, dovuto all'elevato numero di flaconi, ha evitato il blow up nei flaconi siliconati riempiti con 5% w/w di saccarosio + 0,02% w/v Tween 80.

Figura 4.1: Da sinistra a destra l'immagine mostra il prodotto ottenuto dalla liofilizzazione di 5% w/w saccarosio in flaconi non trattati, 5% w/w saccarosio in flaconi siliconatati e 5% w/w saccarosio + 0,02% w/v Tween 80 degassata in flaconi siliconati.

Quindi, i flaconi siliconati riempiti con 5% w/w di saccarosio + 0,02% w/v Tween 80 e degassati sono stati la migliore combinazione trovata per eseguire la nucleazione controllata in flaconi aventi superficie interna idrofoba ottenendo un prodotto con eccellente morfologia mediante liofilizzazione.

L'ebollizione in flaconi siliconati o TopLyo® è stata eliminata grazie all'utilizzo del tensioattivo non ionico Tween 80 ad una concentrazione superiore alla sua CMC. Tensioattivi di questo tipo sono comunemente presenti nei farmaci dove svolgono la funzione di protezione della proteina da aggregazione, adsorbimento superficiale e/o precipitazione. Pertanto, queste soluzioni possono essere sottoposte a VISF, dopo il degassamento, senza l'aggiunta di altri componenti.

1. Introduction

1.1 Importance of Lyophilization

Lyophilization, or freeze-drying, is a process used in the pharmaceutical industry, but not only, to remove the solvent (water or other) from a drug without damaging the molecular structure of the active substance, therefore working at low temperature and pressure. In fact, molecular structures are often very sensitive to thermal gradients and if the temperature at which the product is heated is excessively high will be obtained unacceptable results. The goal of freeze-drying is to guarantee a sufficient long shelf life of proteins and this can often only be obtained by bringing them in solid form. In the solid state, in fact, the degradation reactions are inhibited or sufficiently slowed down ensuring long-term stability. Another advantage of solid products over liquid product is greater ease of handling in storage and shipping. Despite this, the freeze-drying process can also generate various stresses that can denature the protein. At the end of the treatment, a porous and friable solid will be obtained which can be easily and quickly rehydrated to obtain again the starting solution with the same properties. Another non-secondary aspect of freeze-drying is the possibility of avoiding contamination from the external environment and therefore working in conditions of sterility.

To date, around 50% of biopharmaceuticals are obtained by freeze-drying (Kasper and Friess, 2011). Although it requires very long times and the investment costs, both fixed and operational, are very high, freeze-drying is therefore the most used technique. An optimal choice of equipment, processes and service conditions is essential to make it usable on a large scale.

1.1.1 Historical Background

The history of freeze-drying can be roughly contained in the 20th century. In reality, centuries before, the Incas used the sun's energy to dry frozen meat, moreover this civilization developed in the Andes at high altitudes where the atmosphere can begin to be considered partially rarefied. Returning to more recent history in 1890 Altmann reported having managed to remove water from frozen tissues in order to produce histological sections (Altmann, 1890).

In 1906 Bordas and d'Arsonval at the Académie des Sciences in Paris showed for the first time that it was possible to moderately reduce the aqueous content of a delicate product in the frozen state using a partial vacuum. The authors also reported that the same technique could have been used to prolong the storage of serums and vaccines (Bordas and d'Ansonval, 1906).

The first patent regarding freeze-drying was filed by Tival in 1927, but commercially the first implications were in 1935 thanks to Flosdorf and Mudd which, in addition to studying freezing, also gave the name lyophilization (Flosford and Mudd, 1935; Flosdorf, 1949). The term derives from the Greek in which it means "love the solvent", this is due to the ability of the product obtained to regain its original characteristics if placed in contact with water. In the 1940s Flosdorf from America (Flosford *et al*., 1940) and Greaves from England (Greaves, 1946) created, for war purposes, plants to produce dried plasma.

Over the next 50 years, despite the limits given by the costs of freezing and the subsequent sublimation, enormous progress has been made. The fields most attracted by freeze-drying were the food and pharmaceutical ones. The food industry was interested by the possibility of storing food at room temperature in a time in which the freezers were not yet in every home. The pharmaceutical industry was the one that benefited the most from the technology and still guides its development today.

There has been various progress in the second half of the last century that is worth mentioning. Ernst Chain has been the first to use the freeze dryer to produce antibiotics and sensitive biochemicals. Isidore Gersh, Tokio Nei and Fritjof Sjøstrand obtained electron microscope images of biological structures with specimens prepared by freeze-drying. Charles Merieux achieved important results for the industrial production of vaccines and serums, moreover he found a bone bank in which the US Navy Medical Corps invested heavily. Basilio Luyet, Alan Parkes, Audrey Smith, Harry Meryman, Christopher Polge, Peter Mazur and others have been very important in the field of cryobiology (Rey and May, 2004).

To nowadays, investments continue to be made to improve the quality and reduce the costs of freeze-dried products and this process has become a leader in the conservation of sensitive products at environmental conditions.

1.2 Principles of Freezing

The freeze-drying process consists of three phases: freezing, primary drying and secondary drying. During freezing, the solvent will separate from the solute turning into ice. Cooling the water, which in the initial state is at room temperature, it does not freeze at the equilibrium freezing temperature (0 °C) but continues to be liquid even below this threshold. This phenomenon is called supercooling. Super-cooling is closely related to the composition of the solution and the freezing method (Kumar *et al.*, 2008). In the ideal case of cooling water without any impurities, it will freeze at -48 °C (Kawasaki *et al*., 2018). The degree of supercooling therefore depends on the degree of purity of the water and the freezing conditions.

The temperature profile of a pharmaceutical solution during freezing is shown in Figure 1.1. In the first step AB the solution is cooled until the nucleation of the ice in B. The nucleation phenomenon is exothermic, and this entails an increase in temperature in the step BC. The formed ice crystals then begin to grow (CD), at an almost constant temperature, by cryoconcentrating the solution. When solidification is completed (D) the solution is further cooled (DE).

Therefore, nucleation and crystal growth are the two phases identified in the ice crystallization.

Ice nucleation is a stochastic phenomenon that leads to the formation of crystals. The morphology and size of these crystals are of great importance in the freeze-drying process. The concentration fluctuations that derive from the Brownian motion of the super cooled liquid water can form clusters with persistent hydrogen bonds (Matsumoto et al., 2002). If nucleation occurs spontaneously, it is called homogeneous nucleation, while if artificially induced, it is called heterogeneous nucleation. Nucleation can also be divided into primary and secondary nucleation. Primary nucleation occurs in systems where solution crystals are not already present; it can be homogeneous or heterogeneous if induced by foreign particles. Secondary nucleation is only of a heterogeneous type and occurs when crystals such as those that will be formed are already present in the solution.

In homogeneous nucleation, the overall excess free energy, ΔG, is equal to the sum of the excess surface free energy, ΔG_S, and the excess volume free energy, ΔG_V. ΔG_S and ΔG_V have opposite effects on the system and depend differently on the radius of the spherical nuclei r. From Figure 1.2 it can be seen that ΔG_S is a positive quantity, proportional to r^2; while ΔG_V is a negative quantity, proportional to r^3 (Helt, 1976). Always from figure 1.2 it can be observed how the free energy of formation ΔG passes through a maximum value ΔG_{CRIT}, which corresponds to a critical dimension of the core r_c which is the minimum size for which a formed nucleus is stable. From this it is possible to deduce that if a particle has a radius smaller than

the critical one it will dissolve because it's the only way in which can it reduce its free energy. While if a particle has a radius greater than the critical one it will continue to grow by reducing its free energy.

At about -40°C the pure water sample will contain at least one spontaneously water nucleus by which can start the ice crystal growth (Kasper and Friess, 2011). However, for such nucleation to occur there must be no impurities in the solution, which is very difficult.

Most primary type nucleation, including that which occurs in all pharmaceutical solutions, is heterogeneous nucleation. Water adsorbs on foreign impurities creating clusters at degrees of supercooling lower than those of homogeneous nucleation. The impurities can be of various type, such as contaminants in water, sites on proteins, or also the surface of the container (Kasper and Friess, 2011).

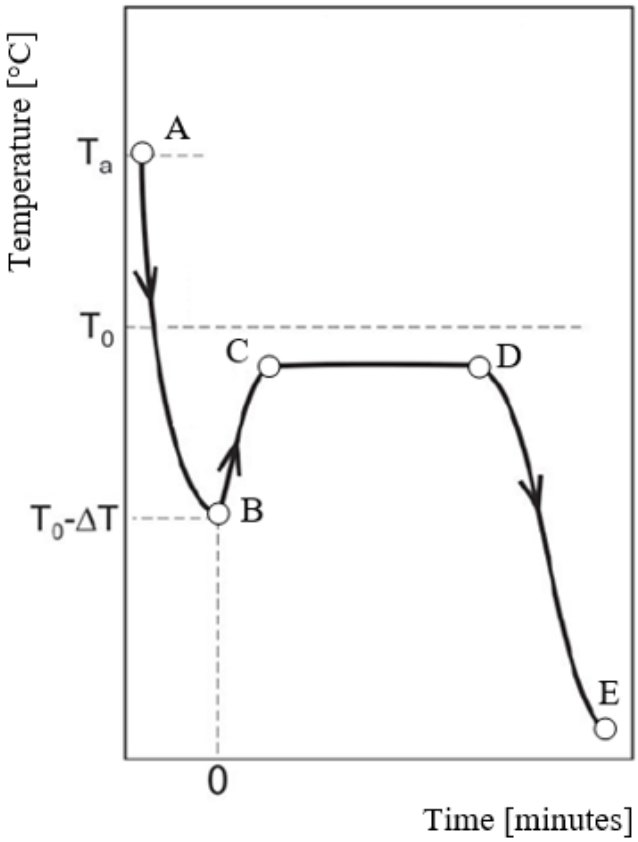

Figure 1.1: Temperature profile of a pharmaceutical solution during freezing. The cooling process starts by ambient temperature T_a to the crystallization temperature T_0-ΔT. The temperature raises because of the exothermic process of solidification till near the equilibrium freezing temperature T_0 and after drop down another time thanks a further cooling. Figure taken from Fan et al., 2018 with modification.

Following nucleation, crystal grow occurs during which water molecules from the increasingly cryoconcentrated solution are added to the nuclei formed. Freezing is not instantaneous because the supercooled solution can absorb 15 cal g^{-1} while the heat released by the solidification process is equal to 79 cal g^{-1} (Lide *et al.*, 2018). A balance is therefore created between the increase in temperature during crystallization and the removal of heat with consequent constant temperature. Once solidification is complete, the temperature decreases

(Fissore *et al.*, 2019). Crystallization at constant temperature and the subsequent decrease in temperature can be observed respectively in the CD and DE sections in Figure 1.1.

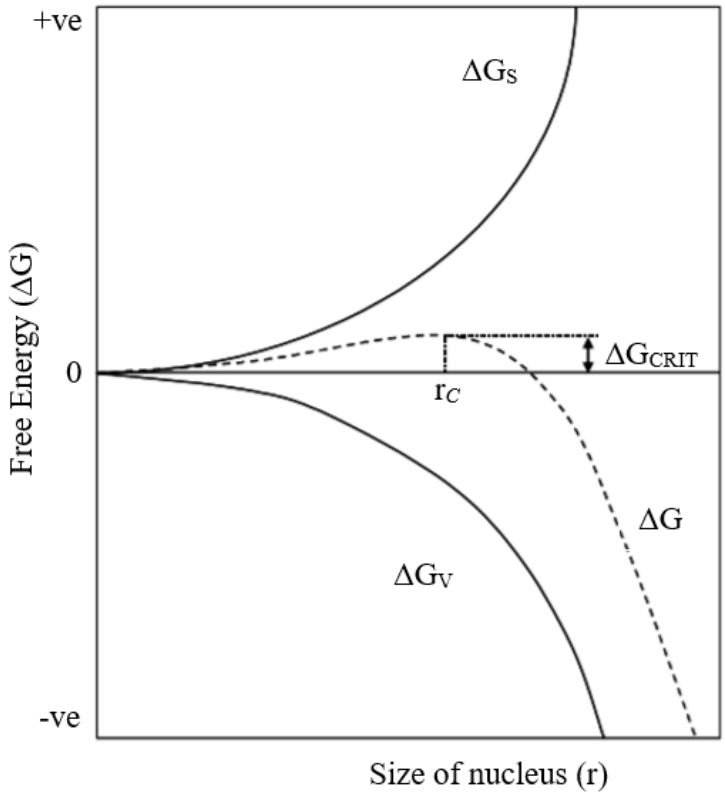

Figure 1.2: Free energy diagram for the nucleation of spherical nuclei. Figure taken from Helt, 1976 with modification.

The number of ice crystals, their size and the rate of ice growth depend on the freezing process, more particularly on the nucleation temperature and the cooling rate. A low cooling rate and/or a high nucleation temperature promote the formation of a few nuclei which will therefore create large ice crystals. Instead, a high cooling rate and/or a low nucleation temperature promote the formation of many nuclei and consequently small ice crystals. Furthermore, freezing conditions are crucial for the development of various polymorphic forms for the crystallizing excipients such as mannitol (Pisano *et al.*, 2019).

The number of crystals formed, and their size will in turn determine the porosity of the freeze-dried cake (Rambhatla *et al.*, 2004). The freezing phase is therefore very important because it is responsible for both within-batch and the within-product variability.

1.3 Freezing Methods for Lyophilization

The supercooling effect obtained on the sample depends on the freezing methods adopted. There are various types of freezing methods, such as liquid nitrogen freezing, loading vials onto precooled shelves, or ramped cooling on the shelves.

Two basic freezing mechanisms can be distinguished (Searles *et al.*, 2001a):

- global supercooling: the supercooling level is almost the same in the entire volume of the liquid, which is generally the case for shelf-ramped freezing;
- local supercooling or directional solidification: only a small volume of the liquid is supercooled, which is the case with high cooling rates, for example with nitrogen immersion.

In the first mechanism, solidification proceeds through the already nucleated volume, in contrast, in the second, the nucleation and solidification fronts are very close in space and time and move further into a non-nucleated solution (Kasper and Friess, 2011). In local supercooling, higher cooling rates result in faster freezing rate (Rey and May, 2004).

1.3.1 Conventional Freezing

The first step of a conventional freeze-drying cycle consists in inserting in the vials a given volume of solution, partially stoppering and placing them on the temperature-controlled shelves of the freeze-dryier. If the solution contains highly volatile organic solvents or active pharmaceutical ingredients which are very unstable at room temperature these steps can be performed at a temperature lower than the ambient temperature, such as 5-10 °C (Fissore *et al.*, 2019). There is, therefore, the cooling process whose duration, final temperature and time for which this temperature is maintained are sought in such a way as to obtain the complete solidification of the vials. The final temperature must be lower than T_g' for non-crystalline excipient or lower than T_{eu} for crystalline materials. By monitoring the cooling rate, the morphology of the ice and subsequently the drying performance are controlled. The range of usable cooling rates is limited and the maximum value lower than 2 °C min^{-1} (Fissore *et al.*, 2019). Studies regarding holding time have shown that if the height of the solution in the vials is less than 1cm then 1 hour is enough, while if the height exceeds this value the minimum time is 2 hours (Tang and Pikal, 2004). High cooling rates promote the formation of small nuclei which, however, are to be avoided in the steps following freezing. However, too low cooling rates are not acceptable if the formulation is prone to phase separation, especially if stabilizers are present (Heller *et al.*, 1999a). A cooling rate lower than 0.5 °C min^{-1} allows proteins and stabilizers to separate with the consequent loss of the stabilizing effect (Heller *et al.*, 1999b). A recommended compromise value for the cooling rate is around 1 °C min^{-1} (Tang and Pikal, 2004).

The lack of control of the degree of supercooling, on which the performance of the process and product quality depend, is the main limit of the conventional method of freezing. (Fissore *et al.*, 2019).

1.3.2 Quench Freezing

The first step of the quench freezing consists in immersing the vials in a cryogenic fluid (liquid nitrogen, dry ice / acetone, dry ice / ethanol) for a time long enough to have its complete solidification (Snell and Cloudman, 1943). The vials are then placed on precooled shelves and freeze-dried. Such rapid cooling produces very small ice crystals.

In order to monitor the extend of supercooling, Zhou has developed a system to control the nucleation temperature and the freezing rate. The vials are placed between two porous metal plates in the cooling chamber. The upper plate has the function of removing the heated cryogen

after contact with the vials. The cooling rate and nucleation temperature depend on the temperature and pressure of the cryogen (Zhou *et al.*, 2014). Currently this method is not used in freeze-drying because it is hardly scalable on a product unit, however the developments introduced by Zhou solve this limitation making practical applications possible (Fissore *et al.*, 2019).

1.3.3 Precooled Shelf Method

The first step in the precooled shelf method is the cooling of the shelves to very low temperatures, such as -40 °C. Only later the vials are loaded on the shelves. In order to prevent the condensation of moist air on the surface of the shelves, the freezing chamber is weakly pressurized with anhydrous nitrogen (Passot *et al*., 2009, Nakagawa *et al*., 2006). The freezing rate depends on the geometry of the vials and their filling volume. Despite the procedure followed in the precooled shelf method, studies have found that loading at very low temperature does not improve the distribution of nucleation temperature (Jiang and Nail, 1998).

1.3.4 Annealing

In order to control the resistance of the product and the drying rate is necessary a minimal variation of the nucleation temperature. Often, moreover, if the cooling is very quick, the freeze-drying concentration process is not completed causing the deformation of the original microstructures of the frozen system during the removal of the water (Pisano *et al.*, 2019).

Annealing is a treatment used during the freezing phase to overcome the ice nucleation heterogeneity and complete the freeze-concentration.

Following the nucleation of the ice in the samples and the lowering the of temperature to -40 °C to favour complete solidification, the temperature of the shelves is increased to a value higher than the glass transition temperature (T_g') of the solution but below the onset of ice melt. As a result of this part of the ice formed begins to melt increasing the molecular mobility of the glass phase which tends to a lower free energy state. Ice crystals larger than a critical size are formed at the expense of the smaller ones. The phenomenon described is identified with the name of Ostwald ripening (Patel *et al.*, 2009). The speed with which the ice melts is inversely proportional to the size of the crystals. By lowering the temperature, the crystals already present will act as a nucleation site during recrystallization inhibiting the formation of new small crystals. Therefore, the annealing treatment produces a frozen structure in which the crystals have a bigger minimum size compared to the absence of this treatment (Fissore *et al.*, 2010).

Thus, annealing can drastically reduce the differences in pore size, pore structure and drying behaviour caused by variations in the degree of supercooling. (Arsiccio *et al.*, 2018a, Rambhatla *et al.*, 2004, Fonte *et al.*, 2016).

The disadvantages of this treatment are the additional times required and the uselessness in case of systems susceptible to phase separation, buffer crystallization, interfacial degradation, or degradation when kept above T_g' (Patel *et al.*, 2009). Furthermore, as the average pore size increases, the product specific surface area is reduced causing also a decrease in the water desorption rate in secondary drying. This may lead to increased residual moisture content in the final product or demand longer secondary drying (Tang and Pikal, 2004).

1.4. Nucleation Temperature Controls

While most of the conventional freezing protocols allow control of the cooling rate, the nucleation temperature remains a stochastic variable, randomly distributed within the batch (Pisano *et al.*, 2019). The nature of the nucleation event is random both as regards the instant and the temperature at which the nucleation occurs (Oddone *et al.*, 2014). This is regarded as a demerit because it leads to large vial to-vial and batch-to-batch variability which are in contrast with the stringent requirements of the pharmaceutical industry in terms of process control and product quality (Pisano *et al.*, 2019). Specifically, the nucleation temperature defines size, number and morphology of ice crystals and thus the drying behaviour on which depends the product stability (Oddone *et al.*, 2020).

It is not currently possible to control nucleation; however, efforts are made to make it as uniform as possible over a batch of vials. To do this, nucleation is forced to take place at a given temperature and the batch temperature is maintained until the nucleation process is completed (Barresi and Pisano, 2018).

Controlled nucleation technology should meet a series of prerequisites (Fissore *et al.*, 2019):

- nucleation occurs with the freezing of the solution regardless of the size of the freeze dryer, the geometry of the vials, the type of stoppers, the formulation and the filling volume;
- nucleation occurs in all vials of the batch in a narrow temperature and time range to minimize vial-to-vial variability;
- nucleation can be easily replicated to minimize batch-to-batch variability;
- the equipment can effectively perform the freezing conditions used in controlled nucleation;
- the process is easily scalable from the laboratory to the production units;
- it does not alter the aseptic conditions of the process;
- it does not affect or alter the qualities of the final product.

Several methods have been proposed to control nucleation.

1.4.1 Nucleating Agents

The addition of impurities to the sample being frozen may act as ice nucleating agents helping to increase the nucleation temperature (Pisano *et al.*, 2019). Ice-nucleating agents (INAs) are mineral dust kaolinite, silver iodide, and bacterium *Pseudomonas syringae*.

INA particles induce ice nucleation in a heterogeneous way because the microscopic structure of their surface resembles the crystalline structure of ice. For example, silver iodide particles can induce freezing of pure water at temperatures down to -4 °C thanks to the fact that they have the same unit cell size as ice crystals. Furthermore, another factor contributing to increase the nucleation temperature is the highly hydrophilic surface of the INA particles. The best characterized bacterial strain that acts as a biological ice nucleator is *Pseudomonas syringae* (Weng *et al.*, 2018).

The main advantage of INAs is the ability to start ice formation heterogeneously without manual or instrumental interruptions. Concerns that arise from the use of INA in biological systems include their biocompatibility, degradability, toxicity, recovery, lack of consistency, cumbersome process if working with many samples and ease of use. Another disadvantage of

producing bacterial hydrogel microspheres is having to maintain the bacterial culture (Weng *et al.*, 2018). The addition of nucleating agents in large-scale units is hardly compatible with the regulatory requirements of pharmaceutical products (Fissore *et al.*, 2019).

1.4.2 Electro-Freezing

The earliest methods proposed to control nucleation was electrofreezing which uses a high-voltage pulse to generate an ice nucleus on a platinum electrode, that afterward initiates ice crystallization. (Oddone *et al.*, 2020)

Scientists have tried to explain the basic mechanism of electrofreezing experimentally and theoretically, but it is still controversial today. Experiments show that the basic mechanism of electrofreezing includes processes dependent on the intensity of the electric field such as the formation of bubbles and their collapse, the influence of the structural and dynamic properties of water and the formation of hydrated metal ion complexes. There is a direct beneficial influence of the electric field on the formation of the nucleus (Petersen *et al*., 2006).

Petersen *et al*. were the first to use this method to control nucleation. The set-up procedure involved balancing the sample at a given temperature to which an electric impulse of 4.5 kV was applied and then the samples were cooled to -45 °C (Petersen *et al.*, 2006). Because of the presence of excipient makes this method less reproducible electrode caps were developed specifically to make the ice nuclei generation independent of the sample composition (Petersen *et al.*, 2006). In fact, additives can inhibit induced nucleation via electrofreezing.

Drawbacks are the need for individual electrodes in each sample and the direct contact between electrode and product which is not practical for good manufacturing practice product manufacture. (Oddone *et al.*, 2020). Moreover, the equipment required by this technique is expensive and diminishes its applicability in manufacturing (Oddone *et al.*, 2014). This method cannot be applied in large-scale units due to the limitations in the salt content of the solutions and the high voltage required to promote the formation of ice crystals (Fissore *et al.*, 2019).

1.4.3 Ultrasound-Induced Ice Nucleation

Ultrasonic vibrations can be used to induce ice nucleation in supercooled water thanks to an ultrasound transducer (Oddone *et al.*, 2020; Inada *et al.*, 2001). Although the detailed nucleation mechanisms of solid crystal from liquid solution are still controversial, bubble cavitation produced by ultrasound has been shown to be of fundamental importance in nucleus formation processes (Ohsaka and Trinh, 1998).

Power ultrasounds are acoustic waves between 20 and 100 kHz which induce the formation of cavitation bubbles. The collapse of these bubbles and the consequent microstreaming increase the transfer of mass and heat, influencing the nucleation of the ice. According to Hickling (Hickling, 1965) the increase in pressure due to the collapse of the cavitation bubble increases the equilibrium freezing temperature of the solution. This phenomenon simultaneously enhances the degree of supercooling which increases the number of nuclei (Pisano *et al.*, 2019). Hunt and Jackson (Hunt and Jackson, 1966) have instead proposed another model according to which nucleation is induced by depression following the collapse of the bubble. Furthermore, the movement of cavitation bubbles also plays a role in nucleation (Zhang *et al.*, 2003). Saclier *et al*. have proposed a theoretical model of ice nucleation induced by acoustic cavitation, starting from the Hickling theory, and have observed that the number of nuclei can be increased by lowering the temperature or increasing the acoustic pressure (Saclier *et al*., 2010). The presence of ice crystals of smaller dimensions on

the bottom of the vial than on the overlying part indicates that the formation of the first ice crystals takes place there. This suggests that the growth mechanisms of ice crystals are the same for ultrasound-nucleated samples and spontaneously nucleated samples. To reduce this intra-vial heterogeneity, annealing treatments can be used (Nakagawa *et al.*, 2006).

The ultrasound technique is particularly interesting thanks to the possibility of application without contact, which makes this technique chemically non-invasive (Pisano *et al.*, 2019). On the opposite side there are concerns related to the high localized temperatures generated by cavitation which can potentially damage or favour the aggregation of very sensitive products (Pisano *et al.*, 2019). The main problems of this technique are related to the difficulty of effectively propagating ultrasonic waves and the scalability of the process that makes the optimal ultrasonic frequency vary (Barresi and Pisano, 2018). In addition, expensive equipment is required for ultrasound-induced ice nucleation and this hinders its applicability in production (Oddone *et al.*, 2020).

1.4.4 Depressurization Method

The depressurization method involves pressurization at about 1,5-4,5 bar and subsequent rapid depressurization inside the chamber (Oddone *et al.*, 2014). This initiates nucleation in the samples, previously equilibrated at a temperature below the equilibrium freezing point (Pisano *et al*., 2019). Then the nucleated vials are cooled to the final shelf temperature which can be -40 °C or lower. The effectiveness of the method varies with the type of gas used to pressurize, the most effective being argon (Kostantinidis *et al.*, 2011).

Despite exists many theories that try to explain how depressurization induces nucleation the mechanism is still controversial. Gasteyer proposed three main mechanisms (Gasteyer *et al.*, 2017). In the first one the initial high pressure increases the concentration of dissolved gas in the liquid; these gases are then quickly released thanks to the depressurization forming bubbles that initiates the nucleation. In the second one the evaporation induced by the depressurization decreases the surface temperature of the liquid triggering the nucleation. In the last one the cold vapours produced by the depressurization freeze particles on the surface which act as a nucleation site. Differently, Geidobler and Winter identified mechanical vibrations (pressure waves) generated by rapid depressurization as responsible for the nucleation (Geidobler and Winter, 2013).

The main advantage of the depressurization method are that is easily scalable, can allow aseptic conditions and does not add nothing to the lyophilized product. This approach, however, requires freeze-dryer designed to withstand the high pressure and this equipment-adaptation is very cost-intensive (Geidobler and Winter, 2013).

1.4.5 Ice-Fog Techniques

The ice fog technique, to nucleate samples at a selected temperature, was suggested by T. W. Rowe in 1990 and applied to freeze-drying for the first time by Rambhatla *et al*. in 2004. The model proposed by T.W Rowe is composed by a series of step:

1. The vials are brought to the temperature at which nucleation is desired.
2. Nitrogen gas is introduced into the humid drying chamber, at a pressure of 10 psig, forming a dense ice fog that seeds the crystallization of ice (Rambhatla *et al.*, 2004). The ice crystals enter the vials because of the slight increase in pressure promoting the nucleation of the solution (Mason and Ludlam, 1951).

3. The vials are cooled down to -45°C.

To be cooled down nitrogen gas is passed, at elevated pressure, through copper coils immersed in liquid nitrogen and then is introduced into the product chamber at a temperature lower than –40°C.

This approach can require more than 30 min to have the nucleation of all the vials enhancing vial-to-vial heterogeneity in terms of morphology of the samples and drying behaviour. In fact, a variable time allowed for Ostwald ripening may result in a non-uniform crystal structure in all the vials. Therefore, Rambhatla *et al*. introduced a new configuration in which a tube with uniformly punched holes was clamped above the shelf to allow a better distribution of the ice fog (Rambhatla *et al*., 2004). Moreover, the temperature of the nitrogen entering the chamber was reduced from -40°C to -50°C. These improvements enabled them to reduce the nucleation time span to 5 min (Rambhatla *et al*., 2004). However, annealing process still occurred in some of the vials that nucleated earlier than the others.

To further enhance the homogeneity of the batch Patel *et al.* proposed to partially depressurize the chamber (approximately to 66 mbar) before the introduction of the cold gas. The chamber was then isolated by closing the valve connecting the chamber and the condenser. Nitrogen gas was introduced into the chamber, pressure begins to increase, ice forms, and the ice fog is forced into the vials. When the chamber pressure was close to the atmospheric one, the isolation valve was quickly opened, and the ice fog pumped into the condenser (Patel *et al.*, 2009). The more uniform distribution of nitrogen in the drying chamber and the greater quantity of nitrogen introduced, thanks to the greater pressure difference between the cold hydrogen chamber and the drying chamber, led to a nucleation time of less than one minute (Assegehegn *et al.*, 2019). This combination of reduced pressure and ice fog, called Reduced Pressure Ice Fog Technique, favoured a more rapid and uniform freezing. However, under full-load conditions, due to higher thermal load, the shelf surface temperature needs to be colder than under partial load condition resulting in a longer drying time.

Some concern about this technique are related the possible contamination by extraneous material entering the vial and the use of liquid nitrogen which makes the process technical demanding and expensive (Pisano *et al.*, 2019).

Over the years many variations of the technique have been proposed. One of these, proposed by Demarco *et al*., involves the use of an ejector to generate the ice fog which is then effectively distributed throughout the drying chamber. To obtain the ice fog are mixed water, liquid nitrogen and the ice fog already circulating in the drying chamber (Demarco *et al.*, 2012).The advantages of the technique introduced by Demarco are nucleation in less than one minute, even on pilot scale units, and the guarantee of sterility.

Weija (Weija, 2012) and Geidobler *et al.* (Geidobler *et al.,* 2012) managed in developing two different processes to obtain an ice fog without the use of liquid nitrogen, thus avoiding all the complexity related to it.

1.4.6 Vacuum-Induced Surface Freezing

The easiest and cheapest way to precise control the nucleation temperature is the vacuum induced surface freezing, VISF. In fact, no hardware and additional equipment are required (Barresi and Pisano, 2018). Moreover, the sterility concerns are only related to sterilization of large valves required for rapid depressurization (Arsiccio *et al.*, 2018a).

The method, which has been proposed and patented (Sennhenn and Kramer, 2004) by Kramer *et al*. consist in lowering the pressure inside the dryer chamber during freezing.

The pressure drop causes a partial evaporation of the water, lowering the product temperature and promoting ice nucleation (Pisano *et al.*, 2019). The temperature and pressure profile characteristic of a VISF cycle are shown in Figure 1.3.

The basic steps of the method proposed are (Kramer *et al.*, 2002):

1. the vials are loaded onto the shelves at room temperature and atmospheric pressure;
2. the vials are cooled down at the fluid temperature T_n which must be above the spontaneously nucleation temperature;
3. the product is held for 1h at T_n in order to minimize the temperature gradients among the vials of the same batch and within the same vial volume;
4. once the temperature of the product reaches a steady-state value, the pressure inside the chamber is reduced and maintained as such for a time specific of the formulation used;
5. as soon as nucleation occurs in all the vials of the batch, atmospheric pressure is re-established to prevent losses due to water boiling;
6. the fluid temperature is decreased down to a value (T_m) below the eutectic temperature and held at this value for about 1 h to increase the size of the ice crystals;
7. the product is cooled down to a temperature between -40°C and -50 °C, following a ramp, to complete the freezing stage.

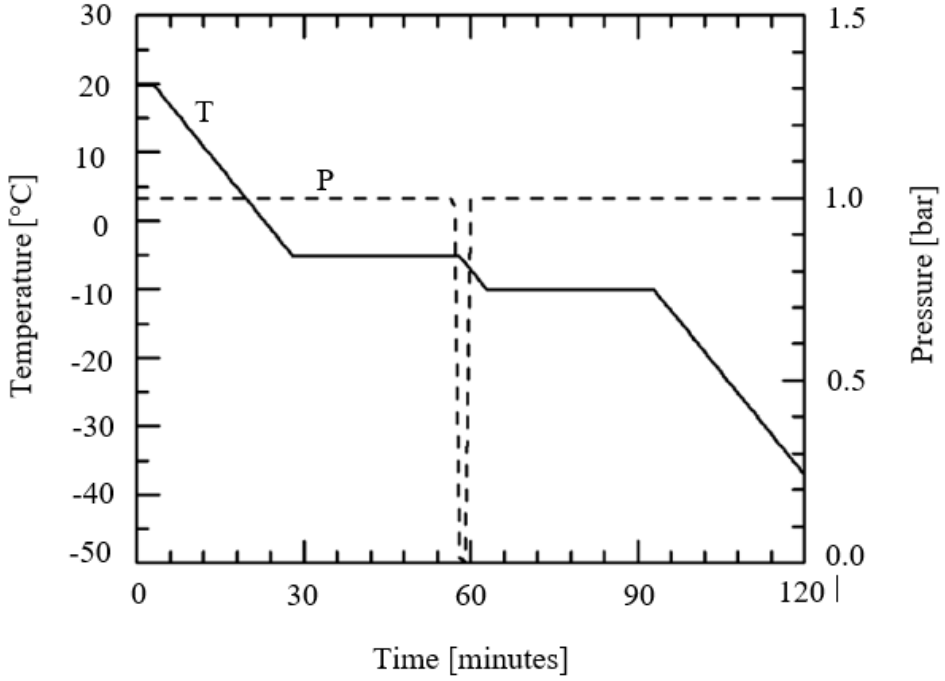

Figure 1.3: Temperature (solid line) and pressure (dashed line) profiles during VISF. Figure taken from Oddone *et al*., 2014 with modifications.

Kramer *et al*. chose 10 °C as the temperature at which to keep the liquid to be frozen for about an hour, however this value led to the formation of a layer of a few mm frozen on the surface while the underlying part freeze only when the shelves were brought to - 40/50 °C. To overcome this two-layer solidification Liu *et al*. chose to balance the solution at -10 °C for about an hour. This temperature continued to be above the spontaneous nucleation temperature but led to the freezing of the entire sample during the depressurization phase (Liu *et al*., 2005).

Because of the method introduced by Kramer *et al*. and validated by Liu *et al*. resulted in the formation of aesthetic defects within the cake structure, such as blow-up and flake formation (Pisano *et al*., 2019), Oddone *et al*. proposed some modification to the previous method solving these problems and producing an elegant cake.

The temperature of the fluid is held at the set point value during vacuum and is decreased only when atmospheric pressure is re-established. Moreover Oddone *et al*. introduced the isolation of the drying chamber from the condenser, once the desired value of vacuum is reached. This result is achieved shutting-off of the valve on the duct between the condenser and the drying chamber which can be identified in Figure 1.5.

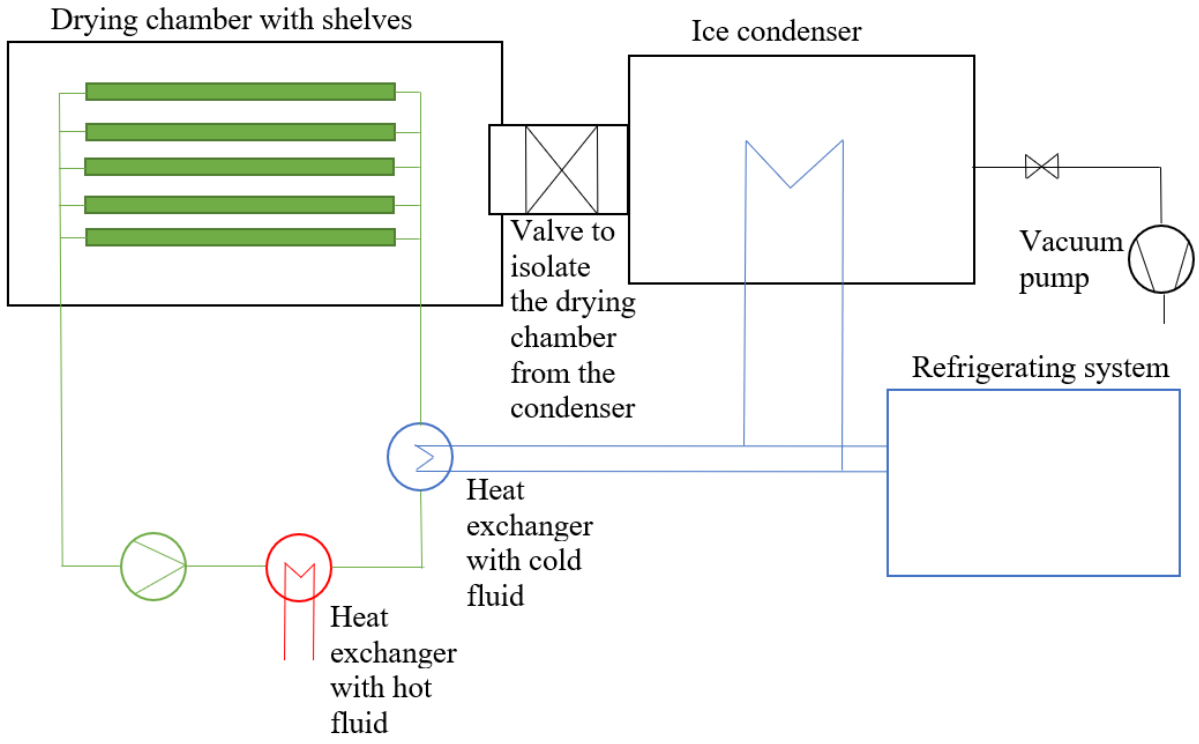

Figure 1.5: simplified configuration of a freeze-dryer. The solution to be freeze-dried is first inserted in vials and then loaded on the shelves of the drying chamber. To realize the manufacturing process the freeze dryer is composed by a vacuum-tight box (drying chamber), holding temperature-controlled shelves, connected by a valve to a condenser chamber, which contains refrigerated coils to trap the water during the drying process (Nireesha *et al*., 2013). The shelves in the drying chamber act as heat exchanger removing or supplying energy to the product thanks to the connection with the silicone oil system. The vacuum level required in the chamber is achieved thanks a vacuum pump.

Therefore, the pressure can increase within the freezing chamber during the vacuum period because of the accumulation of vapor released by the evaporation of the liquid (Oddone *et al*., 2014). Thanks to this the blow-out phenomena is reduced because the evaporation rate is slower. Generally, the optimal duration for vacuum is less than 1 min, at about 1-2 mbar

(Oddone *et al*., 2020). A longer time, such as 1,5 min can produce blow-up of the frozen cake and flake formation on the product surface, while a shorter time may not be enough to induce nucleation in all the vials of the batch (Oddone *et al*., 2014). Before the improvement of the VISF performances introduced by Oddone *et al*. 5 min was needed (Kramer et al., 2014).

A higher value of T_n shows wider variations in terms of pore sizing moving from the top surface of the cake toward the bottom of the container; while the lower T_n is, the more uniform the porous structure is (Oddone *et al.*, 2016).

Following the restoration of the ambient pressure heat is no more removed by water evaporation allowing the temperature of the product to rise, thus promoting the melting back of the ice just formed. If, as soon as atmospheric pressure is established, the fluid temperature is decreased to a value of T_m low enough the whole filling volume freezes when it is still able to rearrange its structure. This promotes the formation of large crystals and uniform batches that are not possible if T_m is not sufficiently low and the freezing happens when the temperature is finally decreased to - 40/50 °C with uncontrolled nucleation. (Oddone *et al.*, 2014)

An increase in the solid content can cause an irregular outgrowth of the crystal at the top surface of the product (Oddone *et al*., 2014).

Actually, with an accurate tuning of temperature, pressure and holding time of the different steps, the VISF technology is extremely effective and commercially available. In addition, the amount of gas dissolved in the solution should be the lowest possible because the degassing during pressure decrease is the main cause of aesthetic defects (Pisano *et al*., 2019).

1.5 Primary drying

During freezing most of the water is converted into ice and is thus available for sublimation during primary drying (Oddone *et al.*, 2017). The primary drying phase represents the majority of the freeze-drying cycle.

The rate of water removal during primary drying J_w through sublimation may be expressed in Equation 1.1 (Rambhatla *et al.*, 2004) as:

$$J_w = \frac{P_{ice} - P_w}{R_p} \tag{1.1}$$

where P_{ice} is the equilibrium vapor pressure of ice at the temperature of the frozen material, P_w is the partial pressure of water inside the chamber and R_p is the resistance of the dried product. The numerator P_{ice} - P_w represent the driving force of the sublimation. This requires that the pressure of the system where the product is being dried, must be less or near to the equilibrium vapor pressure of the frozen solvent. As the ice sublimates, the sublimation interface withdraws from the outside to the inside, forming a porous shell of dried material (cake). The water vapor produced by sublimation is transported by convection and diffusion through the cake, enters the vacuum chamber and finally collects on the condenser plate that must ensure enough surface area and cooling capacity. The temperature of the ice formed in the condenser must be less than that of the product, otherwise the water vapor will tend to return toward the product nullifying the drying process (Liapis and Bruttini, 1994). Typically, the temperature of the condenser coils ranges from -90 °C to -50 °C (Ganguly *et al*., 2010).

From equation 1.1 it can be seen that the rate of removal of the water vapor depends on the resistance of the product, which in turn reflects the way in which the initial solution was frozen. Rambhatla *et al*. found that the dimensions of the pores are inversely correlated to the size of the pores left after the sublimation of the ice crystals formed during freezing. This can be seen in Equation 1.2 (Rambhatla *et al.*, 2004),

$$R_p = \sqrt{\frac{\pi RT}{8M_w}} \frac{3\tau^2}{\varepsilon D_p} \quad (1.2)$$

where *R* is the ideal gas constant, *T* the vapor temperature in Kelvin, *Mw* is the molecular weight of water, ε the dried product's porosity, τ is linked to the pores' interconnectivity and Dp the average pores' size. τ usually is 1.5 (Pikal, 1999). Therefore, the mass transfer and consequently the primary drying rate depend on freezing.

As can be seen in Figure 1.5 the primary drying time decreases with the average pore size up to a limit value of the pore diameter, beyond which no longer varies. Since the curve reaches the asymptote the morphology of the product no longer influences the drying time, therefore the primary drying will no longer be mass transfer controlled but heat transfer controlled. The plateu indicates in fact the point at which the vapor pressure of ice equals the partial pressure of water inside the chamber cancelling the driving force of the sublimation (Franks and Auffret, 2007, Pisano *et al.*, 2011).

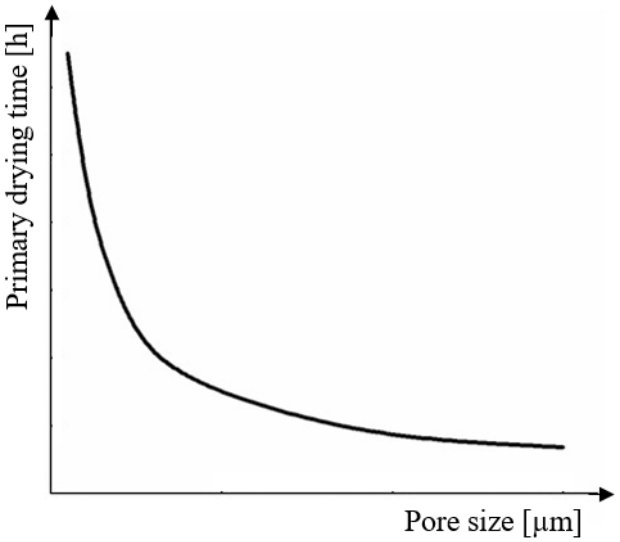

Figure 1.5: relationship between the primary drying time and the average pore size. Figure taken from Fissore *et al*., 2019 with modifications.

During primary drying, the surface temperature must not become too high due to the risk of thermal damage and must be kept below the melting/glass transition point. Therefore, the process can be (Liapis and Bruttini, 1994):

- heat transfer controlled if by increasing the temperature the temperature limit of the external surface is reached first, to further raise the drying speed the thermal conductivity of the dried layer must be increased;
- mass transfer controlled if the melting/glass transition temperature is reached first, to enhance the drying speed the effective diffusivity of the water vapor in the dried layer and therefore the total mass flow must be increased.

The product temperature should be kept as close as possible to the glass transition temperature to ensure a high drying efficiency; however, it does not have to overcome it to avoid product collapse, which will affect aesthetic and physic-chemical characteristics of the dried product.

The values of the effective diffusivity of water vapor in the dried layer and of the total mass flux, could be raised by decreasing the pressure in the drying chamber (Liapis and Bruttini, 1994).

During primary drying, the sublimation rate decreased with increasing chamber pressure and increased with increasing shelf temperature (Patel and Pikal, 2011).

The pressure can be controlled by introducing a non-condensable gas such as nitrogen into the vial chamber. Water vapor and non-condensable gas are forced to pass from the chamber to the condenser by pressure and concentration gradients. The condenser is connected to a vacuum pump for removing non-condensable gases. The typical range of pressures found in freeze drying systems ranges from 10 to 500 mtorr (Ganguly *et al.*, 2010).

Most controlled freezing technologies increase the nucleation temperature by increasing the primary drying rate (Searles *et al.*, 2001a). In the case of uncontrolled freezing the primary drying rate can be enhanced with an annealing treatment (Lu and Pikal, 2004).

When there is no longer a frozen layer and therefore sublimation interface, the primary drying phase ends (Liapis and Bruttini, 1994). Practically this happens when the product temperature approaches the shelf temperature.

1.6 Secondary drying

The remaining unfrozen water (sorbed or bound water), usually 15-20% wt/wt of solute (Rambhatla *et al.*, 2004), requires a secondary drying step (desorption step) for its removal. This step starts at the end of the primary drying. Non-frozen water could be absorbed on the solute surface, it could be in the solute phase as hydrated water and it could be in the solute phase dissolving in amorphous solid particles (Pikal *et al.*, 1990). The secondary drying is performed under vacuum at shelf temperatures that are higher than primary drying shelf temperatures. The shelf temperature must be increased gradually so as not to damage the lyophilized product (Pisano *et al.*, 2012). High shelf temperature can be used only if the product does not undergo undesired phenomena (Hancock and Zografi, 1994). The fact that the lowest pressure can speed up the desorption process has not been proven (Pikal *et al*., 1990).

The desorbed vapor is transported through the pores of the material being dried (Liapis and Bruttini, 1994). Smaller pore size increase both the resistance of the water vapor during primary drying both the specific surface area ensuring faster desorption during secondary drying (Rambhatla *et al*., 2004). It is possible to find this correlation in the Equation 1.3 (Rambhatla *et al*., 2004) assuming a capillary tube model:

$$SSA = \frac{4\varepsilon}{\rho_s(1-\varepsilon)D_p} \tag{1.3}$$

where ρ_s is the density of the solid and $(1-\varepsilon)$ is the solute concentration in volume fraction units. Therefore, SSA and degree of supercooling are directly proportional.

The rate of desorption is affected by the freezing protocol because it depends on the specific surface area and thus on the average pore size of the lyophilized product. The controlled freezing methods induce the nucleation at higher temperature than the conventional freezing, producing larger ice crystals that, on the one hand, speed up primary drying because of lower resistance to vapor flow and, on the other hand, reduce the specific area of the lyophilized product slowing down the desorption step (Oddone *et al.*, 2017). Oddone *et al*. observed that Vacuum Induced Nucleation follow this trend, but overall promotes a substantial reduction in the total drying time and improved vial-to-vial homogeneity in terms of final residual moisture.

This is true for both crystalline and amorphous solutes, but for the first ones the desorption is much faster in secondary drying (Oddone *et al.*, 2017).

The desorption process can be described by a first order mechanism presented in Equation 1.4 (Pikal *et al.*, 1990):

$$\begin{cases} \frac{dC_w}{dt} = -k_d(C_w - C^\circ) \\ C_w(t=0) = C_{w,0} \end{cases} \quad (1.4)$$

where $C_{w,0}$ is the residual moisture of the lyophilized product at the end of primary drying, C° is the equilibrium water content and k_d is the desorption rate constant. The model, initially proposed for an amorphous system, is adequate also for crystalline solutes (Pikal *et al.*, 1990). The residual humidity decreases until it reaches a plateau level. This value depends on the formulation and the secondary drying temperature, while it does not vary with the freezing protocol used (Oddone *et al.*, 2017).

Both overdrying, that promotes protein activity loss upon storage, and high values of residual moisture, that speed up protein degradation over time should be avoided (Pikal, 1994; Pisano *et al.*, 2013).

1.7 Morphology of the Lyophilized product, Intra-Vial Heterogeneity and Vial-to-Vial Heterogeneity

The product morphology depends by the cooling rate and the nucleation temperature. Within the solution the growth of the ice crystals around the nuclei can occur in different ways depending on the grow rate which in turns depends on the degree of supercooling (Petzold and Aguilera, 2009):

- if time is enough the molecules organize themselves in hexagonal crystals called dendrites;
- if the growth rate of the molecules is greater the water molecules are incorporated into the starting nucleus randomly to form ‘‘irregular dendrites’’;
- at even higher growth rates from the crystallization centre are formed many ice spears without side branches, these structures are called spherulites.

Higher is the degree of supercooling more ice crystals of small size are formed (Pikal *et al*., 2002; Pisano and Capozzi, 2017). Regarding the influence of the freezing mechanism on the ice morphology global solidification leads to spherulitic ice crystals, while directional solidification results in directional lamellar morphologies with connected pores (Searles *et al*., 2001a). Moreover, some solutes at high concentrations lead to a depression of the freezing point of the solution resulting in faster ice nucleation according to Raoult's Law (Nail *et al*., 2002).

If the cooling rate is low the ice crystal size is determined by the ice nucleation temperature (Morris *et al*., 2004). As aforementioned controlled nucleation, consequently higher nucleation temperature (low supercooling), lead to the formation of larger ice crystals and enhanced lyophilized cake uniformity respect to the conventional shelf-ramped freezing (Hottot *et al*., 2007). In particular, the vacuum induced nucleation thanks to the vacuum and the reduction in the shelf temperature promoted the growth of dendritic ice crystals, resulting in the formation of long, chimney-like ice crystals (Oddone *et al*., 2014). Larger crystals upon sublimation leave larger pores. A less compact structure has a lower mass transfer resistance, which facilitate water vapor diffusion, and a smaller ice freeze concentrate interface (Oddone *et al*., 2020). The first one lead to a reduction in the primary drying time thanks to a faster

sublimation (Pikal, 2001; Kochs *et al*., 1991; Fissore and Pisano, 2015) and a slower desorption, while the second one to an improve in the stability of sensitive products (Pisano *et al*., 2019). The controlled nucleation not only increased the mass flow rate with respect to spontaneous nucleation, but also decreased the mass flow rate variability (Scutellà *et al*., 2018). However, in case of controlled nucleation the moisture content during drying is higher because of a lower desorption rate; bigger pore means lower SSA (Oddone *et al.*, 2020). Whereas a high supercooling results in many small crystals, large SSA, and thus slow primary drying but fast secondary drying.

The factors on which the within-product (intra-vial) homogeneity mostly depends are T_n and the filling volume; T_m only becomes important if it is high enough to cause the melting back of the frozen solution (Oddone *et al*., 2016). In case of high filling volume large pores and a dendritic structure are observed in the central part of the cake, while spherical and smaller pores are present close to top and bottom of the cake. This happens because, thanks to the pressure reduction, only the upper part of the product freezes and the still liquid lower part will freeze later. Therefore, smaller filling volume lead to more uniform internal structure. Regarding T_n a value not low enough causes a morphology of the cake like which of a high filling volume because it promotes the freezing only of a thin layer of ice at the top surface of the product, while the remaining liquid will freeze with the following temperature decrease (Oddone *et al*., 2015). Therefore, at the bottom of the cake the pores are smaller due to the larger temperature gradients given by the contact with the shelf (Oddone *et al*., 2016). Moreover, the presence of cryoconcentration effects at the top of the cake promote the formation of smaller ice crystals (Oddone *et al*., 2020).

Even, in case of amorphous solutions the controlled nucleation promoted the formation of bigger ice crystals in comparison with an uncontrolled cycle, but the differences are less relevant.

The freezing conditions can influence the morphology of crystalline excipients. For example, mannitol after drying can be present either as an amorphous product or as three different crystalline forms (α, β, δ) which have different thermodynamic stability and have different impact on the stability of the product during its storage (Cao *et al*., 2006; Liao *et al*., 2007). In fact, at the end of the freeze-drying process the matrix formed by the excipients must be stable over time in order not to destabilize the active pharmaceutical ingredients immobilized in it (Pisano *et al*., 2019). The desirable thermodynamically stable form of mannitol is the β form, while the α and δ ones are both metastable. High freezing rates promote the formation of amorphous mannitol which over the time transforms in one of the metastable forms. Instead, freezing rates below 2°C min^{-1} produce crystalline mannitol which vary in the polymorph composition depending on the process conditions (Cavatur *et al*., 2002). As concerns VISF Oddone *et al*. found that if the nucleation is induced at a temperature of -5°C, or higher, promote a mixture of δ (predominant) and α forms (minor), while if the nucleation is induced at a lower temperature generates only β form. The addition of an annealing step promotes the formation of the stable β-form (Oddone *et al*., 2016). Controlling the freezing condition is, also, possible to avoid the vial breaking phenomenon. The vials break happens when metastable forms generate during freezing convert into a stable one (Williams and Dean, 1991; Williams *et al*., 1986).

The temperature profile during the sublimation step is important in determining qualities of the dried cake like the reconstruction time and the moisture content (Pikal and Shah, 1990; Patel *et al*., 2017). To optimize the primary drying phase, but still avoiding the collapse of the dry porous structure, the sublimation temperature must be close to the collapse temperature T_c (e.g., glass transition temperature for amorphous product), but always lower than it (Johnson,

2011). During sublimation the lower part of the cake is the most probable to be subjected to shrinkage due to the higher temperature than the rest of the sample (Passot *et al*., 2009). A collapsed cake loses its aesthetic properties and has a higher moisture content that can damage the active ingredients (Pisano *et al*., 2019).

Furthermore, respect to the uncontrolled freezing, the controlled nucleation lead to more uniform batches (Oddone *et al*., 2014). The inter vial variability causes heterogeneous behaviour during drying because of difference from vial to vial in the heat transfer rate and the mass transfer resistance to vapor flow in the dried layer (Searles *et al*., 2011). One of the main causes of inter-vial variance is the radiation effect from chamber walls (Gan *et al*., 2005; Oetjen and Haseley, 2004): there is an increase in the sublimation rate close to the chamber walls. Also, the position of the condenser duct influences the inter-vial variability: close to the condenser duct the pressure drop across each shelf decreases. The radiation contribution from the chamber walls is more relevant in small scale apparatus, while the pressure drop across the shelves is proportional to the shelf dimension (Barresi *et al*., 2010). Another factor that can affect the drying time of the vials, and so the variability of the batch, is the addition of an inert gas to control the pressure because it can affects the equilibrium temperature and the local partial pressure of water by which depends the driving force for the mass transfer (Barresi *et al*., 2010).

The annealing treatment can reduce the intra-vial heterogeneity and promote the growth of bigger ice crystals but has no effect on the homogeneity of the batch (Oddone *et al*., 2016). This technique, however, tend to prolong the reconstruction time (Webb *et al*.,2003). Nevertheless, it is difficult to identify a general trend about reconstruction time because this also depends on a combination of pore size and specific surface area (Kasper and Friess, 2011).

1.8 Activity and Stability of Lyophilized Proteins

The freeze-drying process generates numerous stresses, which can lead to the loss of biopharmaceutical activity with the disruption of secondary and tertiary structure of the protein or the formation of aggregates (Wang, 2000). The biological activity depends on the 3D conformation of the protein which may be easily lost because of:

- exposure to high or low temperature;
- solute concentration;
- change in ionic strength;
- presence of interfaces;
- pH shifts;
- phase separations;
- removal of the protein hydration shell.

Cold denaturation can occur if the product is subjected to low temperatures during freezing. Denaturation is due to the exposure of the hydrophobic core of the protein to the solvent since the solubility of non-polar groups in water increases with decreasing temperature (Jaenicke, 1990; Privalov, 1990; Franks, 1995; Graziano *et al*., 1997; Lopez *et al*., 2008; Matysiak *et al*., 2012). However, the impact of cold denaturation on freeze-drying is minimal both because it usually occurs at temperatures lower than those reached during freezing and because it is very slow compared to the duration of freeze-drying (Bhatnagar *et al*., 2007; Tang and Pikal, 2005). The function that describes the protein's free energy of unfolding has a

parabolic trend, therefore there will be negative values both at low and high temperatures (Dill, 1990; Randolph, 1997).

Important problems related to protein stability arise with the crystallization of ice in a solution that promotes the freeze concentration and leads to a large ice-water interface. Freeze concentration occurs because of the exclusion of solutes from the ice crystals and their spatial confinement between the freezing interfaces (Miller *et al*., 2013). With the increase in solute concentration the ionic strength and the relative composition of solute change reducing or accelerating the rate of chemical reactions and possibly destabilizing the protein (Wang, 2000; Pikal, 2010). At the ice-water interface there can be the adsorption of proteins which lose their native fold denaturing (Strambini and Gabellieri, 1996). Two different hypotheses have been formulated to explain this phenomenon:

1. protein stability is influenced by the generation of an interfacial electric field through the preferential partitioning of an ionic species in the ice lattice (Workman and Reynolds, 1950);
2. the driving force for the unfolding of proteins derives from the absorption of proteins at the interface with the ice because this leads to unlocking ordered structures of water molecules (Norde, 1986).

Controlling the cooling rate and the nucleation temperature is possible to control the size of the ice crystal and therefore the extension of the ice water interface; bigger is the ice water interface more protein unfolds. If stability of the protein is greater in the bulk of the solution than at the freezing interface must be avoided high cooling rates and low nucleation temperature that lead to small ice crystals and large ice water interface. In this case it is possible to raise the nucleation temperature choosing a controlled nucleation technique, such as the VISF (Pisano, 2019), or adding stabilizers and excipients (Arsiccio *et al.*, 2018b; Chang *et al*.,1996). Another way to reduce the impact of surface driven denaturation is to increase the protein concentration as only a finite number of proteins can be absorbed at the ice water interface (Carpenter *et al*., 1992; Sarciaux *et al*., 1999; Arsiccio *et al*., 2020). On the contrary if the stability of the protein is greater at the ice interface than in the bulk the worst solution to reduce the unfolding is a low cooling rate that allow easily conformational changes. A high cooling rate allow a fast immobilization of the protein in a cryoconcentrated glassy matrix (Ohtake *et al*., 2011; Arsiccio *et al*., 2020).

The effect of introducing a slow thawing step is controversial because, while on the one hand it promotes the growth of crystals, which is positive for the surface induced denaturation phenomena, on the other it introduces stresses for proteins at the ice-water interface (Arsiccio *et al*., 2020). Different is a fast thawing rate that is beneficial for both bulk denaturation phenomena and surface denaturation phenomena because it minimizes process duration and possibility of recrystallization (Cao *et al*., 2003).

Furthermore, because of freeze concentration some components of the formulation can phase separate creating an interface that can lead to surface-induced denaturation and loss of the stabilizing effect of the excipient because their concentration became too small (Heller *et al*., 1997; Al-Hussein and Gieseler, 2012).

During freezing the solute concentration and the selective crystallization of some buffering species can lead to pH shift that can denature the protein because of strong repulsion forces between equal charges (Gomez *et al*., 2001; Murase and Franks, 1989). A fast cooling rate may limit this phenomenon (Franks, 1993; Chang and Randall, 1992), while annealing should be avoided (Searles *et al*., 2001b). The occurring of a pH shift during freezing can have consequences also on the storage stability because of a “pH memory” (Costantino *et al*., 1997).

A fully hydrated protein is covered by an hydratation shell which basically is a monolayer of water. This hydratation shell is partially removed during lyophilization causing protein aggregation, inactivation of active site in which the water has a functional role and therefore denaturation. Moreover, is possible to have a non-uniform moisture distribution that can lead to localized overdrying and so protein denaturation (Pikal and Shah, 1997).

Therefore, during the lyophilization process, protein can have no changes in their conformation, can be affected by reversible or irreversible denaturation (Wang, 2000).

1.8.1 Mechanism of protein stabilization

Excipients are added to enhance the stability of the protein (biopharmaceuticals). Sugars and polyols, amino acids, polymers, surfactants, buffer, proteins, alcohols and preservatives can act as stabilizers.

The stabilization mechanisms change with the quantity of water available and therefore between the freezing phase and the drying phase (Carpenter *et al*., 1993). During freezing, thermodynamic stabilization prevails, while subsequently the mechanism is kinetic (Arsiccio and Pisano, 2018b). Excipients may be more suitable for one phase than another and therefore be cryoprotectant or lyoprotectant (Arsiccio *et al*., 2019; Arsiccio and Pisano, 2018d). Stabilization during the freezing phase is described by the mechanism of preferential exclusion. According to this mechanism, excipients that are poorer solvent for the peptide chain than water are added to the solution. Increasing the concentration of excipients increases the stability of the protein. The native fold of the protein is stabilized because is thermodynamically more stable than the expanded unfolded ones (Arsiccio *et al*., 2019). Furthermore, the addition of excipients increases the viscosity of the solution by decreasing the protein unfolding rate. The kinetic mechanism, typical of the drying phase, performs its stabilizing function by forming a compact network of hydrogen bonds (Arsiccio and Pisano, 2018a). A cage structure of excipients molecules is then formed around the protein that generates water entrapment and hydrogen bonds with the protein which prevent it from being unfolded. This is accompanied by an increase in viscosity. The most important characteristic for an excipient in this mechanism is therefore to be rich in hydrogen-bonding sites easily accessible (Arsiccio and Pisano, 2017).

Surfactants are a type of excipients used to prevent surface-induced denaturation. They have a different stabilizing action depending on whether the interface is of the air-water, ice-water or silica-water type. In the first case, the surfactant molecules are positioned at the interface, inhibiting protein adsorption (Arsiccio *et al.*, 2018). In the second case, the surfactant molecules form clusters around the proteins, towards which the hydrophilic heads turn, avoiding the exposure of the hydrophobic residues in case of unfolding (Arsiccio *et al.*, 2018). Finally, in the last case, the surfactant molecules cover the interface turning the hydrophobic tails to the protein and thus stabilizing the nonpolar surfaces derived from unfolding (Arsiccio *et al.*, 2018). The latter mechanism is like that surfactants show in the bulk of the solution (Arsiccio and Pisano, 2018c). Surfactants can also promote protein refolding by reducing aggregation in the reconstitution phase (Carpenter *et al*., 2002; Jones *et al*., 2001).

1.9 Effects of the container

The correct choice of the primary packaging is of great importance both for the freeze-drying process of the product and for its stability and integrity during storage. To date vials constitute the 50–55% of small volume injectable packaging, syringes 25–30%, while ampoules and cartridges fill the rest (Sacha *et al*., 2010).

The vials are available in different sizes and qualities. Despite risk of breakage, small heat transfer coefficient and ability to interact with the product, glass is the most used material thanks to its chemical durability, inertity, cleanliness, low gas permeability, possibility of terminally sterilization and transparency (Schaut *et al*., 2014). The appearance of plastic and glass vials look identical, however plastic vials face difficulties in being handled by filling system because of the lighter weight compared to glass and can potentially interact with the drug product (absorption, adsorption, migration) (Sacha *et al*., 2010).

For parenteral drugs, generally type I borosilicate glass is used. Type I glass container are composed mainly of silicon dioxide (~81%) and boric oxide (~13%), with low levels of the non-network-forming oxides (such as sodium and aluminium oxides). It is a chemically resistant glass (low leachability) also having a low thermal coefficient of expansion (Sacha *et al*., 2010).

The oxide that cannot enter in the structural network of glass are relatively free to migrate into the solution into the container. The leaching process is a diffusion-controlled ion-exchange process involving exchange of protons from an aqueous solution for the alkali ions present in the glass (e.g. Li^{+}, Na^{+}, K^{+}, Mg^{++}, Ca^{++} and Mg^{+++}). This loss of hydronium ions during leaching leads to rising pH values in the product solution and potential instabilities of biomolecules. (Sacha *et al*., 2010; Ennis *et al*., 2001). The occurrence of a leaching reaction depends on the pharmacological product, for example acid drug formulations lead to leaching, while basic formulations lead to dissolution of the glass surface (Doremus, 1979). Glass dissolution reaction involves breakdown of the silicate backbone by hydroxide ions causing the release of metal ions and other inorganic materials (Borchert *et al*., 1989).

During the storage of parental drugs in glass containers, the surface of the glass in contact with the solution may be subject to delamination (Ditter *et al*., 2018a). Delamination is the result of chemical attack of the glass surface forming visible or subvisible flakes and particulates which are generally unacceptable (Cailleteau *et al*., 2008; Iacocca and Allgeier, 2007). To overcome this problem, the containers can be coated internally.

In addition to the delamination of the glass, the differences in the surface properties of a vial can lead to "fogging" (Ditter *et al*., 2018b): streaks, branches, spots, or even uniform thin layers of product deposited on the internal surface of the glass container above the cake (Langer *et al*., 2020). From cosmetic defect it becomes a critical defect if it compromises the container closure integrity (Huang *et al*., 2019). If the surface tension of the solution is lower than the surface energy of the container, the solution spreads over the surface and creeps up itself into the container wall, while if the surface tension of the formulation is higher than the surface energy of the container wall the solution does not spread along the surface. The fogging factors are inversely related to the contact angles (the angle between the liquid surface and the outline of the contact surface) of the glass surfaces (Langer *et al*., 2020). Therefore, fogging results from Marangoni flow which is driven by a surface tension gradient (Patel *et al*., 2017). The presence of surfactant can reduce the surface tension of the solution favouring the wetting of the glass surfaces with consequent worsening of the fogging (Huang *et al*., 2019; Abdul-Fattah *et al*., 2013). The best way to minimize or eliminate fogging are containers with hydrophobic surface, such as siliconized containers, thanks to their lesser tendency to be wetted by an aqueous solution (Langer *et al*., 2020).

Finally, the glass can to adsorb significant quantities of protein from the solution (Petty and Cunningham, 1974; Hoger *et al*., 2015; Grohganz *et al*., 2004)). To ensure the accurate dosage it is possible to overfill the containers applying a higher filling volume or/and a higher concentration, but this causes an increase in the cost (Hoger *et al*., 2015). Other solutions may be the addition of excipients (Duncan *et al*., 1995; Wendorf *et al*., 2004) or the selection of

containers capable of decreasing the loss of protein content or activity due to adsorption (Kondo and Mihara, 1996).

When choosing a material for containers, compliance with hydrolytic class I is often not enough. Treated or coated surfaces can improve the quality of the container and minimize its interactions with the formulation (Ditter *et al*., 2018b).

1.10 Objectives of the thesis

The purposes of this master's degree project were:

- evaluate the effect of surface treatments on the feasibility of controlled nucleation (VISF);
- find the best combination of type of vials and solutions for performing VISF;
- implement VISF through an automatic mode.

No previous literature on these topics was found.

This research has its starting point in the understanding of the principles of freezing, the techniques to control the nucleation temperature, the drying steps and the effect of the container's properties on the final product. In this chapter the state of the art of these aspects has been introduced.

At the end of this document, a comparison between the various coatings of the containers examined has been presented in order to highlight limits, strengths and differences.

2. Materials and Methods

2.1 Materials

2.1.1 Vials

The vials tested were:

I. Untreated vials (S-);

II. Sulphate treated vials (ST);

III. Siliconized vials (S+);

IV. TopLyo® vials (TL).

2.1.1.1 Drawings and Dimensional Aspects

All vials used were produced according to ISO 8362-1. The size designation of all the vials is 2R.

In Figure 2.1 there is an untreated vial with the main dimensions. This Figure can also be considered valid for the siliconized vials because these are obtained applying a siliconization treatment to the untreated ones.

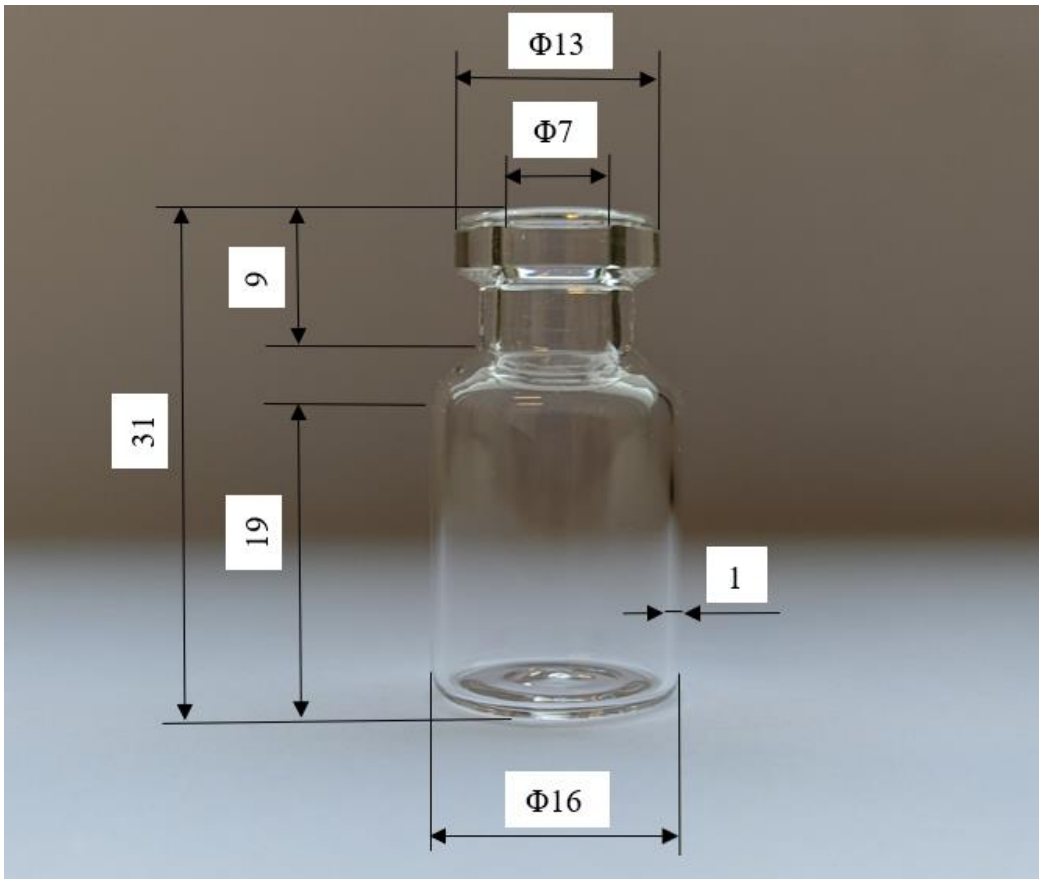

Figure 2.1: Main dimensions of untreated and siliconized vials.

In Figure 2.2 there is a sulphate treated vial with the main dimensions. This figure also applies the TopLyo vials.

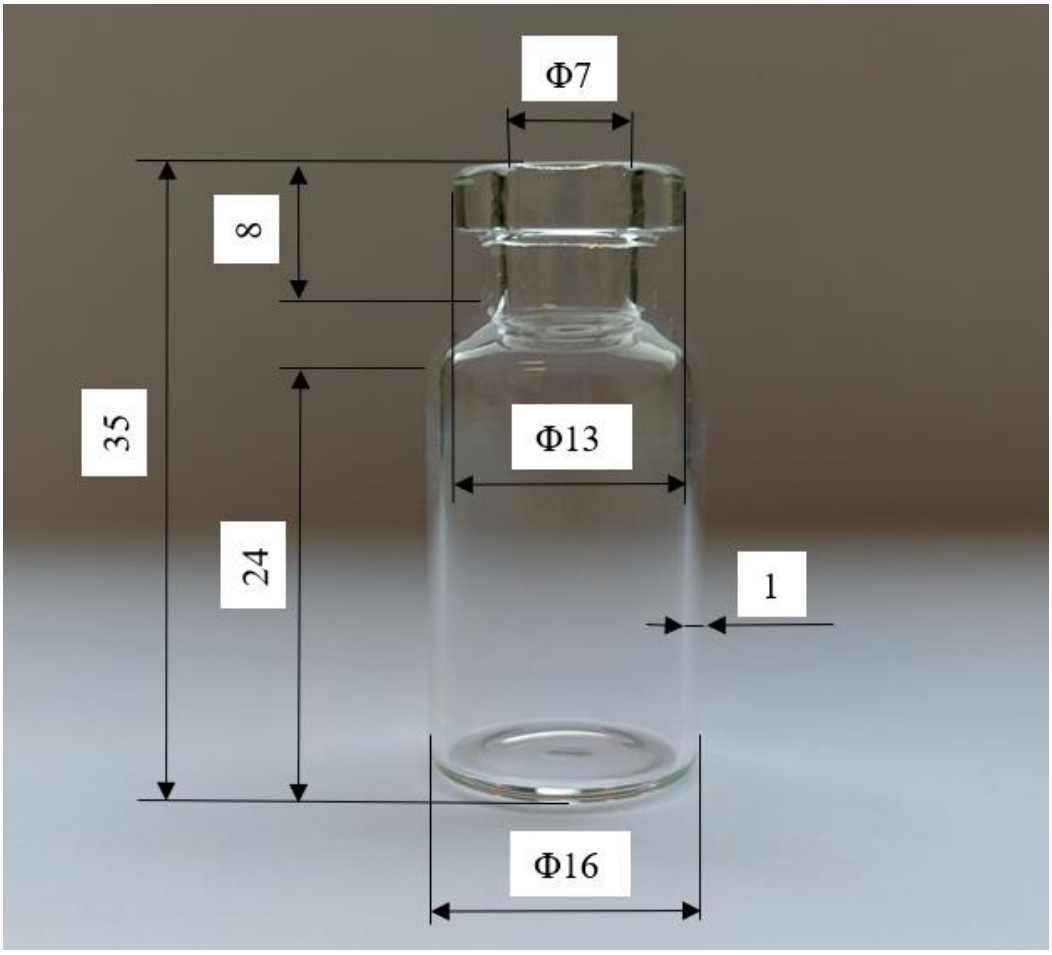

Figure 2.2: Main dimensions of sulphate treated and TopLyo® vials.

2.1.1.2 Untreated Vials

These vials were purchased at Müller + Müller (Holzminden, Germany). Untreated vials are made of clear borosilicate glass of Type I. Also known as "neutral, “type I” is a borosilicate glass with a high hydrolytic resistance due to the chemical composition of the glass itself. The hydrolytic stability of the glass containers is given by the resistance to the release of water-soluble mineral substances from the internal surface of the container to the solution contained therein. Hydrolytic resistance is assessed by titrating released alkalis (Council of Europe, 2010). Type I is also characterized by low leachability and low thermal expansion coefficient (Sacha *et al.*, 2010). It is used for drugs requiring the least reactive containers.

The main components of borosilicate glass are silicon dioxide (over 70%) and boric oxide (about 10%) with low percentages of other oxides, such as sodium and aluminium oxides, that do not contribute to the formation of the network (Sacha *et al.*, 2010). Reactions with water, acids and alkalis can lead to leaching and extraction of the components from the glass surface.

2.1.1.3 Sulphate Treated Vials

These vials were purchased at Stevanato Group (Bad Oeynhausen, Germany). The sulphate-treated vials consist of Type I glass to which a sulphurization treatment with ammonium sulphate salt has been applied.

The treatment consists in bringing the ammonium sulphate to high temperatures (>490°C) in such a way that it decomposes. This vapor reacts with the surface alkalis (cationic metals) to form water-soluble sodium and potassium salts and to displace calcium with hydrogen from decomposing acid ammonium sulphate. After washing, a silica-enriched layer is formed which acts as a barrier for the further elution of alkali (Mochel *et al*., 1966; Preston and Anderson, 1984; Preston and Anderson, 1985; Sacha *et al*., 2010). Therefore, the sulphurization treatment reduces the surface alkalinity (Iacocca *et al*., 2010) and suppresses the particle formation (Ogawa *et al*., 2013). This glass treatment reduces also potential metallic leachates, but it can pit the surface of the vial enhancing delamination (Roseman *et al*., 1976; Ennis *et al*., 2001; Sacha *et al*., 2010). The costs of the treatment are contained.

2.1.1.4 Siliconized Vials

The treatment of siliconization has been applied by GSK Vaccine (Rixensart, Belgium) at the untreated vials purchased at Müller + Müller (Holzminden, Germany) and therefore on Type I glass.

The use of silicones was introduced many years ago in pharmaceutical production as an antifoam, tube material and for the siliconization of container surfaces (Höger *et al*., 2015). The first patent for the siliconization of pharmaceutical containers dates back to 1949 (Goldman, 1950).

To carry out the siliconization on the internal surface of the vials was used SILBIONE EMULSION 70001 SP which is a non-ionic emulsion of dimethicone oil in water at 35 %.

Polydimethylsiloxane (PDMS), also known as dimethicone, is a polymeric organosilicon compound characterized by the basic structure $(\text{-OSi}(CH_3)_2\text{-})_n$ with many methyl groups ($\text{-}CH_3$) which gives the hydrophobic property (Jothi and Nageswaran, 2019).

SILBIONE EMULSION 70001 SP is generally used in the form of a dilution with an active ingredient content of approximately 0.2 to 1.2%. The typical properties of SILBIONE EMULSION 70001 SP are reported in Table 2.1.

The key benefits of SILBIONE EMUL 70001 SP are the following:

- Non-ionic;
- Easily dispersible;
- Chemically inert;
- Harmless;
- Non-toxic;
- Good skin tolerance.

Appearance	Smooth milky liquid
Colour	White to creamy white
Odour	None to slight
Total solids content, %, approx.	40
Active ingredient content, %, approx.	35
Specific gravity at 25°C, approx.	1,0
pH	2,5 to 4,5
Emulsifier	Non-ionic
Thinner	Water

Table 2.1: SILBIONE EMULSION 70001 SP typical properties. Data taken from Elkem, SILBIONE EMUL 70001 SP Brochure.

The film obtained after that the emulsion has been applied offers excellent water-repellent, anti-adherent and heat-resistant properties.

The vials are subjected to:

- Stable washing process;
- Stable sterilization:
    - Depyrogenation (1hour at a 260°C).

Siliconized vials contain lesser quantities of Na and B and more of Si and C than untreated vials (Huang *et al*., 2019).

The silicone coating inhibits the hydrogen bond between water and silanol and siloxane groups at glass surfaces (Kawano *et al*., 2017). Also, the interaction between the various phases given by the van der Waals force are lower for coating glass (Kawano *et al*., 2017). Therefore, thanks to the coating the surface free energy is lower than for an untreated glass. This causes a reduction in the adhesive energy (Kawano *et al*., 2017).

The advantages of the siliconization of the internal surface of the containers, used for freeze-drying, are several:

- The coating suppresses the contact between solution and glass of the vials which is rich in cations (Ogawa *et al*., 2013);
- The coating acts as a barrier against the alkali elution from the glass (White *et al*., 2008; Iacocca *et al*., 2010);
- The coating avoids delamination from the glass surface (White et al., 2008; Ogawa *et al*., 2016);
- The coating reduces the leaching of ions from glass surfaces to acceptable levels;
- The coating results in a hydrophobic surface that resists nonspecific binding reducing sample losses caused by this type of interactions with the container, minimizing protein absorption to the surface and increasing shelf life stability;

- Less disruption of the lyo cake thanks to the limited climbing at the vial edges (Schott TopLyo® Vials Brochure);
- The fogging is limited thanks to the reduction of the surfactant driven Marangoni flow;
- The surfaces, thanks to the hydrophobic coatings, are very homogeneous preventing the adhesion of the freeze-dried substances to the inside walls of the vials. The consequences are a perfect transparency of the glass and an almost complete drainage of the product/solution from the vials that allows a better dosage. Overfilling the vials to ensure accurate dose delivery is significantly reduced, leading to measurable cost savings (Hoger *et al*., 2015);
- The products look good and redissolve faster in water.

However, there is a higher potential for protein aggregation in presence of silicone oil in the internal surface coating (Jones *et al*., 2005) and SiO_2 coating doesn't suppress the particle formation in the solution (Ogawa *et al*., 2013).

2.1.1.5 TopLyo® Vials

These vials were produced by Schott (Müllheim, Germany). TopLyo® vials consist of SCHOTT Type I glass combined with a transparent and nonporous Si-O-C-H layer.

Thanks to the hydrophobic PICVD (Plasma-Impulse Chemical Vapor Deposition) coating this type of vial is especially recommended for freeze-drying. Plasma Impulse Chemical Vapour Deposition (PICVD) is a technology, developed by Schott, used for thin film deposition. The PICVD process apply an oxide coating at the internal surface of the vials using a pulsed plasma in combination with oxygen and a volatile precursor gas. The process is particularly advantageous for the interior deposition of hollow bodies because of the precursor gas is exchanged after every pulse maintaining a constant gas concentration close to the surface and therefore, ensuring a uniform coating distribution (Schott PICVD brochure).

The surface composition of TopLyo® vials is dominated by C, Si and O (Huang *et al*., 2019).

In Table 2.2 and Table 2.3 are presented the physical and the chemical properties of the ultra-thin layer of TopLyo® vials.

Physical data
Layer thickness of ~ 40 nm
Stable against mechanical load
Stable washing process
Stable sterilization: · Autoclaving (121 °C, 30 min) · Depyrogenation (dry heat treatment at 250 °C – 350 °C)

Table 2.2: TopLyo® physical data. Data taken from Schott, TopLyo® Vials Brochure.

Chemical data
Chemical layer properties: Si-O-C-H
Long-term stable layer system during storage
Bond covalently to the material and chemically uniform
Dense and non-porous coating
Contact angle for water of ~100 °

Table 2.3: TopLyo® chemical data. Data taken from Schott, TopLyo® Vials Brochure.

The characteristics of the TopLyo® vials are therefore similar to those of the siliconized vials produced by GSK Vaccines, but the superior quality treatment makes them more hydrophobic. TopLyo® vials can therefore boast all the advantages for freeze-drying described in section 2.1.1.4.

2.1.1.6 Stoppers

All the different types of vials are closed with the same igloo stoppers (Helvoet FM 460 type) that can be seen in Figure 2.3. The stoppers are made of an ultra-pure bromobutyl formulation with extremely high chemical purity and low gas permeability. The level of moisture absorption is really low.

Figure 2.3: Stopper Igloo Helvoet FM 460 type.

2.1.2 Solutions

The formulation tested were:

I. Drinking Water (W);
II. Water for injection (WFI);
III. Demineralized water (DW);
IV. Demineralized water + 0,02% w/v Tween 80 (DW+TW80);
V. 5% w/w sucrose (Suc);
VI. 5% w/w sucrose + 0,02% w/v Tween 80 (Suc+TW80);
VII. 5% w/w mannitol (MAN);
VIII. 5% w/w mannitol+ 0,02% w/v Tween 80 (MAN+TW80).

All the solutions are filtered with a 0,22 μm pore size filter.

2.1.2.1 Water for injection

Water for injection refers to water by which are removed inorganic particles, minerals, salts, bacteria and viruses. Following the United States Pharmacopeia WFI contains:

- less than 10 CFU/100 ml of Aerobic bacteria;
- fewer than 500 ppb of total organic carbon;
- fewer than 0.25 EU/ml endotoxins;
- conductivity of less than 1.3uS/cm @ 25 C.

It is used in the manufacture of parenteral drugs. This highly purifies water is produced by distillation or reverse osmosis.

2.1.2.2 Demineralized water

Demineralized water refers to water by which are removed minerals and salts. It is used in applications were low salt content and conductivity are required. Demineralized water is obtained thanks to resins which exchange ions in the water. Small amount of mineral can remain in the water.

2.1.2.3 Sucrose

Sucrose is the sugar most used in the freeze-drying of biopharmaceuticals (Fissore *et al*., 2019). It is an amorphous disaccharide given by glucose and fructose linked via a glycosidic bond. It can act as both cryoprotectant and lyoprotectant. Thanks to the Tg' of -32 °C and the Tg of 74 °C sucrose also increases storage stability (Heljo, 2013). Moreover, sucrose is a nonreducing disaccharide. Elegant cakes and isotonic products after reconstitutions are given by sucrose concentrations up to 10% w/w (Franks, 1998). The breakdown of the glycosidic linkage produces monosaccharides that give Maillard reactions with protein or amino group-carrying excipients (O'Brien, 1996).

2.1.2.4 Mannitol

The mannitol is a type of sugar alcohol that can be used as bulking excipients for protein lyophilization. The ability to stabilize mannitol proteins is limited to its amorphous form, unfortunately it has a low *Tg′* of -32 °C and -25 °C and a very low *Tg* of 12.6 °C and therefore crystallizes easily (Cavatur *et al*., 2002; Yu *et al*., 1998). Mannitol can form different polymorphs and hemihydrates depending on the temperature, the crystallization rate and the annealing step (Hawe and Friess, 2006). Following the crystallization, a frame is formed which gives elegance to the cake and allows to reach temperatures higher than *Tg′* or *Tc* of the product during primary drying (Fissore *et al*., 2019).

2.1.2.5 Tween 80

Polysorbate 80, also known as Tween 80, is a synthetic nonionic surfactant composed of fatty acid esters of polyoxyethylene sorbitan (Kerwin, 2008). Nonionic surfactants in a protein formulation protect the protein by aggregation, surface adsorption and/or precipitation that can be caused by agitation, freezing, interfacial and/or drying stresses (Kiese *et al*., 2008; Hillgren *et al*., 2002; Wang, 2005). It is necessary the concentration of 0,001% w/v of Tween 80 to reduce the aggregation of protein (Arsiccio *et al*., 2020). More generally Polysorbate 80 can be used in drug formulations as a solubilizer, stabilizer, or emulsifier (Schwartzberg and Navari, 2018; Khan *et al*., 2015).

If the protein unfolding is mainly surface driven the polysorbates lead to a significant increase in protein stability (Arsiccio *et al*., 2020). Polysorbate 80 is an amphiphilic molecule with hydrophobic and hydrophilic components (Kerwin, 2008; Khan *et al*., 2015). At the air-water interface or at the solid-water interface, such as that found in vials, surfactant molecules orient their hydrophobic portions and correspondingly begin to assemble as micelles in solution as the concentration of the surfactant increases above the critical micelle concentration (CMC) of 0,01% (weight/volume).

Polysorbate 80 can undergo oxidation, autoxidation and hydrolysis depending on pH, temperature and oxygen level (Fissore *et al*., 2019). These degradations are more likely in the liquid form than once freeze-dried (Hall *et al*., 2016; Martos *et al*., 2017).

Along with the positive effect at the interface, unfortunately, Tween 80 has a denaturant effect in the bulk where, however, it is found in lesser quantities.

The addition of sucrose as an excipient can counteract the denaturing effect of Tween 80. In the case of the addition of mannitol, the part that crystallizes creates another surface on which adsorption and unfolding can occur, while the fraction that remains in the amorphous phase contrasts the denaturation effect of Tween 80 but to a lesser extent than sucrose (Arsiccio *et al*., 2020).

2.1.3 Lyophilizer

All the experiments were performed in a pilot-scale freeze-dryer (HETO DW 8030 by Thermo Fisher Scientific, Waltham, MA, USA) which can be seen in Figure 2.4.

The samples to be processed are loaded onto the heat/cool shelves of a 0,12 m^3 vacuum chamber. The total cooling surface provided by the shelves is 0,6 m^2. The refrigeration system, necessary to achieve low temperatures, is composed of a compressor, a condenser, an expansion device and an evaporator. In the Table 2.4 are reported the ice condenser specification. A butterfly valve inside a duct divide the condenser by the chamber and allows the isolation of

the latter. A vacuum pump evacuates the incondensable gases by the condenser to reach low pressures. For an easy, safe and controlled stoppering there is a pneumatic stoppering arrangement. The construction allows free inspection of the condenser during the freeze-drying processes.

Figure 2.4: pilot-scale freeze-dryer HETO DW 8030. Figure taken from Heto-Holten Lab Equipment brochure with modifications.

Cooling capacity -50°C	8 kg/ 24 h
Volume	60 Litres
Material	Stainless AISI 316

Table 2.4: Ice condenser specification. Data taken from Heto-Holten Drywinner DW 8 service manual.

2.1.4 Tempris sensors

Tempris sensors are used to detect the temperature of the solution inside the vials which are in the vacuum chamber. It is a wireless temperature monitoring system: the probes are inserted inside the vials in contact with the solution, while the receiver is mounted on the door of the vacuum chamber and connected to a computer that show the data. The probes are shown in Figure 2.5.

Figure 2.5: Tempris probe on the left and Tempris probe correctly inserted in a vial on the right.

2.1.5 Thermovac

The pressure has been measured thanks to the vacuum meter Thermovac TM 101 which is placed on the duct between vacuum chamber and condenser, on the side of the latter. The electronic Thermovac TM 101 is capable of measuring pressures within the pressure range of 1200 to $5*10^{-4}$ mbar.

A piezo-resistive pressure sensor for the upper pressure range combined with a Pirani sensor for the lower pressure range make pressure measurement above 15 mbar independent of the type of gas. The Figure 2.6 shows the vacuum meter.

Figure 2.6: Vacuum meter Thermovac TM 101 placed on the duct between vacuum chamber and condenser on the side of the latter.

2.2 Methods

2.2.1 Validation of the shelf

Five probes of the Tempris sensor were fixed on the two side walls and on the central shelf of the vacuum chamber of the freeze-dryer HETO DW 8030. The three probes positioned on the central shelf were placed 4 cm by the front edge, one on the left, one in the middle and one on the right. To improve the heat transfer between the probes and the shelf/wall a thermally conductive silicone compound (Dow Corning® 340) was applied in the contact points. The temperature of the five probes were noted down for 45 minutes since the start of the freezing phase every 5 minutes.

2.2.1.2 Freezing procedure and cycle details

When placing the probes in the vacuum chamber the shelf temperature was 4 °C. After the preparation phase the freeze dryer began the freezing phase. The temperature setting of the shelf remained constant at 4 °C for 15 minutes, after which in 15 minutes the shelf reached -11,5 °C and remained constant until the experiment was completed.

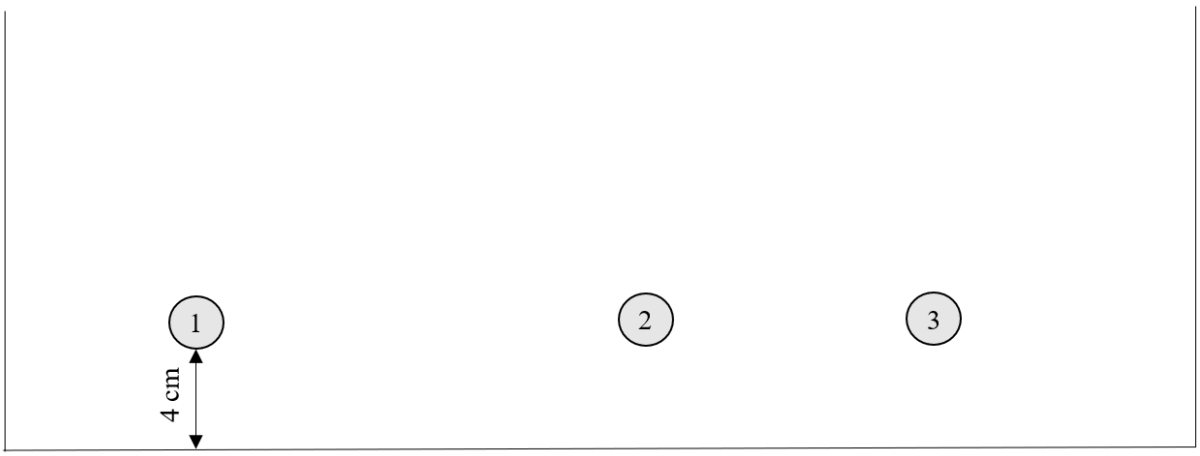

Figure 2.7: disposition of the three probes on the central shelf for its validation.

2.2.2 Determination of P_{first} and P_{last} (Experiment 1)

A sufficient number of vials were loaded on the shelf of the vacuum chamber of the freeze-dryer HETO DW 8030. These vials were equilibrated at a temperature T_n = -5°C or T_n = -10°C and atmospheric pressure. When the vials reached T_n, the vacuum pump was switched on decreasing the pressure in the chamber. The pressure values P_{first} and P_{last}, which corresponded respectively to the pressure value at which nucleation was first observed in some vials and the pressure value at which the last vial nucleated, were noted down. After that the last vial was nucleated the atmospheric pressure could be re-established.

The formulation tested in the experiment 1 were the following:

- Demineralized water (DW);
- Demineralized water + 0,02% w/v Tween 80 (DW+TW80);
- 5% w/w sucrose (Suc);
- 5% w/w sucrose + 0,02% w/v Tween 80 (Suc+TW80);
- 5% w/w mannitol (MAN);
- 5% w/w mannitol+ 0,02% w/v Tween 80 (MAN+TW80).

The type of vials tested in the experiment 1 were the following:

- Untreated vials (S-);
- Sulphate treated vials (ST);
- Siliconized vials (S+);
- TopLyo® vials (TL).

In the Table 2.5 are presented the Cycles details for the experiment 1.

Cycle details							
S-		ST		S+		TL	
Solution	T_n[°C]	Solution	T_n[°C]	Solution	T_n[°C]	Solution	T_n[°C]
DW	-5,0	DW	-5,0	DW	-5,0	DW	-5,0
DW	-10,0	DW	-10,0	DW	-10,0	DW	-10,0
DW+TW80	-5,0	DW+TW80	-5,0	DW+TW80	-5,0	DW+TW80	-5,0
DW+TW80	-10,0	DW+TW80	-10,0	DW+TW80	-10,0	DW+TW80	-10,0
Suc	-5,0	Suc	-5,0	Suc	-5,0	Suc	-5,0
Suc	-10,0	Suc	-10,0	Suc	-10,0	Suc	-10,0
Suc+TW80	-5,0	Suc+TW80	-5,0	Suc+TW80	-5,0	Suc+TW80	-5,0
Suc+TW80	-10,0	Suc+TW80	-10,0	Suc+TW80	-10,0	Suc+TW80	-10,0
MAN	-5,0	MAN	-5,0	MAN	-5,0	MAN	-5,0
MAN	-10,0	MAN	-10,0	MAN	-10,0	MAN	-10,0
MAN+ TW80	-5,0	MAN + TW80	-5,0	MAN + TW80	-5,0	MAN + TW80	-5,0
MAN + TW80	-10,0	MAN + TW80	-10,0	MAN + TW80	-10,0	MAN + TW80	-10,0

Table 2.5: Cycle details for experiment 1 and experiment 2.

2.2.2.1 Samples preparation

Selected the type of vials, twenty vials were filled with 0,5 ml of the chosen solution and a probe of the Tempris sensor was inserted in three of them in order to monitor the temperature. The vials had to be partially stoppered with igloo stoppers (Helvoet FM 460 type) in order to put in communication the headspace of the vials with the vacuum chamber. The vials were then placed on the central shelf of the vacuum chamber in a staggered way at a distance of 4 centimetres from the front edge of the shelf. The probes were always placed in the same positions shown in Figure 2.8.

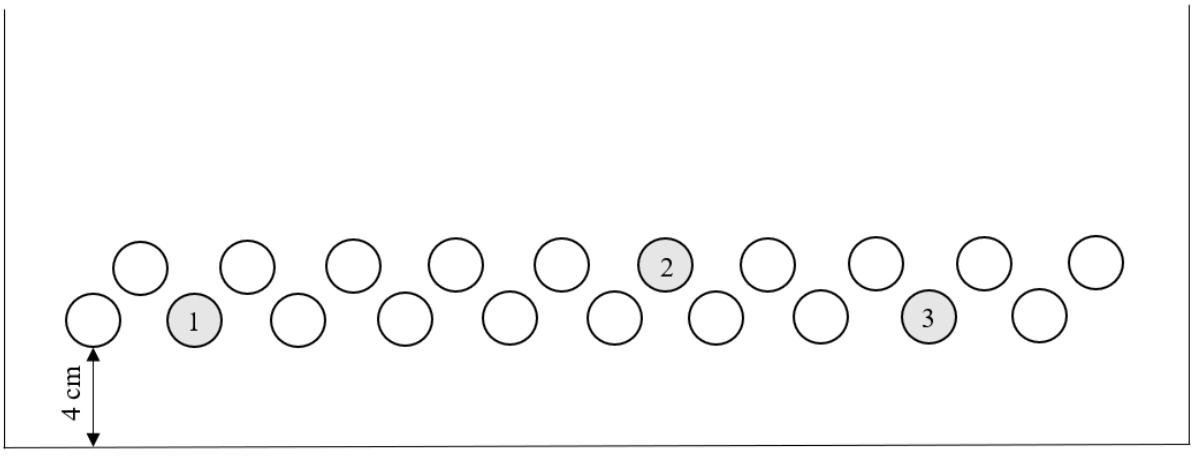

Figure 2.8: Disposition of the vials on the shelf and position of the three probes.

2.2.2.2 Freezing procedure and cycle details

When loading, the shelf temperature was 4 °C. After loading, the freeze dryer began the freezing phase that changed if T_n=-5°C or T_n=-10°C.

If T_n=-5°C the temperature setting of the shelf remained constant at 4 °C for 15 minutes, after which in 10 minutes the shelf reached -6,5 °C and remained constant until the experiment was completed. It was necessary to set a shelf temperature of -6,5 °C to reach a temperature of -5 °C in the vials because if the shelf temperature were identical to the one to be reached in the solution the driving force would be too low and the times too high.

While, if T_n=-10°C the temperature setting of the shelf remained constant at 4 °C for 15 minutes, after which in 15 minutes the shelf reached -11,5 °C and remained constant until the experiment was completed. It was necessary to set a shelf temperature of -11,5 °C to reach a temperature of -10 °C in the vials because if the shelf temperature were identical to the one to be reached in the solution the driving force would be too low and the times too high.

2.2.3 Determination of t_n (Experiment 2)

A sufficient number of vials were loaded on the shelf of the vacuum chamber of the freeze-dryer HETO DW 8030. These vials were equilibrated at a temperature T_n = -5°C or T_n = -10°C and atmospheric pressure. When the vials reach T_n, the vacuum pump was switched on decreasing the pressure in the chamber to the value P_n. The value P_n was obtained with the empirical Equation 2.1:

$$P_n = P_{first} - \frac{P_{first} - P_{last}}{c} \quad (2.1)$$

Where c is a coefficient assumed equal to 3, P_{first} and P_{last} were value of pressure obtained in the corresponding experiment 1. Once the P_n value was reached, the valve between the condenser and the vacuum chamber was closed thus isolating the latter. The vacuum chamber must remain isolated until nucleation was observed in all vials. The time t_n required to induce nucleation should be noted down. After nucleation has been triggered, atmospheric pressure can be re-established. If less than 70% of the vials were nucleated in a maximum time of 5 minutes the experiment was repeated by decreasing the value of c by one unit or half a unit. The minimum value of c that could be reached is 1 to which the nucleation of all vials was certainly observed as in the corresponding Experiment 1.

The formulations and the vials tested were the same as in experiment 1. In the Table 2.5 are presented the cycles details for the experiment 2.

2.2.3.1 Sample preparation

The sample preparation is the same as presented in the section 2.2.2.1.

2.2.3.2 Freezing procedure and cycle details

The freezing procedure and cycle details are the same as presented in section 2.2.2.2.,

2.2.4 Determination of the influence of the type of water

Three groups of TopLyo® vials filled with drinking water, water for injection and demineralized water were loaded on the shelf of the vacuum chamber of the freeze-dryer HETO DW 8030. These vials were equilibrated at a temperature T_n = -5°C and atmospheric pressure. When the vials reached T_n, the vacuum pump was switched on decreasing the pressure in the chamber. The objective of the experiment was to monitor the boiling phenomenon and the

nucleation of the vials in the different groups of vials. After that the last vial was nucleated the atmospheric pressure could be re-established.

2.2.4.1 Sample preparation

Three groups of five TopLyo® vials were filled with 0,5 ml of drinking water, water for injection and demineralized water. A probe of the Tempris sensor was inserted in each of the three groups to monitor the temperature, as shown in Figure 2.9. The vials had to be partially stoppered with igloo stoppers (Helvoet FM 460 type) in order to put in communication, the headspace of the vials with the vacuum chamber. The vials were then placed, in a staggered way, on the central shelf of the vacuum chamber forming three groups at a distance of 4 centimetres from the front edge of the shelf.

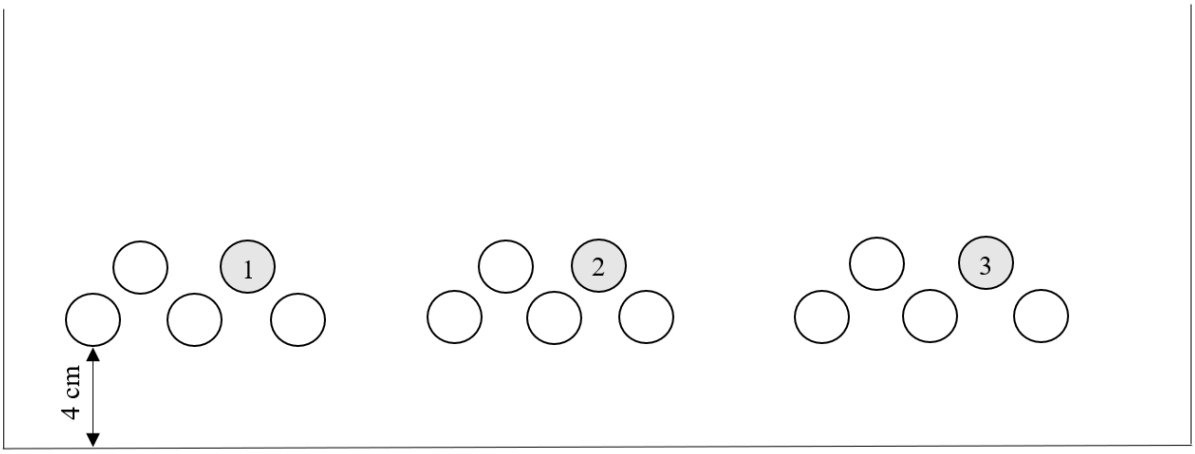

Figure 2.9: Disposition of the vials on the shelf and position of the three probes.

2.2.4.2 Freezing procedure and cycle details

When loading, the shelf temperature was 4 °C. After loading, the freeze dryer began the freezing phase. The temperature setting of the shelf remained constant at 4 °C for 15 minutes, after which in 10 minutes the shelf reached -6,5 °C and remained constant until the experiment was completed.

2.2.5 Determination of the influence of the degasification process

A group of TopLyo® vials filled with the chosen solution was loaded on the left part of the shelf of the vacuum chamber of the freeze-dryer HETO DW 8030. These vials were equilibrated at a temperature T_n = 10°C and degassed. The solution was degassed directly inside the vials to avoid subsequent displacements that could nullify the effectiveness of the treatment. At the end of the degasification the pressure in the vacuum chamber was brought back to the atmospheric one and a second group of TopLyo® vials filled with the same solution was loaded on the right part of the same shelf. All the vials were equilibrated at a temperature T_n = -5°C and atmospheric pressure. When the vials reached T_n, the vacuum pump was switched on decreasing the pressure in the chamber. The objective of the experiment was to monitor the boiling/bubbling phenomena in the different groups of vials. After that the last vial was nucleated the atmospheric pressure could be re-established.

The formulation tested were the following:

- Demineralized water;
- Demineralized water + 0,02% w/v Tween 80;
- 5% w/w sucrose + 0,02% w/v Tween 80;
- 5% w/w mannitol+ 0,02% w/v Tween 80.

2.2.5.1 Samples preparation

One group of ten TopLyo® vials was filled with 0,5 ml of the solution chosen, while another group of ten TopLyo® vials was filled with 0,6 ml of the same solution. To take into account the evaporation of the solution during the degasification one of the two group was filled 0,1 ml more than the other. A probe of the Tempris sensor was inserted in each group to monitor the temperature, as shown in Figure 2.10. The vials had to be partially stoppered with igloo stoppers (Helvoet FM 460 type) in order to put in communication, the headspace of the vials with the vacuum chamber. The group of vials filled 0,6 ml was placed, in a staggered way, on the left part of the central shelf of the vacuum chamber at a distance of 4 centimetres from the front edge of the shelf. Finished the degasification the second group of vials, filled 0,5 ml was loaded, in a staggered way, on the right part of the central shelf of the vacuum chamber at a distance of 4 centimetres from the front edge of the shelf.

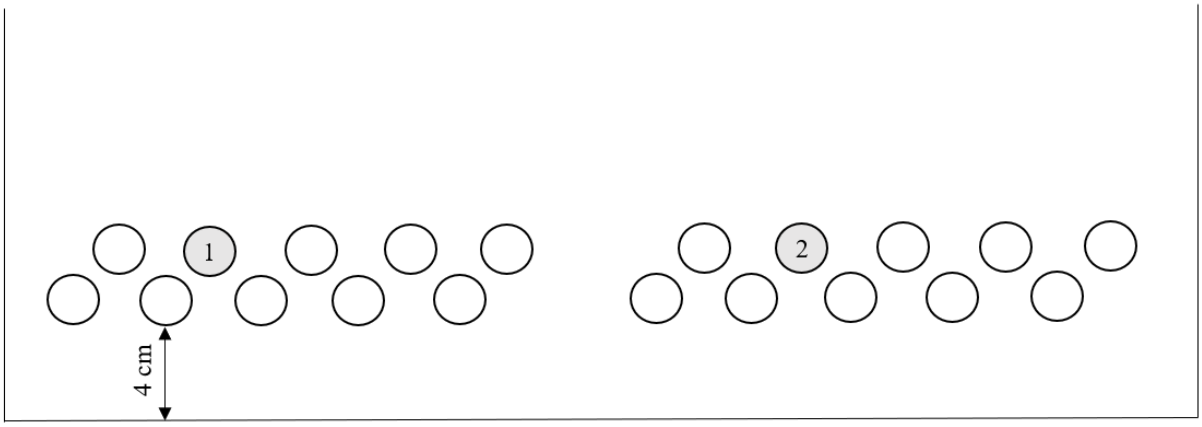

Figure 2.10: Disposition of the vials on the shelf and position of the two probes.

2.2.5.2 Degasification procedure

When loading the first group of vials, the shelf temperature was 10 °C. The temperature of 10 °C was kept constant for all the degasification phase. The degassing procedure changed if Tween 80 was present in the solution or not. If tween 80 was not present to avoid nucleation caused by boiling from 5 mbar, the treatment was carried out at a higher pressure. In presence of Tween 80 the pressure was not decreased under 4 mbar to prevent evaporation from lowering the temperature excessively leading to nucleation. When the temperature of the solution in the vials reached 10 ± 1°C and the pressure was the atmospheric one, the vacuum pump was switched on decreasing the pressure in the chamber.

In the absence of Tween 80:

1. lower the pressure inside the vacuum chamber to 10 mbar and keep it at this value for 10 minutes by switching the vacuum pump on and off;
2. lower the pressure inside the vacuum chamber to 7 mbar and keep it at this value for 20 minutes by switching the vacuum pump on and off.

In presence of Tween 80:

1. lower the pressure inside the vacuum chamber to 10 mbar and keep it at this value for 5 minutes by switching the vacuum pump on and off;
2. lower the pressure inside the vacuum chamber to 7 mbar and keep it at this value for 10 minutes by switching the vacuum pump on and off;
3. lower the pressure inside the vacuum chamber to 4 mbar and keep it at this value for 15 minutes by switching the vacuum pump on and off.

In both cases the vials were kept at a pressure lower than the atmospheric one for a time equal to 30 minutes and after the atmospheric pressure was restored in the vacuum chamber.

2.2.5.3 Freezing procedure and cycle details

When loading the second group of vials, the shelf temperature was 4 °C. After loading, the freeze dryer began the freezing phase. The temperature setting of the shelf remained constant at 4 °C for 15 minutes, after which in 10 minutes the shelf reached -6,5 °C and remained constant until the experiment was completed.

2.2.6 Analysis of the freeze-dried product

2.2.6.1 Experiment A

One tray of untreated vials filled with 5% w/w sucrose and one tray of siliconized vials filled with the same solution were loaded on the shelves of the vacuum chamber of the freeze-dryer HETO DW 8030. These vials were equilibrated at a temperature T_n = -5 °C and atmospheric pressure. When the vials reached T_n, the vacuum pump was switched on decreasing the pressure in the chamber to the value P_n. Once the P_n value was reached, the valve between the condenser and the vacuum chamber was closed, thus isolating the latter. After an amount of time equal to t_n the atmospheric pressure could be re-established in the vacuum chamber. The value of P_n was the smaller between the values of P_n corresponding to untreated and siliconized vials found in experiment 2 (determination of t_n) for the solution chosen at T_n = -5. The value of t_n was which that corresponded to P_n. Therefore, by the Table 2.6 can be seen that the lower value of P_n was 0,9 mbar to which corresponded a t_n of 7 s.

Type of vial	**Solution**	**Experiment**	***T*n [°C]**	***P*n [mbar]**	***t*n [s]**
S-	Suc	2	-5	1	1
S+	Suc	2	-5	0,9	7

Table 2.6: Values of P_n and t_n obtained in the experiment 2 (determination of t_n) for a solution 5% w/w of sucrose.

To obtain the final product the vials were then subjected to freezing, primary drying and secondary drying. Once the secondary drying was completed, the freeze dryer automatically

did the plugging of the vials to isolate the headspace of the vials by the vacuum chamber and so avoid that humidity could come in contact with the product unloading the freeze dryer.

2.2.6.1.1 Sample preparation

One tray composed of 378 untreated vials was filled with 5% w/w sucrose and another tray composed of 378 siliconized vials was filled with the same solution. For the vials of both the trays the filling volume was 0,5 ml. Three probes of the Tempris sensor were inserted in three siliconized vials in the position shown in Figure 2.11 in order to monitor the temperature. The vials had to be partially stoppered with igloo stoppers (Helvoet FM 460 type) so that the headspace of the vials was in communication with the vacuum chamber. The tray of siliconized vials was placed on the central shelf of the vacuum chamber which occupied completely, while the tray of untreated vials was placed on the shelf above.

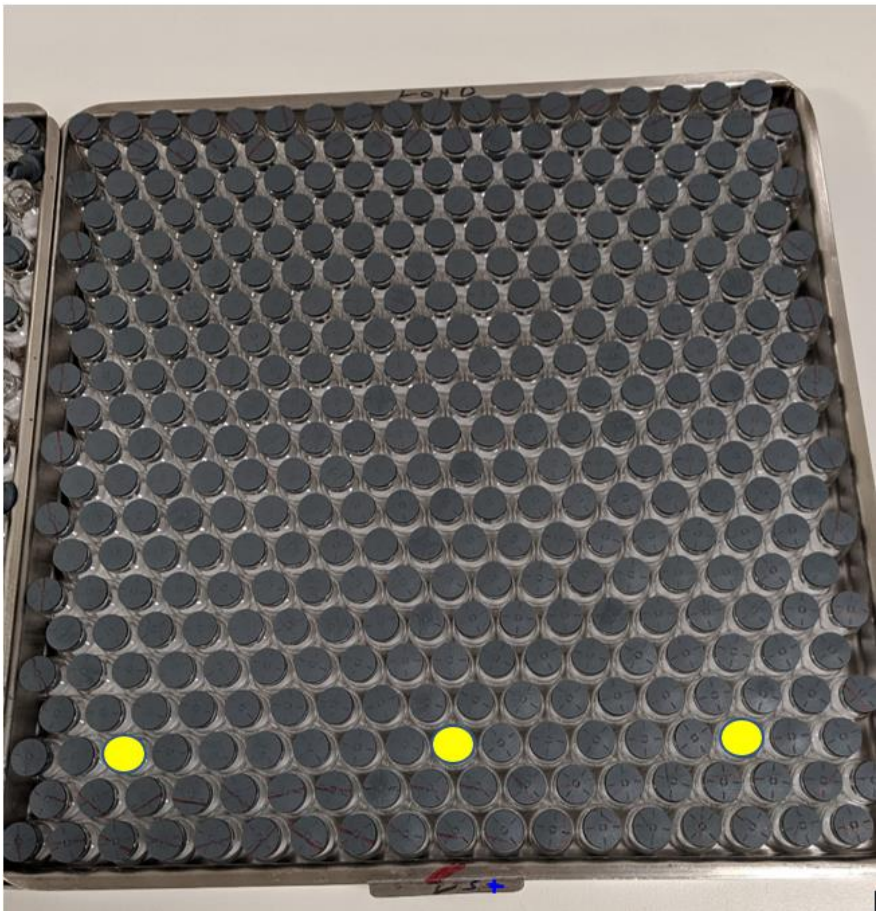

Figure 2.11: Three yellow circle identify the position of the three probes on the tray filled with 378 siliconized vials.

2.2.6.1.2 Freezing procedure and cycle details

When loading, the shelf temperature was 4 °C. After loading, the freeze dryer began the freezing phase. The temperature setting of the shelf remained constant at 4 °C for 15 minutes, after which in 10 minutes the shelf reached -6,5 °C and remained constant until the vials were nucleated.

The vials were then subjected to freezing, primary drying and secondary drying, the details of which are shown in Tables 2.7, 2.8 and 2.9 respectively.

Freezing details	
t [min]	*T* [°C]
60	-52,0

Table 2.7: Freezing details.

Primary drying details			
Sequence	*t* [min]	*T* [°C]	*P* [µbar]
1	1200	-23,0	65
2	360	-10,0	65

Table 2.8: Primary drying details.

Secondary drying details			
Sequence	*t* [min]	*T* [°C]	*P* [µbar]
1	300	+37°C	65
2	480	+37°C	15

Table 2.9: Secondary drying details.

2.2.6.2 Experiment B

One tray of untreated vials filled with 5% w/w sucrose + 0,02% w/v Tween 80 and one tray of siliconized vials filled with the same solution were loaded on the shelves of the vacuum chamber of the freeze-dryer HETO DW 8030. These vials were equilibrated at a temperature T_n = -5°C and atmospheric pressure. When the vials reached T_n, the vacuum pump was switched on decreasing the pressure in the chamber to the value P_n. Once the P_n value was reached, the valve between the condenser and the vacuum chamber was closed, thus isolating the latter. After an amount of time equal to t_n the atmospheric pressure could be re-established in the vacuum chamber. The value of P_n was the smaller between the values of P_n corresponding to untreated and siliconized vials found in experiment 2 (determination of t_n) for the solution chosen at T_n = -5. The value of t_n was which that corresponded to P_n. Therefore, by the Table 2.10 can be seen that the lower value of P_n was 0,9 mbar to which corresponded a t_n of 1 s.

Type of vial	**Solution**	**Experiment**	**T_n [°C]**	**P_n [mbar]**	**t_n [s]**
S-	Suc + TW80	2	-5,0	1,0	0,0
S+	Suc + TW80	2	-5,0	0,9	1,0

Table 2.10: Values of P_n and t_n obtained in the experiment 2 (determination of t_n) for a solution 5% w/w sucrose + 0,02% w/v Tween 80.

To obtain the final product the vials were then subjected to freezing, primary drying and secondary drying. Once the secondary drying was completed, the freeze dryer automatically did the plugging of the vials to isolate the headspace of the vials by the vacuum chamber and so avoid that humidity could come in contact with the product unloading the freeze dryer.

2.2.6.2.1 Sample preparation

One tray composed of 378 untreated vials was filled with 5% w/w sucrose + 0,02% w/v Tween 80 and another tray composed of 378 siliconized vials was filled with the same solution. For the vials of both the trays the filling volume was 0,5 ml. Three probes of the Tempris sensor were inserted in three siliconized vials in the position shown in Figure 2.10 in order to monitor the temperature. The vials had to be partially stoppered with igloo stoppers (Helvoet FM 460 type) so that the headspace of the vials was in communication with the vacuum chamber. The tray of siliconized vials was placed on the central shelf of the vacuum chamber which occupies completely, while the tray of untreated vials on the shelf above.

2.2.6.2.2 Freezing procedure and cycle details

The freezing procedure and cycle details were the same as presented in the section 2.2.6.1.2.

2.2.6.3 Experiment C

One tray of siliconized vials filled with 5% w/w sucrose + 0,02% w/v Tween 80 was loaded on the shelf of the vacuum chamber of the freeze-dryer HETO DW 8030. These vials were equilibrated at a temperature T_n = 10°C and degassed. The solution was degassed directly inside the vials to avoid subsequent displacements that could nullify the effectiveness of the treatment. At the end of the degasification the pressure in the vacuum chamber was brought back to the atmospheric one and the vials were equilibrated at a temperature T_n = -5°C. When the vials reached T_n, the vacuum pump was switched on decreasing the pressure in the chamber to the value P_n. Once the P_n value was reached, the valve between the condenser and the vacuum chamber was closed, thus isolating the latter. After an amount of time equal to t_n the atmospheric pressure could be re-established in the vacuum chamber. The value of P_n was which found for a siliconized vial filled with 5% w/w sucrose + 0,02% w/v Tween 80 in the experiment 2 (determination of t_n) for the solution chosen at T_n = -5. The value of t_n was which that corresponded to P_n. Therefore, the value of P_n was 0,9 mbar to which correspond a t_n of 1 s as could be seen by the Table 2.10.

To obtain the final product the vials were then subjected to freezing, primary drying and secondary drying. Once the secondary drying was completed, the freeze dryer automatically did the plugging of the vials to isolate the headspace of the vials by the vacuum chamber and so avoid that humidity could come in contact with the product unloading the freeze dryer.

2.2.6.3.1 Sample preparation

One tray composed of 378 siliconized vials was filled with 5% w/w sucrose + 0,02% w/v Tween 80. The filling volume of the vials was 0,6 ml instead of 0,5 ml of the cases before to take into account the evaporation of the solution during the degasification. Three probes of the Tempris sensor were inserted in three vials in the position shown in Figure 2.11 in order to monitor the temperature. The vials had to be partially stoppered with igloo stoppers (Helvoet

FM 460 type) to put in communication the headspace of the vials with the vacuum chamber. The tray of siliconized vials was placed on the central shelf of the vacuum chamber which occupied completely.

2.2.6.3.2 Degasification procedure

The degasification procedure is the same as presented in section 2.2.5.2 in presence of Tween 80.

2.2.6.3.3 Freezing procedure and cycle details

The freezing procedure and cycle details are the same as presented in the section 2.2.6.1.2.

3. Results

3.1 Validation of the shelf

Following the procedure described in sections 2.2.1, the validation of the shelf 1 was done to detect if the temperature of the shelf is uniform or not.

From the result reported in Table 3.1 is possible to observe both the higher temperature on the right side of the shelf compared to the left side, and the slower cooling of the temperature of the walls which acted as a thermal flywheel.

	Left wall	Left side of the shelf	Middle of the shelf	Right side of the shelf	Right wall
***t* [min]**	***T* [°C]**				
0	15,1	4,3	4,7	5,4	15
5	14,8	4	4,2	4,7	14,7
10	14,6	4,2	4,3	4,5	14,4
15	14,4	4,2	4,3	4,4	14,2
20	14,1	1,2	2,3	3,5	13,9
25	13,6	-3,8	-2,5	-0,4	13,4
30	13	-8,2	-7,1	-4,7	12,9
35	12,1	-11,3	-10,8	-8,8	12,1
40	11,2	-10,4	-10,3	-9,8	11,2
45	10,8	-11	-10,7	-10,1	10,8

Table 3.1: Result of the shelf validation. The temperature data were taken from the Tempris sensor probes every 5 minutes from the beginning of the freezing phase. The probes were placed on the two side walls of the vacuum chamber and on the left, in the middle and on the right of the central shelf at a distance of 4 cm from the front edge.

The temperature gradient from the left to the right of the shelf was due to the path that the silicone oil took inside the shelf: the freshly cooled silicone fluid entered the shelf on the left side, flowed inside it following a coil and exited at a higher temperature on the right side of the shelf. As the silicone fluid flowed through the coil it cooled the shelf by heating itself, therefore the right side of the shelf, where was positioned the probe number 3, tended to be less cold than the left part of the shelf where was positioned the probe number 1. The position of the probes of the Tempris sensor can be seen in Figure 2.7, while the direction of circulation of the silicone oil is shown in Figure 3.1.

The shelf validation was performed starting from the vacuum chamber at room temperature, for this reason the wall temperature was so high and did not have time to reach values below zero. By performing several freezing cycles one after the other, the walls would cool down to temperatures below zero and would not have time to return to room temperature

during the loading phases. This condition corresponds to a thermal flywheel effect on the temperature inside the chamber opposite to that seen in the shelf validation experiment.

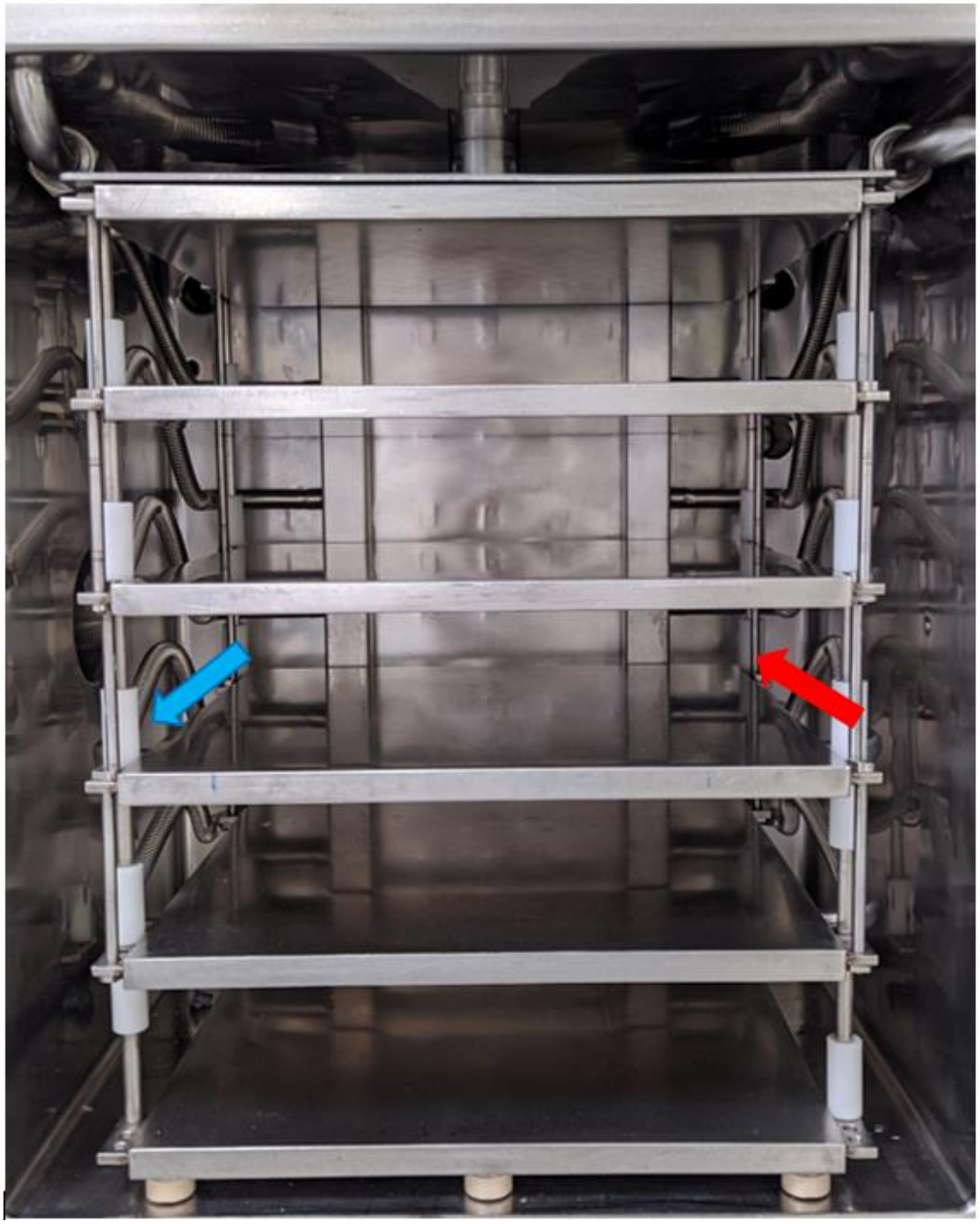

Figure 3.1: Shelves in the vacuum chamber. In the central shelf are highlighted with a blue arrow the tube that feeds the incoming cooled silicone oil, while with a red arrow the tube through which the silicone oil, no longer as cold as at the entrance, leaves the shelf.

3.2 Determination of P_{first} and P_{last} (Experiment 1)

Following the procedure fully described in sections 2.2.2, the experiment 1 was done to detect the pressure value at which nucleation is first observed in some vials and the pressure value at which the last vial nucleates for different formulations and type of vials. The nucleation was detected through visual inspection. At the time of the start of cooling the solution was transparent and clear. When the temperature was well below the equilibrium freezing point, nucleation occurred and the solution became opaque due to the presence of ice crystals. This

was the moment when pressure values were recorded. Following nucleation, the ice crystals grew and the colour of the product changed to milky-white with the completion of freezing.

The results achieved are summarized in Tables 3.2, 3.3, 3.4 and 3.5.

Type of vials	**Solution**	T_n **[°C]**	**Equilibration time [min]**	***T1*** **[°C]**	***T2*** **[°C]**	***T3*** **[°C]**	T_{mean} **[°C]**	P_{first} **[mbar]**	P_{last} **[mbar]**
S-	DW	-5,0	44,0	-5,0	-4,0	-3,7	-4,2	1,3	0,7
S-	DW	-10,0	46,0	-9,9	-10,0	-7,8	-9,2	1,3	0,8
S-	DW+TW80	-5,0	32,0	-5,0	-4,8	-2,8	-4,2	1,2	0,8
S-	DW+TW80	-10,0	46,0	-10,0	-9,9	-8,4	-9,4	1,3	0,8
S-	Suc	-5,0	34,0	-5,0	-5,0	-3,5	-4,5	1,2	0,8
S-	Suc	-10,0	44,0	-9,7	-10,0	-8,7	-9,5	1,2	0,8
S-	Suc+TW80	-5,0	60,0	-5,0	-4,8	-4,2	-4,7	1,2	1,0
S-	Suc+TW80	-10,0	57,0	-10,0	-9,5	-9,0	-9,5	1,2	0,9
S-	MAN	-5,0	44,0	-5,0	-4,8	-3,9	-4,6	1,2	0,7
S-	MAN	-10,0	47,0	-10,0	-10,0	-8,1	-9,4	1,0	0,7
S-	MAN+TW80	-5,0	38,0	-5,0	-4,8	-3,9	-4,6	1,1	0,7
S-	MAN+TW80	-10,0	48,0	-10,0	-9,7	-9,2	-9,6	1,1	0,7

Table 3.2: Experiment 1, results for untreated vials.

Type of vials	**Solution**	T_n **[°C]**	**Equilibration time [min]**	***T1*** **[°C]**	***T2*** **[°C]**	***T3*** **[°C]**	T_{mean} **[°C]**	P_{first} **[mbar]**	P_{last} **[mbar]**
ST	DW	-5,0	46,0	-5,0	-4,4	-4,0	-4,5	1,2	0,9
ST	DW	-10,0	65,0	-9,9	-10,0	-9,4	-9,8	1,3	0,9
ST	DW+TW80	-5,0	42,0	-5,0	-4,9	-4,2	-4,7	1,2	0,9
ST	DW+TW80	-10,0	91,0	-10,0	-9,3	-9,1	-9,5	1,3	0,8
ST	Suc	-5,0	41,0	-5,0	-4,8	-4,3	-4,7	1,1	0,8
ST	Suc	-10,0	70,0	-10,0	-9,9	-9,4	-9,8	1,1	0,8
ST	Suc+TW80	-5,0	40,0	-5,0	-4,9	-4,2	-4,7	1,2	0,9
ST	Suc+TW80	-10,0	103,0	-10,0	-9,7	-9,5	-9,7	1,3	0,9
ST	MAN	-5,0	41,0	-5,0	-4,9	-4,5	-4,8	1,2	0,6
ST	MAN	-10,0	68,0	-10,0	-9,9	-9,6	-9,8	1,3	0,7
ST	MAN+TW80	-5,0	40,0	-5,0	-4,9	-4,7	-4,9	1,2	0,7
ST	MAN+ TW80	-10,0	65,0	-9,9	-10,0	-9,6	-9,8	1,2	0,7

Table 3.3: Experiment 1, results for sulphate treated vials.

Type of vials	Solution	T_n [°C]	Equilibration time [min]	*T1* [°C]	*T2* [°C]	*T3* [°C]	T_{mean} [°C]	P_{first} [mbar]	P_{last} [mbar]
S+	DW	-5,0	40,0	-5,0	-4,3	-3,7	-4,3	1,2	0,8
S+	DW	-10,0	46,0	-10,0	-9,7	-9,2	-9,6	1,2	0,9
S+	DW+TW80	-5,0	40,0	-5,0	-4,9	-4,6	-4,8	1,2	0,9
S+	DW+TW80	-10,0	49,0	-10,0	-9,9	-9,5	-9,8	1,1	0,8
S+	Suc	-5,0	37,0	-5,2	-4,8	-4,3	-4,8	1,1	0,8
S+	Suc	-10,0	59,0	-10,0	-10,0	-9,5	-9,8	1,0	0,8
S+	Suc +TW80	-5,0	40,0	-5,0	-4,8	-4,3	-4,7	1,2	0,8
S+	Suc +TW80	-10,0	49,0	-10,0	-9,9	-9,2	-9,7	1,1	0,9
S+	MAN	-5,0	40,0	-5,2	-4,9	-4,2	-4,8	1,1	0,6
S+	MAN	-10,0	55,0	-10,0	-9,7	-9,3	-9,7	1,2	0,8
S+	MAN+TW80	-5,0	42,0	-5,0	-5,0	-4,4	-4,8	1,1	0,8
S+	MAN+TW80	-10,0	61,0	-9,8	-10,0	-9,7	-9,8	1,2	0,8

Table 3.4: Experiment 1, results for siliconized vials.

Type of vials	Solution	T_n [°C]	Equilibration time [min]	*T1* [°C]	*T2* [°C]	*T3* [°C]	T_{mean} [°C]	P_{first} [mbar]	P_{last} [mbar]
TL	DW	-5,0	44,0	-5,0	-5,0	-4,8	-4,9	1,3	1,2
TL	DW	-10,0	47,0	-10,0	-9,8	-9,3	-9,7	1,2	0,9
TL	DW+TW80	-5,0	37,0	-5,0	-4,8	-4,2	-4,7	1,3	0,7
TL	DW+TW80	-10,0	48,0	-10,0	-9,7	-9,3	-9,7	1,2	0,8
TL	Suc	-5,0	38,0	-5,0	-5,0	-4,5	-4,8	1,2	0,9
TL	Suc	-10,0	47,0	-10,0	-10,0	-9,5	-9,8	1,1	0,8
TL	Suc+TW80	-5,0	35,0	-5,0	-4,9	-4,0	-4,6	1,1	0,7
TL	Suc+TW80	-10,0	48,0	-10,0	-10,0	-9,3	-9,8	1,2	0,8
TL	MAN	-5,0	41,0	-5,0	-4,9	-4,3	-4,7	1,1	0,8
TL	MAN	-10,0	51,0	-10,0	-10,0	-9,2	-9,7	1,2	0,8
TL	MAN+TW80	-5,0	39,0	-5,0	-4,7	-4,0	-4,6	0,9	0,7
TL	MAN+TW80	-10,0	50,0	-10,0	-9,8	-9,1	-9,6	1,1	0,7

Table 3.5: Experiment 1, results for TopLyo® vials.

For the P_{first} determination, pressure values, which may be slightly higher than those chosen but also up to 5-6 mbar, were often discarded. This was done because these were isolated values due to stochastic nature of nucleation and/or possible presence of impurities in the vials. The nucleation pressure values of the vials containing probes of the Tempris sensor were also discarded from the choice because the probes acted as nucleating agents favouring nucleation. In the case of T_n = -10 °C, the nucleation of the vials containing the probes occurred frequently before reaching T_n and therefore at atmospheric pressure.

Again, due to the stochastic nature of nucleation, by repeating the experiment it was possible to obtain small variations in the results.

The average of the equilibration time is about 40 minutes if T_n = -5 °C or slightly more than 50 minutes if T_n = -10 °C. Its wide oscillation is due to when the experiment was performed. If the experiment was carried out after a period of inactivity of the freeze-dryer it took longer because the walls of the vacuum chamber initially at room temperature acted as a thermal flywheel slowing down the cooling of the environment inside the vacuum chamber. On the other hand, if the experiments were carried out in succession the walls once cooled acted as a thermal flywheel reducing the time required for the solution to reach thermal equilibrium.

Again, due to the thermal flywheel action carried out by the walls of the vacuum chamber the T_{mean}, which is the average of *T1*, *T2* and *T3*, it is more distant from T_n if it is the first cycle after some hours of inactivity of the freeze dryer.

Observing the temperature values detected by the probes of the Tempris sensor, it is possible to note that *T1* reaches almost always T_n, *T2* is usually very close to *T1*, while the value of *T3* differs from the previous ones. The reason for this lies in the position of the vials containing the probes on the shelf. The vial containing probe 1, which provides the temperature value *T1*, was located on the left side of the shelf which, as seen in section 3.1, was at a lower temperature than the right side of the shelf where was the vial containing probe 3. Therefore, if the shelf is colder, the vials above it will reach lower temperatures first.

Through the Table 3.6 is easier to visualize and compare experiment done with different T_n and type of vial.

		S-		ST		S+		TL	
Solution	***T_n* [°C]**	***P_{first}* [mbar]**	***P_{last}* [mbar]**	***P_{first}* [mbar]**	***P_{last}* [mbar]**	***P_{first}* [mbar]**	***P_{last}* [mbar]**	***P_{first}* [mbar]**	***P_{last}* [mbar]**
DW	-5,0	1,3	0,7	1,2	0,9	1,2	0,8	1,3	1,2
DW	-10,0	1,3	0,8	1,3	0,9	1,2	0,9	1,2	0,9
DW+TW80	-5,0	1,2	0,8	1,2	0,9	1,2	0,9	1,3	0,7
DW+TW80	-10,0	1,3	0,8	1,3	0,8	1,1	0,8	1,2	0,8
Suc	-5,0	1,2	0,8	1,1	0,8	1,1	0,8	1,2	0,9
Suc	-10,0	1,2	0,8	1,1	0,8	1,0	0,8	1,1	0,8
Suc + TW80	-5,0	1,2	1,0	1,2	0,9	1,2	0,8	1,1	0,7
Suc + TW80	-10,0	1,2	0,9	1,3	0,9	1,1	0,9	1,2	0,8
MAN	-5,0	1,2	0,7	1,2	0,6	1,1	0,6	1,1	0,8
MAN	-10,0	1,0	0,7	1,3	0,7	1,2	0,8	1,2	0,8
MAN + TW80	-5,0	1,1	0,7	1,2	0,7	1,1	0,8	0,9	0,7
MAN + TW80	-10,0	1,1	0,7	1,2	0,7	1,2	0,8	1,1	0,7

Table 3.6: Schematic representation of the results of experiment 1.

By following the horizontal lines in the Table 3.6, it can be seen that there is no marked influence of the type of vials on P_{first} and P_{last} with the same solution used.

Analysing the vertical lines of the Table 3.6, it can be noticed that, with the same T_n and type of vial, the P_{first} and P_{last} values are slightly lower if a solute (sucrose or mannitol) is added to the solvent (water). In particular, the mannitol-containing solutions are which with the lowest pressure values. By adding a non-volatile solute to a solvent, nucleation occurs at lower temperatures (freezing-point depression) than in the case of a pure solvent. This is caused by a decrease in chemical potential or equivalently by a decrease in vapor pressure; both are related

to pressure. In order to reach a lower temperature in the solution in the vials, greater evaporation is required which is obtained at lower pressures in the vacuum chamber.

Looking at table 3.6, keeping the solution and the type of vial constant, the nucleation pressure is slightly higher for T_n = -10 °C than for T_n = -5. Again, a decrease in pressure causes an increase in the evaporation of the solution which, being an endothermic process, lowers the temperature of the solution promoting ice nucleation. Therefore, if the starting temperature of the solution is lower the decrease of the pressure necessary for the nucleation of the solution is lower.

In some types of vials, with certain solutions, boiling and/or bubbling phenomena could be observed during the lowering of the pressure in the vacuum chamber.

Decreasing the pressure in the chamber promotes the degassing of the solution in the vials. For pressures below 50 mbar, small bubbles form between the internal surface of the vials and the solution as can be seen in Figure 3.2.

Figure 3.2: Small bubble in TopLyo® vial filled with Demineralized water + 0,02% w/v Tween 80 with a pressure exerted on the liquid of 30 mbar.

These bubbles continue to grow by decreasing the pressure until they release from 10 mbar going up the bottle and bursting, as can be seen in Figure 3.3. This phenomenon, identified with the name of bubbling, stops for pressures equal to 2-3 mbar.

Figure 3.3: Bubble going up and bursting into untreated vial filled with 5% w/w mannitol+ 0,02% w/v Tween 80 with a pressure exerted on the liquid of 6 mbar.

The other phenomenon observable by decreasing the pressure in the vacuum chamber is boiling. When a liquid reaches its boiling point, its vaporization occurs. The boiling point is the temperature at which the vapor pressure of the liquid is equal to the pressure exerted on the liquid by the surrounding atmosphere. By decreasing the pressure from 35-40 mbar very small bubbles begin to form on the bottom of the vials as can be seen in Figure 3.4. These grow to rise into the surface and burst into the air since 10 mbar to the end of the nucleation as can be seen in Figure 3.5.

Figure 3.4: Small bubble in TopLyo® vial filled with 5% w/w sucrose+ 0,02% w/v Tween 80 with a pressure exerted on the liquid of 20 mbar.

Figure 3.5: Bubble rising and bursting in TopLyo® vial filled with demineralized water with a pressure exerted on the liquid of 4 mbar.

.

Both bubbling and boiling can influence the morphology of the cake. Being both tumultuous processes these phenomena can lead to nucleation of the solution, this is particularly evident in the case of boiling. In Figure 3.6 are reported a series of vials containing irregular cakes nucleated because of boiling, while in Figure 3.7 is reported a vial with a regular cake of the same batch, which was not nucleated because of boiling.

Figure 3.6: Irregular cake in TopLyo® vials filled with demineralized water; the nucleation occurred because of the boiling.

Figure 3.7: Regular cake in TopLyo® vials filled with demineralized water; the nucleation didn't occur because of the boiling.

The presence and intensity of these phenomena was reported, for the cases analysed by experiment 1, in tables 3.7, 3.8, 3.9, 3.10. As regards the presence of boiling and bubbling, the classification includes:

- absent: observed in no vials (the 3 vials containing probes were not counted);
- isolated: observed in less than one third of vials (the 3 vials containing probes were not counted);
- widespread: observed in more one third of vials (the 3 vials containing probes were not counted).

As regards the intensity of boiling and bubbling, the classification includes:

- weak: low frequency of the phenomenon that slightly agitates the solution.
- moderate: phenomenon with a relevant frequency that agitates the solution.
- strong: very tumultuous phenomenon which can lead to the nucleation of some vials and influence the morphology of those cakes.

Type of vials	**Solution**	T_n [°C]	**Bubbling**		**Boiling**	
			Diffusion	Intensity	Diffusion	Intensity
S-	DW	-5,0	Absent		Absent	
S-	DW	-10,0	Absent		Absent	
S-	DW+TW80	-5,0	Isolated	Moderate	Absent	
S-	DW+TW80	-10,0	Isolated	Moderate	Absent	
S-	Suc	-5,0	Isolated	Moderate	Absent	
S-	Suc	-10,0	Isolated	Weak	Absent	
S-	Suc + TW80	-5,0	Isolated	Moderate	Absent	
S-	Suc + TW80	-10,0	Isolated	Moderate	Absent	
S-	MAN	-5,0	Widespread	Moderate	Absent	
S-	MAN	-10,0	Isolated	Weak	Absent	
S-	MAN + TW80	-5,0	Widespread	Moderate	Absent	
S-	MAN + TW80	-10,0	Widespread	Moderate	Absent	

Table 3.7: Diffusion and intensity of bubbling and boiling phenomena for untreated vials.

Type of vials	Solution	T_n [°C]	Bubbling		Boiling	
			Diffusion	Intensity	Diffusion	Intensity
ST	DW	-5,0	Absent		Absent	
ST	DW	-10,0	Absent		Absent	
ST	DW+TW80	-5,0	Widespread	Moderate	Absent	
ST	DW+TW80	-10,0	Widespread	Weak	Absent	
ST	Suc	-5,0	Isolated	Weak	Absent	
ST	Suc	-10,0	Isolated	Weak	Absent	
ST	Suc + TW80	-5,0	Isolated	Moderate	Absent	
ST	Suc + TW80	-10,0	Isolated	Weak	Absent	
ST	MAN	-5,0	Absent		Absent	
ST	MAN	-10,0	Absent		Absent	
ST	MAN + TW80	-5,0	Isolated	Moderate	Absent	
ST	MAN + TW80	-10,0	Isolated	Weak	Absent	

Table 3.8: Diffusion and intensity of bubbling and boiling phenomena for sulphate treated vials.

Regarding the non-siliconized vials from tables 3.6 and 3.7 some considerations can be made. Boiling is never present in untreated and sulphate treated vials thanks to the strong interactions between the internal surface of the vials and the solutions contained in them. Instead, bubbling is always present except for demineralized water and 5% w/w mannitol only in sulphate treated vials. The cases in which bubbling is more intense are those of solutions containing Tween 80. This is because surfactants are compound that lower the surface tension of the liquid facilitating the formation of foam and prevent the bubble rupture thanks to their amphiphilic nature. Also, sucrose and mannitol may be related to the phenomenon of bubbling. Sucrose inhibits bubble coalescence over a concentration range 0.01-0.3 M (Henry and Craig, 2009): the concentration of sucrose in the solutions tested is about 0,15 M and therefore is in the range. Henry and Craig suggested that the bubble coalescence inhibition may be related to the partitioning of the osmolytes at the air-water interface, while there is no correlation with the increasing of the surface tension gradient or with electrostatic mechanism. No evidence has been found in the literature for mannitol and no clear relationship between this excipient and bubbling can be derived from the experiments done.

Bubbling is generally weaker for T_n = -10 °C than for T_n = -5 °C. An explanation for this may be related to the fact that at lower temperature more air can be dissolved in the solution and less is therefore released. Finally, it can be observed that bubbling is slightly less widespread and intense in the sulphate treated vials than in the untreated ones.

As for siliconized and TopLyo® vials, the results of which are shown in tables 3.6 and 3.7, bubbling is always present except for demineralized water and 5% w/w mannitol only in sulphate treated vials. Also, for these types of vials the cases in which the bubbling is more intense are those with which the solutions contain Tween 80 and the bubbling is generally a little weaker for T_n = -10 °C than for T_n = -5 °C.

Boiling is always present if there is no Tween 80. Tween 80 improves the wettability of the internal surface of the vials thanks to its amphiphilic properties. Boiling is more widespread and more intense in TopLyo® vials than in siliconized ones. This is due to the greater contact angle and therefore to the greater hydrophobicity of the former which minimize the interactions between the solution and the container, facilitating boiling.

Type of vials	Solution	T_n [°C]	Bubbling		Boiling	
			Diffusion	Intensity	Diffusion	Intensity
S+	DW	-5,0	Absent		Isolated	Weak
S+	DW	-10,0	Absent		Isolated	Weak
S+	DW+TW80	-5,0	Widespread	Moderate	Absent	
S+	DW+TW80	-10,0	Widespread	Moderate	Absent	
S+	Suc	-5,0	Isolated	Moderate	Isolated	Weak
S+	Suc	-10,0	Isolated	Weak	Isolated	Weak
S+	Suc + TW80	-5,0	Widespread	Moderate	Absent	
S+	Suc + TW80	-10,0	Widespread	Moderate	Absent	
S+	MAN	-5,0	Isolated	Moderate	Isolated	Weak
S+	MAN	-10,0	Isolated	Weak	Isolated	Weak
S+	MAN + TW80	-5,0	Widespread	Moderate	Absent	
S+	MAN + TW80	-10,0	Widespread	Moderate	Absent	

Table 3.9: Diffusion and intensity of bubbling and boiling phenomena for siliconized vials.

Type of vials	Solution	T_n [°C]	Bubbling		Boiling	
			Diffusion	Intensity	Diffusion	Intensity
TL	DW	-5,0	Absentent		Widespread	Strong
TL	DW	-10,0	Absentent		Widespread	Strong
TL	DW+TW80	-5,0	Widespread	Strong	Absentent	
TL	DW+TW80	-10,0	Widespread	Moderate	Absentent	
TL	Suc	-5,0	Isolated	Moderate	Widespread	Strong
TL	Suc	-10,0	Isolated	Moderate	Widespread	Strong
TL	Suc + TW80	-5,0	Widespread	Strong	Absentent	
TL	Suc + TW80	-10,0	Widespread	Strong	Absentent	
TL	MAN	-5,0	Absentent		Widespread	Strong
TL	MAN	-10,0	Absentent		Widespread	Strong
TL	MAN + TW80	-5,0	Widespread	Strong	Absentent	
TL	MAN + TW80	-10,0	Widespread	Strong	Absentent	

Table 3.9: Diffusion and intensity of bubbling and boiling phenomena for TopLyo® vials.

In the case of water, a curve relating to the water boiling point as a function of pressure is shown in Figure 3.8. In this figure have been highlighted the temperatures of -10°C and -5°C (values of T_n) and the corresponding pressure values. The boiling point at T_n = -10 °C is between 2 and 3 mbar, while at T_n = -5 °C it is slightly less than 5 mbar. In experiment 1 the bubbles started to release, for both T_n, when the pressure in the chamber dropped below 10 mbar.

The addition of a non-volatile solute, such as mannitol or sucrose, causes an increase in the boiling point (boiling point elevation) compared to the case of the solvent only. This is due to a decrease in the chemical potential or equivalently to a decrease in the vapor pressure. An increase in the boiling point translates into an upward translation of the curve represented in

Figure 3.8. Consequently, for the same T_n, the boiling occurs for lower pressure values. The boiling point elevation increases as the solute concentration increases. At atmospheric pressure, for a solution of 5% w/w sucrose the boiling point elevation is a degree of magnitude lower than a centigrade degree (Holven, 1936; Tressler *et al*., 1941). Furthermore, with the same concentration of solute, the increase in the boiling point decreases with decreasing pressure (Crapiste and Lozano, 1988). Therefore, the variations of the boiling point between the solutions used are negligible.

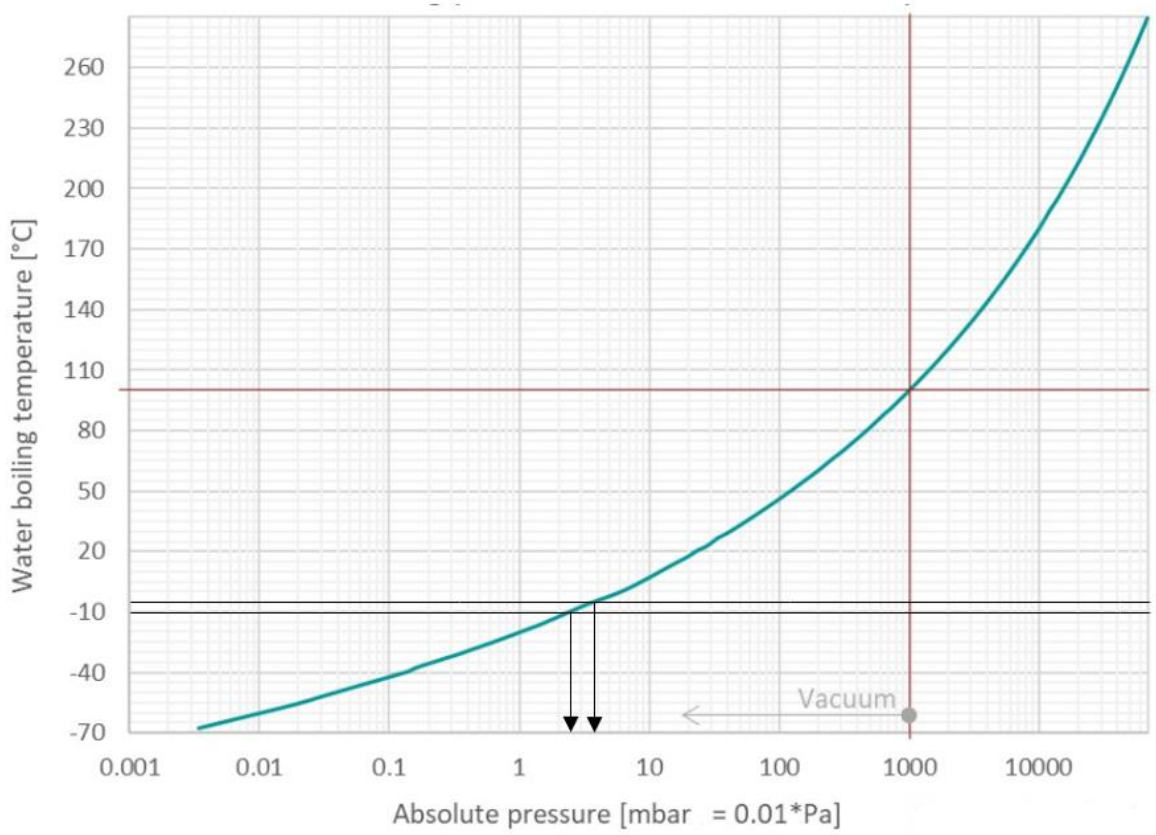

Figure 3.8: Water boiling point as a function of pressure. Figure taken from: https://www.engineeringtoolbox.com/boiling-point-water-d_926.html?vA=0%2C003&units=B#

Another phenomenon observed in the experiment 1 was the fogging, introduced in section 1.9. This cosmetic defect was observed in untreated vials and, to a greater extent, in sulphate treated vials. The causes of fogging are not to be found in bubbling, in fact it occurred even when bubbling was absent, but in the contact angles of the glass surfaces. Fogging is relevant for low contact angles; this is demonstrated by the fact that the phenomenon was absent for siliconized and TopLyo® vials that because of their treatment have hydrophobic surfaces. Hydrophobic surfaces tend to be less wetted by an aqueous solution (Langer *et al*., 2020). From experiment one it emerged that solutions containing mannitol are those for which fogging is more evident.

Figure 3.9 shows on the left sulphate treated vials, while on the right TopLyo vials both filled with 5% w/w mannitol; the vials were just nucleated. Looking at the different transparency of the vials, it is clear that the sulphate treated vials present fogging which is absent in the TopLyo ones.

Figure 3.9: On the left there are sulphate treated vials, while on the right TopLyo® vials both filled with 5% w/w mannitol; the vials were just nucleated.

3.3 Determination of t_n (Experiment 2)

Following the procedure fully described in sections 2.2.3 the experiment 2 was done to detect, for a given solution and a type of vial, the pressure value P_n for which at least 70% of the vials nucleate and the time t_n required for the nucleation at this pressure. The nucleation was detected through visual inspection, in the same way as in experiment 1.

The results achieved are summarized in Tables 3.10, 3.11, 3.12 and 3.13.

Type of vials	Solution	T_n [°C]	P_n [mbar]	t_n [s]	% vials nucleated	Result	Formula
S-	DW	-5,0	1,1	17,0	100%	success	Pn=Pf-(Pf-Pl)/3
S-	DW	-10,0	1,1	15,0	100%	success	Pn=Pf-(Pf-Pl)/3
S-	DW+TW80	-5,0	1,1	21,0	76%	success	Pn=Pf-(Pf-Pl)/3
S-	DW+TW80	-10,0	1,1	7,0	47%	fail	Pn=Pf-(Pf-Pl)/3
S-	DW+TW80	-10,0	1,0	0,0	100%	success	Pn=Pf-(Pf-Pl)/2
S-	Suc	-5,0	1,1	4,0	12%	fail	Pn=Pf-(Pf-Pl)/3
S-	Suc	-5,0	1,0	1,0	100%	success	Pn=Pf-(Pf-Pl)/2
S-	Suc	-10,0	1,0	2,0	82%	success	Pn=Pf-(Pf-Pl)/2
S-	Suc + TW80	-5,0	1,1	2,0	47%	fail	Pn=Pf-(Pf-Pl)/2
S-	Suc + TW80	-5,0	1,0	0,0	100%	success	Pn=Pf-(Pf-Pl)/1,5
S-	Suc + TW80	-10,0	1,0	1,0	100%	success	Pn=Pf-(Pf-Pl)/1,5
S-	MAN	-5,0	0,9	4,0	100%	success	Pn=Pf-(Pf-Pl)/2
S-	MAN	-10,0	0,8	0,0	100%	success	Pn=Pf-(Pf-Pl)/2
S-	MAN + TW80	-5,0	0,9	28,0	94%	success	Pn=Pf-(Pf-Pl)/2
S-	MAN + TW80	-10,0	0,9	21,0	88%	success	Pn=Pf-(Pf-Pl)/2

Table 3.10: Experiment 2, results for untreated vials.

Type of vials	Solution	T_n [°C]	P_n [mbar]	t_n [s]	% vials nucleated	Result	Formula
ST	DW	-5,0	1,0	12,0	100%	success	Pn=Pf-(Pf-Pl)/2
ST	DW	-10,0	1,1	4,0	88%	success	Pn=Pf-(Pf-Pl)/2
ST	DW+TW80	-5,0	1,0	5,0	71%	success	Pn=Pf-(Pf-Pl)/1,5
ST	DW+TW80	-10,0	1,0	3,0	88%	success	Pn=Pf-(Pf-Pl)/1,5
ST	Suc	-5,0	0,9	1,0	88%	success	Pn=Pf-(Pf-Pl)/1,5
ST	Suc	-10,0	0,9	9,0	100%	success	Pn=Pf-(Pf-Pl)/1,5
ST	Suc + TW80	-5,0	1,0	2,0	82%	success	Pn=Pf-(Pf-Pl)/1,5
ST	Suc + TW80	-10,0	1,0	2,0	100%	success	Pn=Pf-(Pf-Pl)/1,5
ST	MAN	-5,0	0,8	2,0	100%	success	Pn=Pf-(Pf-Pl)/1,5
ST	MAN	-10,0	0,9	58,0	100%	success	Pn=Pf-(Pf-Pl)/1,5
ST	MAN + TW80	-5,0	0,9	57,0	59%	fail	Pn=Pf-(Pf-Pl)/2
ST	MAN + TW80	-5,0	0,8	4,0	88%	success	Pn=Pf-(Pf-Pl)/1,5
ST	MAN + TW80	-10,0	0,8	1,0	100%	success	Pn=Pf-(Pf-Pl)/1,5

Table 3.11: Experiment 2, results for sulphate treated vials.

Type of vials	Solution	T_n [°C]	P_n [mbar]	t_n [s]	% vials nucleated	Result	Formula
S+	DW	-5,0	1,0	1,0	100%	success	Pn=Pf-(Pf-Pl)/2
S+	DW	-10,0	1,1	9,0	94%	success	Pn=Pf-(Pf-Pl)/3
S+	DW+TW80	-5,0	1,0	80,0	59%	fail	Pn=Pf-(Pf-Pl)/1,5
S+	DW+TW80	-5,0	0,9	24,0	88%	success	Pn=Pf-(Pf-Pl)/1
S+	DW+TW80	-10,0	0,9	1,0	94%	success	Pn=Pf-(Pf-Pl)/1,5
S+	Suc	-5,0	0,9	7,0	88%	success	Pn=Pf-(Pf-Pl)/1,5
S+	Suc	-10,0	0,9	8,0	100%	success	Pn=Pf-(Pf-Pl)/2
S+	Suc + TW80	-5,0	0,9	1,0	88%	success	Pn=Pf-(Pf-Pl)/1,5
S+	Suc + TW80	-10,0	1,0	1,0	100%	success	Pn=Pf-(Pf-Pl)/2
S+	MAN	-5,0	1,0	24,0	100%	success	Pn=Pf-(Pf-Pl)/1,5
S+	MAN	-10,0	1,0	30,0	88%	success	Pn=Pf-(Pf-Pl)/2
S+	MAN + TW80	-5,0	0,9	1,0	47%	fail	Pn=Pf-(Pf-Pl)/1,5
S+	MAN + TW80	-5,0	0,8	1,0	53%	fail	Pn=Pf-(Pf-Pl)/1
S+	MAN + TW80	-5,0	0,7	1,0	100%	success	Pn < Pl
S+	MAN + TW80	-10,0	1,0	0,0	35%	fail	Pn=Pf-(Pf-Pl)/2
S+	MAN + TW80	-10,0	0,9	2,0	76%	success	Pn=Pf-(Pf-Pl)/1,5

Table 3.12: Experiment 2, results for siliconized vials.

Type of vials	Solution	T_n [°C]	P_n [mbar]	t_n [s]	% vials nucleated	Result	Formula
TL	DW	-5,0	1,2	26,0	100%	success	Pn=Pf-(Pf-Pl)/1
TL	DW	-10,0	1,0	3,0	100%	success	Pn=Pf-(Pf-Pl)/1,5
TL	DW+TW80	-5,0	0,9	28,0	88%	success	Pn=Pf-(Pf-Pl)/1,5
TL	DW+TW80	-10,0	0,9	1,0	100%	success	Pn=Pf-(Pf-Pl)/1,5
TL	Suc	-5,0	1,0	31,0	76%	success	Pn=Pf-(Pf-Pl)/1,5
TL	Suc	-10,0	0,9	0,0	94%	success	Pn=Pf-(Pf-Pl)/1,5
TL	Suc + TW80	-5,0	0,8	7,0	100%	success	Pn=Pf-(Pf-Pl)/1,5
TL	Suc + TW80	-10,0	0,9	0,0	94%	success	Pn=Pf-(Pf-Pl)/1,5
TL	MAN	-5,0	0,9	0,0	100%	success	Pn=Pf-(Pf-Pl)/1,5
TL	MAN	-10,0	1,0	17,0	76%	success	Pn=Pf-(Pf-Pl)/2
TL	MAN + TW80	-5,0	0,7	0,0	94%	success	Pn=Pf-(Pf-Pl)/1
TL	MAN + TW80	-10,0	0,8	3,0	76%	success	Pn=Pf-(Pf-Pl)/1,5

Table 3.13: Experiment 2, results for TopLyo® vials.

From the tables showing the results of experiment 2, the data relating to *T1*, *T2*, *T3* and T_{mean} have been omitted for reasons of space and clarity. Their trends, and consequently the considerations on them, are analogous to those of experiment 1 developed in the section 3.2. The same applies to the bubbling and boiling phenomena that occurred with the same diffusivity and intensity of experiment 1.

To calculate the percentage of vials nucleated, both in the number of nucleated vials and in the total number of vials are not counted those containing probes of the Tempris sensor because these act as nucleating agents favouring nucleation.

If 100% of nucleated vials had not been obtained, 300 seconds were waited before the end of experiment 2. The tables show for each case the value of t_n corresponding to the time duration between chamber insulation and nucleation of the last vial. Generally, t_n does not vary much and is quite small: the average between the various solutions settles on 9 seconds for the different type of vials, as shown in Figure 3.10. The optimal duration for vacuum is less than 1 min because a longer time, such as 1.5 min can produce blow-up of the frozen cake and flake formation on the product surface (Oddone *et al*., 2020). If the time t_n is zero, it means that at the time of the vacuum chamber isolation all the vials were already nucleated and therefore the chamber could also had been isolated a few moments earlier. The percentage of nucleated vials is not always 100%. This is partly because the P_n values are almost always higher than those of P_{last} found by experiment 1, partly due to the fact that the pressure inside the vacuum chamber tends to increase over time due to evaporation of the solutions. If the nucleation of 100% of the vials is obtained at a pressure P_n higher than P_{last}, it is because by keeping the pressure at values close to P_n the evaporation continues and with it the decrease of the temperature in the solution up to nucleation. The pressure increase effect obtained by isolating the vacuum chamber from the condenser is intended to reduce the blow-out phenomena thanks to a slower evaporation rate. Given an experiment 2 performed with untreated vials filled with 5% w/w sucrose + 0,02% w/v Tween 80, at T_n = -5 and P_n = 1 mbar, after about 20 seconds from the insulation of the vacuum chamber the pressure inside it reached 2 mbar, after 160 seconds it reached 3 mbar and remained the same for up to 300 seconds (time limit of experiment 2).

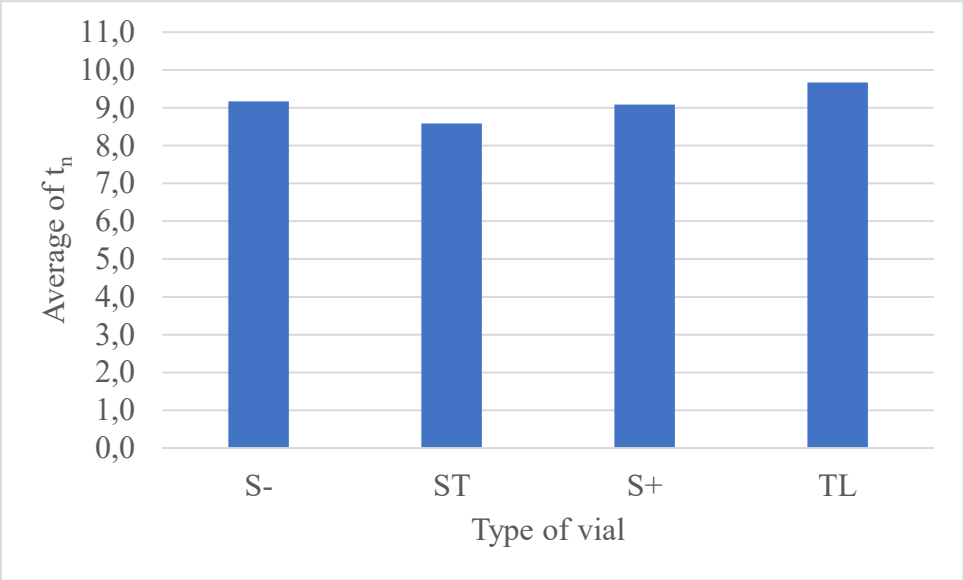

Figure 3.10: Average of the time t_n required to induce the nucleation of the vials with the same type of vial and different solutions.

The P_n value is generally between P_{first} and P_{last}, from which it is calculated using the Formula 2.1. However, there was an exception in which not all the vials in the chamber were nucleated by a value of P_n=P_{last}, therefore lower pressures had to be used. This is a demonstration of the stochastic nature of nucleation which can occur for different P_n repeating the experiment.

Figure 3.11 shows the average, among the various solutions, of the values of c for the various types of vials. For untreated vials, nucleation occurs for P_n values closer to P_{first} than to P_{last}, while for other types of vials P_n is about half between P_{first} and P_{last} (c = 1,5).

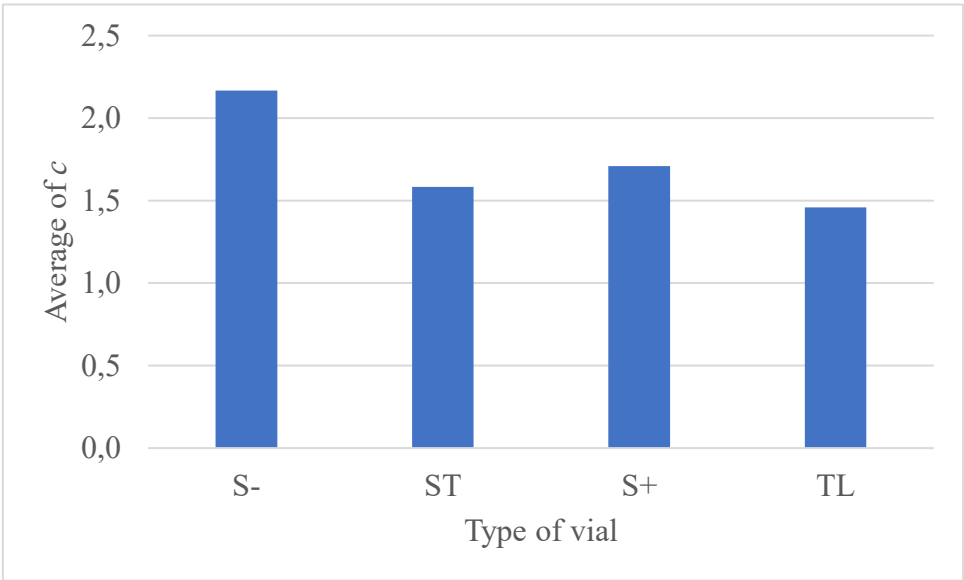

Figure 3.11: Average, among the various solutions, of the values of c for the various types of vials.

Through the Table 3.14 is easier to visualize and compare the value of P_n obtained by the experiment 2 done with different T_n, solutions, and type of vials.

		S-	ST	S+	TL
Solution	***T*$_n$ [°C]**	***P*$_n$ [mbar]**	***P*$_n$ [mbar]**	***P*$_n$ [mbar]**	***P*$_n$ [mbar]**
DW	-5,0	1,1	1,0	1,0	1,2
DW	-10,0	1,1	1,1	1,1	1,0
DW+TW80	-5,0	1,1	1,0	0,9	0,9
DW+TW80	-10,0	1,0	1,0	0,9	0,9
Suc	-5,0	1,0	0,9	0,9	1,0
Suc	-10,0	1,0	0,9	0,9	0,9
Suc + TW80	-5,0	1,0	1,0	0,9	0,8
Suc + TW80	-10,0	1,0	1,0	1,0	0,9
MAN	-5,0	0,9	0,8	1,0	0,9
MAN	-10,0	0,8	0,9	1,0	1,0
MAN + TW80	-5,0	0,9	0,8	0,7	0,7
MAN + TW80	-10,0	0,9	0,8	0,9	0,8

Table 3.14: Schematic representation of the values of P_n obtained by experiment 2.

By following the horizontal lines in the Table 3.14, it can be seen that there is no marked influence of the type of vials on P_n with the same solution used.

Analysing the vertical lines of the Table 3.6, it can be noticed that, with the same T_n and type of vial, the values of P_n are similar for the different solutions, only those of the solutions containing mannitol are slightly lower than the others. As explained in the section 3.2 the consequence of adding a non-volatile solute to a solvent is a freezing-point depression.

Due to the low P_n values it is possible that after the nucleation the cake rises inside the vial, as shown in Figure 3.12. The phenomenon is known as "blow up of the cake" or "flying cake". In case of blow up with solutions containing Tween 80 remains of solution not yet solidified may form bubbles under the cake that solidify with this morphology, as shown in Figure 3.13. The blow up of the cake should be avoided because it leads to an unacceptable product.

Tables 3.15 and 3.16 show the presence of blow up of the cake for the combinations of solutions and types of vials tested in experiment 2. By comparing them it is possible to notice that the blow up is not related to the value of t_n, but to the type of vials. For untreated and sulphate treated vials there is generally no presence of blow up, which instead is usually present in siliconized and TopLyo® vials. This is because the last two types of vials, thanks to the hydrophobic coatings, are very homogeneous thus reducing the friction between the cake and the internal surface of the container. So, for the same P_n value in a vial with a silicone coating, blow up can occur, which instead is not present in a vial without silicone coating.

		S-			ST		
Solution	T_n **[°C]**	P_n **[mbar]**	t_n **[s]**	**Blow up**	P_n **[mbar]**	t_n **[s]**	**Blow up**
DW	-5,0	1,1	17,0	absent	1,0	12,0	absent
DW	-10,0	1,1	15,0	absent	1,1	4,0	absent
DW+TW80	-5,0	1,1	21,0	absent	1,0	5,0	absent
DW+TW80	-10,0	1,0	0,0	absent	1,0	3,0	absent
Suc	-5,0	1,0	1,0	absent	0,9	1,0	absent
Suc	-10,0	1,0	2,0	present	0,9	9,0	absent
Suc + TW80	-5,0	1,0	0,0	present	1,0	2,0	absent
Suc + TW80	-10,0	1,0	1,0	present	1,0	2,0	absent
MAN	-5,0	0,9	4,0	absent	0,8	2,0	absent
MAN	-10,0	0,8	0,0	absent	0,9	58,0	absent
MAN + TW80	-5,0	0,9	28,0	absent	0,8	4,0	absent
MAN + TW80	-10,0	0,9	21,0	absent	0,8	1,0	absent

Table 3.15: Experiment 2, blow up presence in untreated and sulphate treated vials.

		S+			TL		
Solution	T_n **[°C]**	P_n **[mbar]**	t_n **[s]**	**Blow up**	P_n **[mbar]**	t_n **[s]**	**Blow up**
DW	-5,0	1,0	1,0	absent	1,2	26,0	present
DW	-10,0	1,1	9,0	absent	1,0	3,0	present
DW+TW80	-5,0	0,9	24,0	absent	0,9	28,0	absent
DW+TW80	-10,0	0,9	1,0	absent	0,9	1,0	absent
Suc	-5,0	0,9	7,0	present	1,0	31,0	present
Suc	-10,0	0,9	8,0	present	0,9	0,0	present
Suc + TW80	-5,0	0,9	1,0	present	0,8	7,0	present
Suc + TW80	-10,0	1,0	1,0	present	0,9	0,0	present
MAN	-5,0	1,0	24,0	present	0,9	0,0	present
MAN	-10,0	1,0	30,0	present	1,0	17,0	present
MAN + TW80	-5,0	0,7	1,0	present	0,7	0,0	present
MAN + TW80	-10,0	0,9	2,0	present	0,8	3,0	present

Table 3.16: Experiment 2, blow up presence in siliconized and TopLyo® vials.

Figure 3.13: TopLyo® vials filled with 5% w/w mannitol at the end of the Experiment 2.

Figure 3.14: TopLyo® vials filled with 5% w/w sucrose + 0,02% w/v Tween 80 at the end of the Experiment 2.

3.4 Determination of the influence of the type of water

Following the procedure fully described in sections 2.2.4 the experiment was done to monitor the boiling phenomenon and the nucleation of the vials with water differently treated. The vials were all TopLyo® type, but once they were filled with drinking water, another with demineralized water and the last group with water for injection. The choice of the type of vials fell on TopLyo® because the most critical case in terms of bubbling and boiling phenomena.

All three types of solution presented the phenomenon of boiling by decreasing the pressure in the vacuum chamber, which can also induce nucleation. Some vials filled with drinking water nucleated before vials filled with the other two solutions. The reason for this is the presence of impurities in the drinking water that act as nucleating agents, as explained in the section 1.4.1. Therefore, the drinking water is not suitable for a controlled nucleation process. The phenomenon of boiling had equal intensity in demineralized water and water for injection. This can be seen in Figure 3.15 in which there are vials filled on the left with DE, while on the right with WFI; in both groups bubbles, which then led to boiling, formed with equal size and diffusion on the bottom of the vials.

This test confirms that the freeze drying process does not require the use of water for injection which becomes mandatory if the final product has constraints on bacterial and viral load.

Figure 3.15: Two group of TopLyo® vials filled on the left with demineralized water, while on the right with water for injection. Decreasing the pressure both the solutions formed bubbles on the bottom of the container, as typical of the boiling phenomenon.

3.5 Determination of the influence of the degasification process

Following the procedure fully described in sections 2.2.5 the test was done to investigate, for a given solution in a TopLyo® vial, the influence of the degassing process on the bubbling and boiling phenomena. The choice of the type of vials fell on TopLyo® because the most critical case in terms of bubbling and boiling phenomena.

3.5.1 Demineralized water

During the degassing of the solution, in the vials subjected to this treatment, the phenomenon of boiling occurred but not that of bubbling. This is in accordance with the results of experiment 1 presented in section 3.1, in fact the pressure in the vacuum chamber was 7 mbar and the boiling is evident under 10 mbar.

By lowering the pressure in the chamber to have the nucleation of the water, the phenomenon of boiling took place equally widespread for the group of samples subjected to degassing and those not, while as regards the intensity of the boiling it was slightly lower for degassed vials. This can be observed in Figure 3.16 where on the left of the red line there are the samples subject to degassing while on the right those not. The slightly greater intensity of the boiling in the non-degassed vials may be due to the air dissolved in the water which in the case of degassing had already been released by lowering the pressure the first time.

Figure 3.16: Two group of TopLyo® vials filled with demineralized water. The group of samples on the left was subject to degassing, while the group on the right was not. In both could be observed boiling phenomenon due to the decrease in pressure in the vacuum chamber.

As can be seen in Figure 3.17, the morphology of the cake obtained after nucleation is not acceptable, even for degassed samples, due to boiling.

Figure 3.17: Two group of TopLyo® vials filled with demineralized water at the end of the nuclation process. The group of samples on the left was subject to degassing, while the group on the right was not.

3.5.2 Demineralized water + 0,02% w/v Tween 80

During the degassing of the solution, in the vials subjected to this treatment, the phenomenon of bubbling occurred but not that of boiling thanks to the presence of the Tween 80. This is in accordance with the results of experiment 1 presented in section 3.1, in fact the pressure in the vacuum chamber was 4 mbar and the bubbling is evident under 10 mbar.

By lowering the pressure in the chamber to have the nucleation of the solution, the phenomenon of bubbling took place only in samples that had not been subjected to degassing. This can be observed in Figure 3.18 where on the left of the red line there are the samples subjected to degassing while on the right those not. It is therefore evident that the presence of Tween 80 eliminates the phenomenon of boiling, thanks to an improvement in the wettability of the internal surface of the vials, and in turn the bubbling caused by Tween 80 in water can be eliminated with a degassing process.

It is important following the degassing of the samples to avoid transferring the solution to other containers with pipettes because this would nullify the process just completed. For this reason, degassing was carried out directly in the vials with a small increase in filling volume to take account of the evaporation caused in the 30 minutes of degassing at low pressure.

As can be seen in Figure 3.19, the morphology of the cake obtained after nucleation is acceptable for the cake subjected to degassing, while for the samples not degassed the cakes present small defects due to bubbling.

Figure 3.18: Two group of TopLyo® vials filled with demineralized water + 0,02% w/v Tween 80. The group of samples on the left was subject to degassing, while the group on the right was not. In the group on the right could be observed bubbling phenomenon due to the decrease in pressure in the vacuum chamber.

Figure 3.19: Two group of TopLyo® vials filled with with demineralized water + 0,02% w/v Tween 80 at the end of the nuclation process. The group of samples on the left was subject to degassing, while the group on the right was not.

3.5.3 5% w/w sucrose + 0,02% w/v Tween 80

During the degassing of the solution, in the vials subjected to this treatment, the phenomenon of bubbling occurred but not that of boiling thanks to the presence of the Tween 80. This is in accordance with the results of experiment 1 presented in section 3.1, in fact the pressure in the vacuum chamber was 4 mbar and the bubbling is evident under 10 mbar.

By lowering the pressure in the chamber to have the nucleation of the solution, the phenomenon of bubbling took place only in samples that had not been subjected to degassing. This can be observed in Figure 3.20 where on the left of the red line there are the samples subjected to degassing while on the right those not. It is therefore evident that the presence of Tween 80 eliminates the phenomenon of boiling, thanks to an improvement in the wettability of the internal surface of the vials, and in turn the bubbling caused by Tween 80 can be eliminated with a degassing process.

Following the degassing of the samples, it is important to avoid transferring the solution to other containers with pipettes because this would nullify the process just completed. For this reason, degassing was carried out directly in the vials with a small increase in filling volume to take account of the evaporation caused in the 30 minutes of degassing at low pressure.

As can be seen in Figure 3.21, the cakes obtained after nucleation are subjected to blow up, even for degassed samples, but perhaps this could have been avoided by isolating the vacuum chamber for a given P_n value, as done in experiment 2. Without blow up, the morphology of the cake obtained after nucleation is acceptable for the samples subjected to degassing, while for the non degassed samples the cakes have small defects due to bubbling. Furthermore, in the case of non-degassed samples, bubbles are present under the cake due to Tween 80, this defect is also eliminated by degassing.

Figure 3.20: Two group of TopLyo® vials filled with 5% w/w sucrose + 0,02% w/v Tween 80. The group of samples on the left was subject to degassing, while the group on the right was not. In the group on the right could be observed bubbling phenomenon due to the decrease in pressure in the vacuum chamber.

Figure 3.21: Two group of TopLyo® vials filled with with 5% w/w sucrose + 0,02% w/v Tween 80 at the end of the nuclation process. The group of samples on the left was subject to degassing, while the group on the right was not.

3.5.4 5% w/w mannitol+ 0,02% w/v Tween 80

During the degassing of the solution, in the vials subjected to this treatment, the phenomenon of bubbling occurred but not that of boiling thanks to the presence of the Tween 80. This is in accordance with the results of experiment 1 presented in section 3.1, in fact the pressure in the vacuum chamber was 4 mbar and the bubbling is evident under 10 mbar.

By lowering the pressure in the chamber to have the nucleation of the solution, the phenomenon of bubbling took place only in samples that had not been subjected to degassing. This can be observed in Figure 3.22 where on the left of the red line there are the samples subjected to degassing while on the right those not. It is therefore evident that the presence of Tween 80 eliminates the phenomenon of boiling, thanks to an improvement in the wettability of the internal surface of the vials, and in turn the bubbling caused by Tween 80 can be eliminated with a degassing process.

Following the degassing of the samples, it is important to avoid transferring the solution to other containers with pipettes because this would nullify the process just completed. For this reason, degassing was carried out directly in the vials with a small increase in filling volume to take account of the evaporation caused in the 30 minutes of degassing at low pressure.

As can be seen in Figure 3.23, the cakes obtained after nucleation are subjected to blow up, even for degassed samples, but perhaps this could have been avoided by isolating the vacuum chamber for a given P_n value, as done in experiment 2. Without blow up, the morphology of the cake obtained after nucleation is acceptable for the samples subjected to degassing, while for the non-degassed samples the cakes have small defects due to bubbling. Furthermore, in the case of non-degassed samples, bubbles are present under the cake due to Tween 80, this defect is also eliminated by degassing.

Figure 3.22: Two group of TopLyo® vials filled with 5% w/w mannitol + 0,02% w/v Tween 80. The group of samples on the left was subject to degassing, while the group on the right was not. In the group on the right could be observed bubbling phenomenon due to the decrease in pressure in the vacuum chamber.

Figure 3.23: Two group of TopLyo® vials filled with with 5% w/w mannitol + 0,02% w/v Tween 80 at the end of the nuclation process. The group of samples on the left was subject to degassing, while the group on the right was not.

Therefore, the results are similar to those obtained for a solution of 5% w/w sucrose + 0,02% w / v Tween 80 presented in section 3.5.3.

3.6 Analysis of the freeze-dried product

Following the procedure fully described in sections 2.2.6 the test was done to investigate the morphology of the freeze-dried product.

For their advantages, presented in the section 2.1.1.4, the vials of interest were the siliconized ones while the untreated ones were used as a comparison. The solutions tested were those based on sucrose (5% w/w sucrose and 5% w/w sucrose + 0,02% w/v Tween 80) because its presence guarantees a final solid residue and allows to have P_n higher than mannitol, as seen in the section 3.3.

The choice of T_n between -5 °C and -10 °C is almost indifferent. In the following experiments T_n = -5 °C was used, however a T_n = -10 °C could allow to use slightly higher P_n, as explained in the section 3.2. Having a higher P_n decreases the risk of blow up. By inducing nucleation at higher temperatures, larger ice crystals are produced which, on the one hand, accelerate the primary drying due to the lower resistance to the flow of steam and, on the other hand, reduce the specific area of the freeze-dried product causing a slowing of the desorption phase (Oddone *et al*., 2017).

In experiments A, B and C following the procedure necessary for nucleation with the P_n and t_n obtained from experiment 2, for visual inspection, all vials were nucleated despite the percentage of nucleated vials reported in Table 3.12 is 88% for the solutions used. The merit of this may be the time required to lower the pressure in the chamber which with 378, and even more with 756 vials, is at least one order of magnitude higher than that with the 20 vials of experiment 2. A longer time at values of pressure close to P_n before isolating the chamber allows more solution to evaporate, lowering the temperature in the vials more and therefore increasing the percentage of nucleated vials at P_n compared to the experiment 2. If in some vials the solution was not nucleated by lowering the pressure to P_n, it would do so in an uncontrolled way with the subsequent freezing that leads to -52 °C.

3.6.1 Experiment A

The samples tested were one tray of untreated vials filled with 5% w/w sucrose and one tray of siliconized vials filled with the same solution.

In the case of untreated vials, the freeze-dried cakes are all on the bottom of the vials and have a fairly good morphology. The absence of blow-up is a confirmation of the results of experiment 2, presented in Table 3.15. There is some small surface defect probably due to slight bubbling, observed in the same conditions in experiment 1. Because of the good interactions between glass and solution there is the presence of dry material pulling from the edge and the curvature of the cake surface is convex, as can be seen in Figure 3.23. The glass of the vials does not show stains of solution and the stoppers are clean, despite the bubbling.

Figure 3.23: Product obtained after freeze drying by an untreated vial filled with 5% w/w sucrose.

In the case of siliconized vials, only 4,5% of the freeze-dried cakes are on the bottom of the vials, while the other 95,5% are flying cakes. In the vials count, for calculating the percentages, those containing thermocouples which may have distorted the results are excluded. The presence of blow-up is a confirmation of the results of experiment 2, presented in Table 3.16. The surface of the cake has many defects and overall, the result is not acceptable. The defects may be due to the moderate/weak bubbling and boiling phenomena observed even in the same conditions in experiment 1. The coating results in a hydrophobic surface that resists nonspecific binding reducing sample losses caused by this type of interactions with the container. Thanks to this the climbing of the product at the vial edges is avoided and the surface of the cake has a concave curvature, as can be seen in Figure 3.24. In the case of flying cakes, residues of product adhering to the glass can be found under them. The vials stoppers are clean, despite the bubbling.

Whether the vials are untreated or siliconized, between the bottom of the cakes and the bottom of the vials there are no hints of bubbles. This is in accordance with what seen in section 3.3, in which the presence of these bubbles is attributed to the Tween 80 absent in this test.

Figure 3.24: Product obtained after freeze drying by a siliconized vial filled with 5% w/w sucrose. On the left there is a vial in which the blow up is absent, while on the right one in which it is present.

3.6.2 Experiment B

The samples tested were one tray of untreated vials filled with 5% w/w sucrose + 0,02% w/v Tween 80 and one tray of siliconized vials filled with the same solution.

In the case of untreated vials 60,6% of the freeze-dried cakes are on the bottom of the vials, while the other 39,4% are flying cakes. In the vials count, for calculating the percentages, those containing thermocouples which may have distorted the results are excluded. Because of the good interactions between glass and solution there is the presence of dry material pulling from the edge and the curvature of the cake surface is convex, as can be seen in Figure 3.25. The glass of the vials shows some stains of product, but the stoppers are clean, despite the bubbling.

Figure 3.25: Products obtained after freeze drying by an untreated vial filled with 5% w/w sucrose + 0,02% w/v Tween 80. On the left there is a vial in which the blow up is absent, while on the right one in which it is present.

In the case of siliconized vials, only 27,6 % of the freeze-dried cakes are on the bottom of the vials, while the other 72,4 % are flying cakes. In the vials count, for calculating the percentages, those containing thermocouples which may have distorted the results are excluded.

The coating results in a hydrophobic surface that resists nonspecific binding reducing sample losses caused by this type of interactions with the container. Thanks to this the climbing of the product at the vial edges is avoided and the surface of the cake has a concave curvature, as can be seen in Figure 3.26. For the same reason, there are no residues of product adhering to the glass. The vials stoppers are clean, despite the bubbling.

Figure 3.26: Product obtained after freeze drying by a siliconized vial filled with 5% w/w sucrose + 0,02% w/v Tween 80. On the left there is a vial in which the blow up is almost absent, while on the right one in which it is present.

In both the case of untreated and siliconized vials the surface of the cake has small defect caused by the bubbling phenomena, which has been observed in the same conditions also in experiment 1.

What makes the product unacceptable, in both cases, is the high percentage of flying cakes and the presence between the bottom of the cakes and the bottom of the vials of bubbles. This is in accordance with what seen in section 3.3, in which the presence of these bubbles has been attributed to the Tween 80. For siliconized vials the percentage of flying cakes exceeds 70% while for untreated vials this is less than 40% because, as introduced in section 3.3, the hydrophobic coatings reduce the friction between the cake and the internal surface of the container.

Therefore, on one hand the presence of Tween 80 eliminates the phenomenon of boiling, thanks to an improvement in the wettability of the internal surface of the vials. While, on the other hand the Tween 80 increases the phenomenon of bubbling because lower the surface tension of the liquid facilitating the formation of foam and prevent the bubble rupture thanks to its amphiphilic nature.

3.6.3 Experiment C

The samples tested were one tray of untreated vials filled with 5% w/w sucrose + 0,02% w/v Tween 80 that underwent the degassing procedure before the freezing one.

The freeze-dried cakes have a good morphology thanks to the absence of bubbling and boiling phenomena prior to nucleation. The presence of Tween 80 eliminates the phenomenon

of boiling, thanks to an improvement in the wettability of the internal surface of the vials, and in turn the bubbling caused by Tween 80 is eliminated by the degassing process.

Contrary to the predictions that could have been made from the results of experiment 2, presented in section 3.3 and from the tests on degassing, presented in section 3.5.3, the internal surface of the vials is siliconized but all the cakes are perfectly adherent to the bottom of the container. The reason for this could lie in the fact that, as introduced at the beginning of section 3.5, thanks to the large number of vials, the pressure in the vacuum chamber drops more slowly.

Degassing also eliminates any hints of bubbles, that usually accompany the presence of Tween 80.

The coating results in a hydrophobic surface that resists nonspecific binding reducing sample losses caused by this type of interactions with the container. Thanks to this the climbing of the product at the vial edges is avoided and the surface of the cake has a concave curvature, as can be seen in Figure 3.27. For the same reason, there are no residues of product adhering to the glass, with the exception of two isolated cases in which there are splashes of product on the vials due to bubbling in the degassing phase. The vials stoppers have no traces of product, despite the bubbling in the degasification process.

Figure 3.27: Product obtained after freeze drying by a siliconized vial filled with 5% w/w sucrose + 0,02% w/v Tween 80 that underwent the degassing procedure before the freezing one.

4. Conclusions

4.1 Objectives and achievements

This master's degree project aimed at a deep investigation of the effect of surface treatments on the feasibility of controlled nucleation using the Vacuum-Induced Surface Freezing technique. Two were the main objectives that have been set:

- acquire an extensive knowledge on the principles of freezing, the techniques to control the nucleation temperature, the drying steps and the various treatments that can be applied to a container suitable for freeze-drying;
- analyse the effect of vials with different surface treatments and filled with different solutions on the product obtained by VISF.

To achieve the first purpose, a deep literature research has been done.

Regarding the second goal, various experiments, presented in section 2.2, have been carried out in GSK Vaccines (Rixensart).

In the experiment, 1 for vials in equilibrium at a given T_n, a pressure range was identified in which nucleation occurs. The fact that nucleation does not occur in all vials at the same time confirms its stochastic nature. Comparing untreated vials, sulphate treated vials, siliconized vials and TopLyo® vials there is no marked influence of the type of vials on P_{first} and P_{last}, with the same solution used. While changing the type of solution, experiment 1 proved that by adding a non-volatile solute to a solvent, nucleation occurs at lower temperatures (freezing-point depression). If the value of T_n is -5 °C instead of -10 °C, greater evaporation is required which is obtained by lowering the pressure in the vacuum chamber slightly more. Bubbling has been reported for all combinations tested, except for demineralized water and 5% w/w mannitol only in sulphate treated vials. Bubbling is more intense and widespread in cases where Tween 80 is present in the solution. This is because surfactants are compound that lower the surface tension of the liquid facilitating the formation of foam and prevent the bubble rupture thanks to their amphiphilic nature. Also, sucrose and mannitol may be related to the phenomenon of bubbling. Sucrose inhibits bubble coalescence over a concentration range 0.01-0.3 M (Henry and Craig, 2009): the concentration of sucrose in the solutions tested is about 0,15 M and therefore is in the range. Henry and Craig suggested that the bubble coalescence inhibition may be related to the partitioning of the osmolytes at the air-water interface, while there is no correlation with the increasing of the surface tension gradient or with electrostatic mechanism. No evidence has been found in the literature for mannitol and no clear relationship between this excipient and bubbling can be derived from the experiments done. The phenomenon of boiling is present in all vials with internal silicone coatings but is inhibited by the presence of Tween 80 in the solution that improves the wettability of the internal surface of the vials thanks to its amphiphilic properties. Boiling is more widespread and more intense in TopLyo® vials than in siliconized ones. This is due to the greater contact angle and therefore to the greater hydrophobicity of the former which minimize the interactions between the solution and the container, facilitating boiling. Both bubbling and boiling lead to obtaining products with an unacceptable morphology. The fogging, another cosmetic defect, was observed in untreated vials and, to a greater extent, in sulphate treated vials. Fogging is relevant for low contact angles; this is demonstrated by the fact that the phenomenon was absent for siliconized and TopLyo® vials because of their hydrophobic surfaces. The sulphate treated vials therefore gave results very similar to the untreated vials, only the bubbling was slightly less intense in the former, but on the other hand the fogging was worse.

In experiment 2, for each combination of solution and surface treatment of the vials, was determined a pressure value P_n to which the vacuum chamber should be isolated for a time t_n in order to obtain the nucleation of the samples previously in equilibrium at T_n and atmospheric pressure . The values of P_n are similar for the different solutions, only those of the solutions containing mannitol are slightly lower than the others. Generally, t_n is less than 10 seconds. The optimal duration for vacuum is less than 1 min because a longer time, such as 1,5 min can produce blow-up of the frozen cake and flake formation on the product surface (Oddone *et al*., 2020). The pressure increase effect obtained by isolating the vacuum chamber from the condenser is intended to reduce the blow-out phenomena thanks to a slower evaporation rate. However, usually the blow up was present in siliconized and TopLyo® vials because of the hydrophobic coatings reduce the friction between the cake and the internal surface of the container. In case of blow up with solutions containing Tween 80 remains of solution not yet solidified may form bubbles under the cake that solidify with this morphology. The blow up of the cake should be avoided because it leads to an unacceptable product. The considerations on bubbling and boiling obtained from experiment 1 were also confirmed in experiment 2.

The influence of the degassing process on the bubbling and boiling phenomena was investigated for a given solution in TopLyo® vials which are the most critical case in terms of bubbling and boiling phenomena. Degassing demineralized water has shown that the phenomenon of boiling is slightly less intense in the subsequent nucleation phase since the air dissolved in the water had already been released by lowering the pressure the first time. Since it did not lead to a substantial reduction in boiling, degassing was applied to solutions containing Tween 80 which causes strong bubbling but eliminates boiling. Solutions containing Tween 80 degassed did not present bubbling and boiling during VISF and consequently the morphology of the cakes was good. The degassing therefore allows the VISF controlled nucleation technique to be applied also to solutions contained in vials with internal silicone coating.

Tests were then carried out to find a combination of treatment of the vials and solution that could give, through controlled nucleation with the VISF method and subsequent freeze-drying, a product with an acceptable morphology. In these experiments, thanks to P_n and t_n values determined in experiment 2 for each combination of solution and surface treatment of the vials, it was possible to implement VISF through an automatic mode without the need for manual pressure adjustments by visual inspection of the samples.

For their advantages, presented in the section 2.1.1.4, the vials of interest were the siliconized ones. Among those tested, the solution that led to the best results was 5% w/w sucrose + 0,02% w/v Tween 80. Sucrose was chosen because it allows to have higher P_n than mannitol, as seen in the section 3.3. Unlike mannitol, sucrose remains amorphous during freeze-drying and therefore a secondary drying phase was necessary to obtain the freeze-dried product. In fact, in amorphous solutes, about 20% of unfrozen water is associated with the solid solution, which must be removed by a diffusion process during secondary drying, while in crystalline material nearly all water is frozen and can easily be removed during primary drying (Nail *et al*., 2002). A process with a crystalline solute could be more efficient because the eutectic melting temperatures are usually higher than the glass transition temperatures, allowing a higher product temperature during primary drying without the melting/collapsing of the cake (Kasper and Friess, 2011). The choice of T_n between -5 °C and -10 °C is almost indifferent. A T_n = -10 °C could allow to use slightly higher P_n, as explained in the section 3.2, reducing the risk of blow up. By inducing nucleation at higher temperatures, larger ice crystals are produced which, on the one hand, accelerate the primary drying due to the lower resistance to the flow of steam and, on the other hand, reduce the specific area of the freeze-dried product causing a slowing of the desorption phase (Oddone *et al*., 2017).

In Figure 4.1, from left to right, are presented the products obtained by freeze drying of 5% w/w sucrose in untreated vials, 5% w/w sucrose in siliconized vials and 5% w/w sucrose + 0,02% w/v Tween 80 degassed in siliconized vials. Products obtained from non-degassed solutions have shown defects on the surface of the cake due to bubbling and/or boiling. The untreated vials, because of the good interactions between glass and solution, were characterized by the presence of dry material pulling from the edge and the curvature of the cake surface was convex. In the siliconized vials the coating results in a hydrophobic surface that resists nonspecific binding reducing sample losses caused by this type of interactions with the container. Thanks to this the climbing of the product at the vial edges was avoided and the surface of the cake had a concave curvature. The blow up phenomenon was absent in the untreated vials thanks to the good friction between the cake and the internal surface of the container, while it was present in the siliconized one in the absence of degasification. The elimination of bubbling, thanks to degassing, together with the slow lowering of the pressure in the vacuum chamber, due to the high number of vials, avoided the blow up in the siliconized vials filled with 5% w/w sucrose + 0,02% w/v Tween 80.

Figure 4.1: From the left to the right the image shows the product obtained after freeze drying of 5% w/w sucrose in untreated vials, 5% w/w sucrose in siliconized vials and degassed 5% w/w sucrose + 0,02% w/v Tween 80 in siliconized vials.

Siliconized vials filled with 5% w/w sucrose + 0,02% w/v Tween 80 and degassed was therefore the best combination for performing controlled nucleation in siliconized vials obtaining a product with excellent morphology by freeze-drying.

Boiling in vials with an internal silicone coating has been eliminated thanks to the use of the non-ionic surfactant Tween 80 at a concentration higher than its CMC. Surfactants of this type are commonly present in pharmaceutical drugs where protect the protein by aggregation, surface adsorption and/or precipitation. Therefore, these products can be subjected to Vacuum-Induced Surface Freezing, after degassing, without adding other components.

4.2 Perspectives

If working in full load, filling the 5 shelves of the pilot-scale freeze-dryer HETO DW 8030, instead of just one or two, the isolation of the vacuum chamber reached the P_n during experiment 2 may not be necessary. The time required to lower the pressure in the vacuum chamber would probably be large enough to have nucleation at slightly higher P_n values and prevent the pressure from rapidly falling to values for which it is very likely to have flying

cakes. Furthermore, by isolating the chamber, the pressure inside it would rise very quickly due to the evaporation of the solution in the many vials present, blocking further evaporation and nucleation.

It could also be very interesting to repeat these tests in containers different from vials, such as dual chamber syringes or cartridges. Traditionally, the product is freeze-dried in vials, then reconstituted with a diluent and administered with syringes.

Lyophilize the product directly in the syringe, isolate this with a stopper and fill the remaining space with diluent would bring several benefits, such as (Patel and Pikal, 2011; Sacha *et al*., 2010; Badkar *et al*., 2011):

- eliminate the overfill reducing the waste and dosage errors because, unlike vials, syringes contain the exact amount of deliverable dose needed;
- easy and quick reconstruction pushing the plunger;
- the guarantee of sterility is increased, as fewer manipulations are needed;
- lower costs.

List of symbols

c	Coefficient used to evaluate P_n
$C°$	Equilibrium water content during the desorption process
$C_{w,0}$	Residual moisture of the lyophilized product at the end of primary drying
D_p	Average pore size diameter
J_w	Rate of water removal during primary drying
k_d	Desorption rate constant
Mw	Molecular weight of water
P	Vacuum chamber pressure
P_{first}	Pressure value at which nucleation was first observed in some vials
P_{ice}	Equilibrium vapor pressure of ice at the temperature of the frozen material
$P_{last,}$	Pressure value at which the last vial nucleated
P_n	Pressure value at which the valve between the condenser and the vacuum chamber was closed
P_w	Partial pressure of water inside the chamber
R	Ideal gas constant
r	Radius of the spherical nuclei
r_C	Minimum radius for which a formed nucleus is stable
R_p	Resistance of the dried product
T	Temperature
t	Time
T_0	Equilibrium freezing temperature
T_1	Temperature of the first probe of the Tempris sensor
T_2	Temperature of the second probe of the Tempris sensor
T_3	Temperature of the third probe of the Tempris sensor
T_a	Ambient temperature
T_c	Collapse temperature
T_{eu}	Eutectic temperature
T_g	Glass transition temperature
T_g'	Glass transition temperature for maximally freeze-concentrated solutions
T_m	Holding temperature after the induction of nucleation
T_{mean}	Average of *T1*, *T2* and *T3*
T_n	Holding temperature before the induction of nucleation

t_n	Time required to induce the nucleation of the vials isolated inside the vacuum chamber
ΔG	Overall excess free energy in homogeneous nucleation
ΔG_S	Excess surface free energy in homogeneous nucleation
ΔG_V	Excess volume free energy in homogeneous nucleation

Greek symbols

ε	Void volume fraction
ρ_s	Density of the dried product
τ	Factor linked to pores' interconnectivity

Abbreviations

CMC	Critical Micelle Concentration
DW	Demineralized water
DW+TW80	Demineralized water + 0,02% w/v Tween 80
INAs	Ice-Nucleating Agents
MAN	5% w/w mannitol
MAN+TW80	5% w/w mannitol+ 0,02% w/v Tween 80
PICVD	Plasma-Impulse Chemical Vapor Deposition
S-	Untreated vials
S+	Siliconized vials
SSA	Specific Surface Area
ST	Sulphate treated vials
Suc	5% w/w sucrose
Suc+TW80	5% w/w sucrose + 0,02% w/v Tween 80
TL	TopLyo® vials
VISF	Vacuum-Induced Surface Freezing
W	Drinking Water
WFI	Water for injection

References

Abdul-Fattah A.M., Oeschger R., Roehl H., Bauer Dauphin I., Worgull M., Kallmeyer G. and Mahler H.C., 2013, Investigating factors leading to fogging of glass vials in lyophilized drug products. *European Journal of Pharmaceutics and Biopharmaceutics*, **85**, 314-326.

Al-Hussein A. and Gieseler H., 2012, The effect of mannitol crystallization in mannitol-sucrose system on LDH stability during freeze-drying. Journal of Pharmaceutical Sciences, 101, 2534-2544.

Altmann R., 1890, *Die Elementarorganismen und ihre Beziehungen zu den Lellen*, Veit and Co., Leipzig.

Arsiccio A. and Pisano R., 2017, Stability of protein in carbohydrates and other additives during freezing: The human growth. *Journal of Physical Chemistry B*, **121**, 8652-8660.

Arsiccio A. and Pisano R., 2018a, Water entrapment and structure ordering as protection mechanism for protein structural preservation. *The Journal of Chemical Physics*, **148**, 55-102.

Arsiccio A. and Pisano R., 2018b, Clarifying the role of cryo- and lyo- protectants in the biopreservation of proteins. *Physical Chemistry Chemical Physics*, **20**, 8267-8277.

Arsiccio A. and Pisano R., 2018c, Surfactants as stabilizers for biopharmaceuticals: An insight into the molecular mechanisms for inhibition of protein aggregation. *European Journal of Pharmaceutics and Biopharmaceutics*, **128**, 98-106.

Arsiccio A. and Pisano R., 2018d, Design of the formulation for therapeutic proteins – How to improve stability of drugs during freezing and in the dried state. *Chemistry Today*, **36**, 16-18.

Arsiccio A., Barresi A.A., De Beer T., Oddone I., Van Bockstal P. and Pisano R., 2018a, Vacuum Induced Surface Freezing as an effective method for improved inter- and intra-vial product homogeneity. *European Journal of Pharmaceutics and Biopharmaceutics*, **128**, 210–219.

Arsiccio A., McCarty J., Pisano R. and Shea J.-E., 2018b, Effect of surfactants on surface induced denaturation of proteins: evidence of an orientation-dependent mechanism. *Journal of Physical Chemistry B*,**122**(49), 11390-11399.

Arsiccio A., Paladini A., Pattarino F. and Pisano R., 2019, Designing the optimal formulation for biopharmaceuticals: A new approach combining molecular dynamics and experiments. *Journal of Pharmaceutical Sciences*, **108**, 431-438.

Assegehegn G., Brito-de la Fuente E., Franco J. and Gallegos C., 2019, The importance of understanding the freezing step on freeze-drying process performance. *Journal of Pharmaceutical Science*, **108**, 1378-1395.

Badkar A., Wolf A., Bohack L. and Kolhe P., 2011, Development of Biotechnology Products in Pre-filled Syringes: Technical Considerations and Approaches. *AAPS PharmSciTech*, **12**(2), 564-572.

Barresi A.A. and Pisano R., 2018, Process intensification and process control in freeze-drying. *Proceedings of 21st International Drying Symposium (IDS'2018)*, València, Spain, 11-14 September 2018.

Barresi A.A., Pisano R., Rasetto V., Fissore D. and Marchisio L.D., 2010, Model-Based Monitoring and Control of Industrial Freeze-Drying Processes: Effect of Batch Nonuniformity. *Drying Technology*, **28**(5), 577-590.

Bhatnagar B.S., Bogner R.H. and Pikal M.J., 2007, Protein stability during freezing: separation of stresses and mechanisms of protein stabilization. *Pharmaceutical Development and Technology*, **12**, 505–523.

Borchert S.J., Ryan M.M., Davison R.L. and Speed W., 1989, Accelerated extractable studies of borosilicate glass containers. *Journal of Parenteral Science and Technology*, **43**(2), 67–79.

Bordas F. and d'Arsonval M., 1906, *C R Acad Sci Paris*, 142-1058.

Cailleteau C., Angeli F., Devreux F., Gin S., Jestin J., Jollivet P. and Spalla O., 2008, Insight into silicate-glass corrosion mechanisms. *Nature Materials*, **7**, 978–983.

Cao E., Chen Y., Cui Z. and Foster P.R., 2003, Effect of freezing and thawing rates on denaturation of proteins in aqueous solutions. *Biotechnology and Bioengineering*, **82**(6), 684-690.

Cao W., Mao C., Chen W., Lin H., Krishnan S. and Cauchon N., 2006, Differentiation and quantitative determination of surface and hydrate water in lyophilized mannitol using NIR spectroscopy. *Journal of Pharmaceutical Sciences*, **95**, 2077–2086.

Carpenter J.F., Arakawa T. and Crowe J.H., 1992, Interactions of stabilizing additives with proteins during freeze-thawing and freeze-drying. *Developmental Biology*, **74**, 225–238.

Carpenter J.F., Chang B.S., Garzon-Rodriguez W. and Randolph T.W., 2002, Rational design of stable lyophilized protein formulations: Theory and practice. In: *Rational design of stable protein formulations – Theory and Practice* (Carpenter J.F. and Manning M.C.). Kluwer Academic/Plenum Publisher, New York.

Carpenter J.F., Prestrelski S.J., Chang B.S. and Arakawa T., 1993, Separation of freezing and drying-induced denaturation of lyophilized proteins using stress-specific stabilization. I. Enzymatic activity and calorimetric studies. *Archives of Biochemistry and Biophysics*, **303**, 456-464.

Cavatur R.K., Vemuri N.M., Pyne A., Chrzan Z., Toledo-Velasquez D. and Suryanarayanan R., 2002, Crystallization behaviour of mannitol in frozen aqueous solutions. *Pharmaceutical Research*, **19**, 894-900.

Chang B.S, Kendrick B.S. and Carpenter J.F., 1996, Surface-induced denaturation of proteins during freezing and its inhibition by surfactants. *Journal of Pharmaceutical Sciences,* **85**(12), 1325-1330.

Chang B.S. and Randall C.S., 1992, Use of subambient thermal analysis to optimize protein lyophilization. *Cryobiology*, **29**(5), 632-656.

Costantino H.R., Griebenow K., Langer R. and Klibanov A.M., 1997, On the pH memory of lyophilized compounds containing protein functional groups, *Biotechnology and Bioengineering*, **53**, 345–348.

Council of Europe, 2010, *European Pharmacopoeia 7th ed*. Strasbourg: Council of Europe, **3.2.1** Glass Containers for pharmaceutical use, 363-367.

Crapiste G.H. and Lozano J.E., 1988, Effect of Concentration and Pressure on the Boiling Point Rise of Apple Juice and Related Sugar Solutions. *Journal of Food Science*, **53**(3), 865-868.

Demarco F., Renzi E., Lee R., and Chakravarty P., 2012, Ice fog as a means to induce uniform ice nucleation during lyophilization. *BioPharm International*, **25**(1), 33-38.

Dill K., 1990, Dominant forces in protein folding. *Biochemistry*, **29**, 7133–7155.

Ditter D., Mahler H.C., Roehl H., Wahl M., Huwyler J., Nieto A. and Allmendinger A., 2018b, Characterization of surface properties of glass vials used as primary packaging material for parenterals. *European Journal of Pharmaceutics and Biopharmaceutics*,**125**, 58-67.

Ditter D., Nieto A., Mahler H.C., Roehl H., Wahl M., Huwyler J. and Allmendinger A., 2018a, Evaluation of Glass Delamination Risk in Pharmaceutical 10 mL/10R Vials. *Journal of Pharmaceutical Sciences*, **107**(2), 624-637.

Doremus R.H., 1979, Chemical durability of glass. In: *Treatise on Materials Science and Technology* (Tomozawa M., Doremus R.H.). Vol. 17: Glass II, New York: Academic Press, pp 41–69.

Duncan M.R., Lee J.M. and Warchol M.P., 1995, Influence of surfactants upon protein/peptide adsorption to glass and polypropylene. *International Journal of Pharmaceutics*, **120**, 179-188.

Elkem, SILBIONE EMUL 70001 SP Brochure.

Ennis R.D., Pritchard R., Nakamura C., Coulon M., Yang T., Visor G.C. and Lee W.A., 2001, Glass Vials for Small Volume Parenterals: Influence of Drug and Manufacturing Processes on Glass Delamination. *Pharmaceutical Development and Technology*, **6**, 393-405.

Fan T.H., Li J.Q., Minatovicz B., Soha E., Sun L., Patel S., Chaudhuri B. and Bogner R., 2018, Phase-Field Modeling of Freeze Concentration of Protein Solutions. *Polimers*, **11**(10).

Fissore D. and Pisano R., 1995, Computer-Aided Framework for the Design of Freeze-Drying Cycles: Optimization of the Operating Conditions of the Primary Drying Stage. *Processes*, **3**, 406–421.

Fissore D., Pisano R. and Barresi A.A., 2010, On the methods based on the pressure rise test for monitoring a freeze-drying process. *Drying Technology*, **29**, 73-90.

Fissore D., Pisano R. and Barresi A.A., 2019, Freeze Drying of Pharmaceuticals Products. In: *Advances in Drying Science and Technology* (Mujumdar A.S.). CRC Press.

Flosdorf E.W. and Mudd S., 1935, Procedure and apparatus for preservation in ‘‘lyophile’’ form of serum and other biological substances. *The Journal of Immunology*. **29**(5), 389-425.

Flosdorf E.W., 1949, *Freezing and Drying*, Reinhold, New York, USA.

Flosdorf E.W., Stokes F. and Mudd S., 1940, *J. Amer. Med. Ass*. U.S. Patent US 2,345,548.

Fonte P., Roque L.P., Seabra V., Almeida A.J., Reis S. and Sarmento B., 2016, Annealing as a tool for the optimization of lyophilization and ensuring of the stability of protein-loaded PLGA nanoparticles. *International Journal of Pharmaceutics*, **503**, 163-173.

Franks F. and Auffret T., 2007, *Freeze drying of pharmaceuticals and biopharmaceuticals*. RSC Publishing, Cambridge.

Franks F., 1993, Solid aqueous solutions. *Pure and Applied Chemistry*, **65**(12), 2527-2537.

Franks F., 1995, Protein destabilization at low temperatures. *Advances in Protein Chemistry*, **46**, 105-139.

Franks F., 1998, Freeze-drying of bioproducts: Putting principles into practice. *European Journal of Pharmaceutics and Biopharmaceutics*, **83**, 367-382.

Gan K.H., Bruttini R., Crosser O.K. and Liapis A.I., 2005, Freeze-drying of pharmaceuticals in vials on trays: Effects of drying chamber wall temperature and tray side on lyophilization performance. *International Journal of Heat and Mass Transfer*, **48**, 1675–1687.

Ganguly A., Nail S.L. and Alexeenko A.A., 2010, Experimental Determination of the Key Heat Transfer Mechanisms in Pharmaceutical Freeze Drying. *School of Aeronautics and Astronautics Faculty Publications*, **27**.

Gasteyer T. H., Sever R. R., Hunek B., Grinter N. and Verdone M. L., 2017, *Lyophilization system and method*. U.S. Patent US 9,651,305 B2, 16 May 2017.

Geidobler R. and Winter G., 2013, Controlled ice nucleation in the field of freeze-drying: fundamentals and technology review. *European Journal of Pharmaceutics and Biopharmaceutics*, **85**(2), 214-222.

Geidobler R., Mannschedel S. and Winter G., 2012, A new approach to achieve controlled ice nucleation of supercooled solutions during the freezing step in freeze-drying. *Journal of Pharmaceutical Science*, **101**, 4409-4413.

Goldman R., 1950, *Drain-clear container for aqueous-vehicle liquid pharmaceutical preparations*. U.S. Patent US 2,504,482, 18 April 1950.

Gomez G., Pikal M.J. and Rodríguez-Hornedo N., 2001, Effect of initial buffer composition on pH changes during far-from-equilibrium freezing of sodium phosphate buffer solutions. *Pharmaceutical Research*,**18**(1), 90-97.

Graziano G., Catanzano F., Riccio A. and Barone G., 1997, A reassessment of the molecular origin of cold denaturation. *Journal of Biochemistry*, **122**(2), 395-401.

Greaves R.I.N., 1946, The Preservation of Proteins by Drying. *Medical Research Council Special Report Series No. 258*, London: HMSO.

Grohganz H., Rischer M. and Brandl M., 2004, Adsorption of the decapeptide Cetrorelix depends both on the composition of dissolution medium and the type of solid surface. *European Journal of Pharmaceutical Sciences*, **21**, 191-196.

Ha E., Wang W. and Wang Y.J., 2002, Peroxide formation in polysorbate 80 and protein stability. *Journal of Pharmaceutical Sciences*, **91**, 2252-2264.

Hall T., Sandefur S.L., Frye C.C., Tuley T.L. and Huang L., 2016, Polysorbates 20 and 80 degradation by group XV lysosomal phospholipase A2 isomer X1 in monoclonal antibody formulations. *Journal of Pharmaceutical Sciences*, **105**, 1633-1642.

Hancock B.C. and Zografi G., 1994, The relationship between the glass transition temperature and the water content of amorphous pharmaceutical solids. *Pharmaceutical Research*., **11**, 471–477.

Hawe A. and Friess W., 2006, Impact of freezing procedure and annealing on the physicochemical properties and the formation of mannitol hydrate in mannitol – sucrose – NaCl formulations. *European Journal of Pharmaceutics and Biopharmaceutics*, **64**, 316-325.

Heljo P., 2013, Comparison of disaccharides and polyalcohols as stabilizers in freeze-dried protein formulations. PhD diss., University of Helsinki.

Heller M.C., Carpenter J.F. and Randolph T.W., 1997, Manipulation of lyophilization induced phase separation: implications for pharmaceutical proteins. *Biotechnology Progress*, **13**(5), 231-238.

Heller M.C., Carpenter J.F. and Randolph T.W., 1999a, Application of a Thermodynamic Model to the Prediction of Phase Separations in Freeze-Concentrated Formulations for Protein Lyophilization. *Archives of Biochemistry and Biophysics*, **363**, 191-201.

Heller M.C., Carpenter J.F. and Randolph T.W., 1999b, Protein Formulation and Lyophilization Cycle Design: Prevention of Damage Due to Freeze-Concentration Induced Phase Separation. *Biotechnology and Bioengineering*, **63**, 166-174.

Helt J.E., 1976, Effects of supersaturation and temperature on nucleation and crystal growth in a MSMPR crystallizer. *Retrospective Theses and Dissertations*, **6213**.

Henry C.L. and Craig V.S.J., 2009, Inhibition of Bubble Coalescence by Osmolytes: Sucrose, Other Sugars, and Urea. *Langmuir*, **25**(19), 11406-11412.

Hickling R., 1965, Nucleation of freezing by cavity collapse and its relation to cavitation damage. *Nature*, **206**(4987), 915-917.

Hillgren A., Lindgren J. and Alden M., 2002, Protection mechanism of Tween 80 during freeze-thawing of a model protein, LDH. *International Journal of Pharmaceutics*, **237**, 57-69.

Höger K., Mathes J. and Frieß W., 2015, IgG1 adsorption to siliconized glass vials-influence of pH, ionic strength, and nonionic surfactants. *Journal of Pharmaceutical Sciences*, **104**(1), 34-43.

Holven A., 1936, Sucrose Solutions: Influence of Pressure on Boiling Point Elevation. *Industrial & Engineering Chemistry Research*, **28**(4), 452-455.

Hottot A., Vessot S. and Andrieu J., 2007, Freeze-Drying of Pharmaceuticals in Vials: Influence of Freezing Protocol and Sample Configuration on Ice Morphology and Freeze-Dried Cake Texture. *Chemical Engineering and Processing*, **46**, 666–674.

Huang M., Childs E., Roffi K., Karim F., Juneau J., Bhatnagar B. and Tchessalov S., 2019, Investigation of Fogging Behavior in a Lyophilized Drug Product. *Journal of Pharmaceutical Sciences*, **108**(3), 1101-1109.

Hunt J.D. and Jackson K.A., 1966, Nucleation of solid in an undercooled liquid by cavitation. *Journal of Applied Physics*, **17**(1), 254-257.

Iacocca R.G. and Allgeier M., 2007, Corrosive attack of glass by a pharmaceutical compound. *Journal of Materials Science*, **42**, 801–811.

Iacocca R.G., Toltl N., Allgeier M., Bustard B., Dong X., Foubert M., Hofer J., Peoples S. and Shelbourn T., 2010, Factors Affecting the Chemical Durability of Glass Used in the Pharmaceutical Industry. *AAPS PharmSciTech*, **11**, 1340–1349.

Inada T., Zhang X., Yabe A. and Kozawa Y., 2001, Active control of phase change from supercooled water to ice by ultrasonic vibration 1. Control of freezing temperature. *International Journal of Heat and Mass Transfer*, **44**(23), 4523-4531.

Jaenicke R., 1990, Protein structure and function at low temperatures. *Philosophical Transactions of the Royal Society B: Biological Sciences*, **326**(1237), 535-551.

Jiang S. and Nail S.L., 1998, Effect of process conditions on recovery of protein activity after freezing and freeze-drying. *European Journal of Pharmaceutics and Biopharmaceutics*, **45**, 249–257.

Johnson L.L.R., 2011, Freeze-drying protein formulations above their collapse temperatures: possible issues and concerns. *American Pharmaceutical Review*, **14**, 50–54.

Jones L.S., Kaufmann A. and Middaugh C.R., 2005, Silicone Oil Induced Aggregation of Proteins. *Journal of pharmaceutical sciences*, **94**(4), 918–927.

Jones L.S., Randolph T.W., Kohnert U., Papadimitriou A., Winter G., Hagmann M.L., Manning M.C. and Carpenter J.F., 2001, The effects of Tween 20 and sucrose on the stability of anti-L-selectin during lyophilization and reconstitution. *Journal of Pharmaceutical Sciences*, **90**, 1466-1477.

Jothi L. and Nageswaran G., 2019, Plasma Modified Polymeric Materials for Biosensors/Biodevice Applications, in "Non – Thermal Plasma Technology for Polymeric Materials", (S. Thomas, M. Mozetic, U. Cvelbar, P. Spatenka and K.M. Praveen, Eds.), Chap. 15, Elsiever, 409-437.

Kasper J.C. and Friess W., 2011, The freezing step in lyophilization: Physico-chemical fundamentals, freezing methods and consequences on process performance and quality attributes of biopharmaceuticals. European Journal of Pharmaceutics and *Biopharmaceutics*, **78**, 248–263.

Kawano Y., Otsu S., Bamba T. and Hanawa T., 2017, Study of Interaction between Fluorinated Coating Glass and the Medicines. *YAKUGAKU ZASSHI*, **137**(11) 1409-1417.

Kawasaki H., Shimanouchi T., Takahashi K. and Kimura Y., 2018, Effect of Controlled Nucleation of Ice Crystals on the Primary Drying Stage during Lyophilization. *Chemical and Pharmaceutical Bulletin*, **66**, 1122–1130.

Kerwin B.A., 2008, Polysorbates 20 and 80 used in the formulation of protein biotherapeutics: structure and degradation pathways. *Journal of Pharmaceutical Sciences*, **97**(8), 2924–2935.

Khan T.A., Mahler H.C. and Kishore R.S., 2015, Key interactions of surfactants in therapeutic protein formulations: a review. *European Journal of Pharmaceutics and Biopharmaceutics*, **97**, 60–67.

Kiese S., Pappenberger A., Friess W. and Mahler H.C., 2008, Shaken, not stirred: Mechanical stress testing of an IgG1 antibody. *Journal of Pharmaceutical Sciences*, **97**, 4347-4366.

Kochs M., Korber C., Nunner B. and Heschel I., 1991, The influence of the freezing process on vapor transport during sublimation in vacuum freeze-drying. *International Journal of Heat and Mass Transfer*, **34**, 2395-2408.

Kondo A. and Mihara J., 1996, Comparison of Adsorption and Conformation of Hemoglobin and Myoglobin on Various Inorganic Ultrafine Particles. *Journal of Colloid and Interface Science*, **177**, 214-221.

Kostantinidis A. L., Kuu W., Otten L., Nail S. L. and Sever R. R., 2011, Controlled nucleation in freeze-drying: effects on pore size in the dried product layer, mass transfer resistance, and primary drying rate. *Journal of Pharmaceutical Science*, **100**, 3453-3470.

Kramer M., Sennhenn B. and Lee G., 2002, Freeze-drying using vacuum-induced surface freezing. *Journal of Pharmaceutical Science*, **91**, 433-443.

Kumar P., Franzese G. and Stanley H.E., 2008, Predictions of Dynamic Behavior under Pressure for Two Scenarios to ExplainWater Anomalies. *PHYSICAL REVIEW LETTERS*, **100**, 105701.

Langer C., Mahler H.C., Koulov A., Marti N., Grigore C., Matter A., Chalus P., Singh S., Lemazurier T., Joerg S. and Mathaes R., 2020, Method to Predict Glass Vial Fogging in Lyophilized Drug Products. *Journal of Pharmaceutical Sciences*, **109**(1), 323-330.

Liao X., Krishnamurthy R. and Suryanarayanan R., 2007, Influence of Processing Conditions on the Physical State of Mannitol. Implications in Freeze-Drying. *Pharmaceutical Research*, **24**, 370–376.

Liapis A.I. and Bruttini R., 1994, A theory for the primary and secondary drying stages of the freeze-drying of pharmaceutical crystalline and amorphous solutes: comparison between experimental data and theory. *Separation and Purification Technology*, **4**.

Lide D.R., 2008, *CRC handbook of chemistry and physics, 88th edn*. CRC Press Taylor & Francis, New York, NY, pp 6-8.

Liu J., Viverette T., Virgin M., Anderson M. and Dalal P., 2005, A study of the impact of freezing on the lyophilization of a concentrated formulation with a high fill depth. *Pharmaceutical Development and Technology*, **10**, 261-272.

Lopez C.F., Darst R.K. and Rossky P.J., 2008, Mechanistic elements of protein cold denaturation. *Journal of Physical Chemistry B*, **112**(19), 5961-5967.

Lu X. and Pikal M.J., 2004, Freeze-drying of mannitol-trehalose-sodium chloride-based formulations: the impact of annealing on dry layer resistance to mass transfer and cake structure. *Pharmaceutical Development and Technology*, **9**(1), 85-95.

Martos A., Koch W., Jiskoot W., Wuchner K., Winter G., Friess W. and Hawe A., Trends on Analytical Characterization of Polysorbates and Their Degradation Products in Biopharmaceutical Formulations, *Journal of Pharmaceutical Sciences*, **106**, 1722-1735.

Mason B.J. and Ludlam F.H., 1951, The microphysics of clouds. *Reports on Progress in Physics*, **14**(1), 147-195.

Matsumoto M., Saito S. and Ohmine I., 2002, Molecular dynamics simulation of the ice nucleation and growth process leading to water freezing. *Nature*, **416**, 409-413.

Matysiak S., Debenedetti P.G. and Rossky P.J., 2012, Role of hydrophobic hydration in protein stability: a 3d water-explicit protein model exhibiting cold and heat denaturation. *Journal of Physical Chemistry B*, **116**(28), 8095-8104.

Miller M.A., Rodrigues M.A., Glass M.A., Singh S.K., Johnston K.P. and Maynard J.A., 2013, Frozen-state storage stability of a monoclonal antibody: Aggregation is impacted by freezing rate and solute distribution. *Journal of Pharmaceutical Sciences*, **102**, 1194–1208.

Mochel E.L., Nordberg M.E. and Elmer T.H., 1966, Strengthening of Glass Surfaces by Sulfur Trioxide Treatment. *Journal of the American Ceramic Society*, **49**(11), 585–589.

Morris J., Morris G.J., Taylor R., Zhai S. and Slater N.K.H., 2004, The Effect of Controlled Nucleation of Ice on the Ice Structure, Drying Rate, and Protein Recovery in Vials Cooled in Modified Freeze-Drier. *Cryobiology*, **49**(3), 308.

Müller + Müller, Vials Brochure.

Murase N. and Franks F., 1989, Salt precipitation during the freeze-concentration of phosphate buffer solutions. *Biophysical Chemistry*, **34**(3), 293-300.

Nail S.L., Jiang S., Chongprasert S. and Knopp S.A., 2002, Fundamentals of freeze-drying. In: *Development and Manufacture of Protein Pharmaceuticals* (Nail S.L. and Akers M.J.). Kluwer Academic/Plenum Publisher, New York.

Nakagawa K., Hottot A., Vessot S. and Andrieu J., 2006, Influence of controlled nucleation on ice morphology of frozen formulations for pharmaceutical proteins freeze-drying. *Chemical Engineering and Process*, **45**, 783-791.

Nireesha G.R., Divya L., Sowmya C., Venkateshan N., Niranjan Babu M. and Lavakumar V., 2013, Lyophilization / freeze drying – an review. *International Journal of Novel Trends in Pharmaceutical Sciences*, **3**, 2277-2782.

Norde W., 1986, Adsorption of proteins from solution at the solid–liquid interface. *Advances in Colloid and Interface Science*, **25**, 267–340.

O'brien J., 1996, Stability of trehalose, sucrose and glucose to nonenzymatic browning in model systems. *Journal of Food Science*, **61**, 679-682.

Oddone I., Arsiccio A., Duru C., Malik K., Ferguson J., Pisano R. and Matejtschuk P., 2020, Vacuum-Induced Surface Freezing for the Freeze-Drying of the Human Growth Hormone: How Does Nucleation Control Affect Protein Stability? *Journal of Pharmaceutical Sciences*, **109**, 254-263.

Oddone I., Barresi A.A. and Pisano R., 2017, Influence of controlled ice nucleation on the freeze-drying of pharmaceutical products: the secondary drying step. *International Journal of Pharmaceutics*, **524**, 134–140.

Oddone I., Bockstal P.-J., De Beer T. and Pisano R., 2016, Impact of vacuum-induced surface freezing on inter- and intra-vial heterogeneity. *European Journal of Pharmaceutics and Biopharmaceutics*, **103**, 167-178.

Oddone I., Fulginiti D., Barresi A.A., Grassini S. and Pisano R., 2015, Non-invasive temperature monitoring in freeze drying: control of freezing as a case study. *Drying Technology*, **33**(13), 1621-1630.

Oddone I., Pisano R., Bullich R. and Stewart P., 2014, Vacuum-induced nucleation as a method for freeze-drying cycle optimization. *Industrial and Engineering Chemistry Research*, **53**, 182365-18244.

Oetjen G.W. and Haseley P., 2004, *Freeze-Drying*, 2nd Ed, Wiley-VCH Verlag, Weinheim.

Ogawa T, Miyajima M, Wakiyama N, Terada K., 2013, Effects of Phosphate Buffer in Parenteral Drugs on Particle Formation from Glass Vials. *Chemical and Pharmaceutical Bulletin*, **61**(5), 539–545.

Ogawa T., Miyajima M., Nishimoto N., Minami H. and Teradab K., 2016, Comparisons of Aluminum and Silica Elution from Various Glass Vials. *Chemical and Pharmaceutical Bulletin*, **64**, 150-160.

Ohsaka K. and Trinh E. H., 1998, Dynamic nucleation of ice induced by a single stable cavitation bubble. *Applied Physics Letters*, **73**, 129-131.

Ohtake S., Kita Y. and Arakawa T., 2011, Interactions of formulation excipients with proteins in solution and in the dried state. *Advanced Drug Delivery Reviews*, **63**(13), 1053-1073.

Passot S., Tréléa I.C., Marin M., Galan M., Morris G.J. and Fonseca F., 2009, Effect of Controlled Ice Nucleation on Primary Drying Stage and Protein Recovery in Vials Cooled in a Modified Freeze-Dryer. *Journal of Biomechanical Engineering*, **131**.

Patel S.M. and Pikal M.J., 2011, Emerging Freeze-Drying Process Development and Scale-up Issues. *American Association of Pharmaceutical Scientists*, **12**(1).

Patel S.M., Bhugra C. and Pikal M.J., 2009, Reduced pressure ice fog technique for controlled ice nucleation during freeze-drying. *American Association of Pharmaceutical Scientists*, **10**, 1406-1411.

Patel S.M., Nail S.L., Pikal M.J., Geidobler R., Winter G., Hawe A., Davagnino J. and Rambhatla Gupta S., 2017, Lyophilized drug product cake appearance: what is acceptable? *Journal of Pharmaceutical Sciences*, **106**, 1706–1721.

Petersen A., Schneider H., Rau G. and Glasmacher B., 2006, A new approach for freezing of aqueous solutions under active control of the nucleation temperature. Cryobyology, **53**, 248-257.

Petty C. and Cunningham N.L., 1974, Insulin adsorption by glass infusion bottles, polyvinyl chloride infusion containers, and intravenous tubing, *Anesthesiology*, **40**, 406-410.

Petzold G. and Aguilera J., 2009, Ice morphology: fundamentals and technological applications in foods. *Food Biophysics*, **4**, 378–396.

Pikal M. J., 1999, Heat and mass transfer in low pressure gases: applications to freeze-drying. In: *Transport process in pharmaceutical systems* (Amidon G., Lee P. and Top L.). Marcel Dekker, New York, USA.

Pikal M.J. and Shah S., 1990, The collapse temperature in freeze drying: dependence on measurement methodology and rate of water removal from the glassy phase. *International Journal of Pharmaceutics*, **62**, 165–186.

Pikal M.J. and Shah S., 1997, Intravial distribution of moisture during the secondary drying stage of freeze drying. *PDA Journal of Pharmaceutical Science and Technology*, **51**, 17–24.

Pikal M.J., 1994, Freeze-drying of proteins. In: *Formulation and Delivery of Proteins and Peptides* (Cleland J.L. and Langer R.). American Chemical Society, Washington DC, 4, 120-133.

Pikal M.J., 2001, Freeze drying. In: *Encyclopedia of Pharmaceutical Technology* (Swarbrick J, Boylan J). Marcel Dekker, New York.

Pikal M.J., 2010, *Mechanisms of Protein Stabilization during Freeze-Drying Storage: The Relative Importance of Thermodynamic Stabilization and Glassy State Relaxation Dynamics*, Informa Healthcare, London, 198-232.

Pikal M.J., Rambhatla S. and Ramot R., 2002, The impact of the freezing stage in lyophilization: effects of the ice nucleation temperature on process design and product quality. *American Pharmaceutical Review*, **5**, 48-52.

Pikal M.J., Shah S., Roy M.L. and Putman R., 1990, The secondary drying stage of freeze drying: drying kinetics as a function of temperature and chamber pressure. *International Journal of Pharmaceutics*, **60**, 203–217.

Pisano R. and Capozzi L.C., 2017, Prediction of products morphology of lyophilized drugs in the case of Vacuum Induced Surface Freezing. *Chemical Engineering Research and Design*, **125**(1), 119-129.

Pisano R., 2019, Alternative methods of controlling nucleationin freeze drying. In: *Lyophilization of Pharmaceuticals and Biologicals* (Ward K. and Matejtschuk P.), New York, NY, Humana Press, 79-111.

Pisano R., Arsiccio A., Nakagawa K. and Barresi A.A., 2019, Tuning, measurement and prediction of the impact of freezing on product morphology: A step toward improved design of freeze-drying cycles. *Drying Technology*, **37**(5), 579-599.

Pisano R., Fissore D. and Barresi A.A., 2011, Freeze-drying cycle optimization using model predictive control techniques. *Journal of Industrial and Engineering Chemistry*, **50**(12), 7363-7379.

Pisano R., Fissore D. and Barresi A.A., 2012, Quality by Design in the Secondary Drying Step of a Freeze-Drying Process. *Drying Technology*, **30**, 11-12, 1307-1316.

Pisano R., Rasetto V., Barresi A.A., Kuntz F., Aoude-Werner D. and Rey L., 2013, Freeze-drying of enzymes in case of water-binding and non-water-binding substrates. *European Journal of Pharmaceutics and Biopharmaceutics*, **85**, 974–983.

Preston W.A. and Anderson N.R., 1984, Glass and rubber closure effects on the pH of water I. A preliminary investigation. *Journal of parenteral science and technology*, **38**(1), 11-16.

Preston W.A. and Anderson N.R., 1985, Glass and rubber closure effects on the pH of water II. A proposed mechanism of interaction. *Journal of parenteral science and technology*, **39**(1), 28-47.

Privalov P.L., 1990, Cold denaturation of proteins. *Critical Reviews in Biochemistry and Molecular Biology*, **25**(4), 281-305.

Rambhatla S., Ramot R., Bhugra C. and Pikal M.J., 2004, Heat and Mass Transfer Scale-up Issues during Freeze Drying: II. Control and Characterization of the Degree of Supercooling. *American Association of Pharmaceutical Scientists*, **5**(4).

Randolph T.W., 1997, Phase separation of excipients during lyophilization: effects on protein stability. *Journal of Pharmaceutical Sciences,* **86**, 1198–1203.

Rey L. and May J. C., 2004, *Freeze-drying/Lyophilization of pharmaceutical and biological products*, Marcel Dekker Inc., New York, USA.

Roseman T.J., Brown J.A. and Scothorn W.W., 1976, Glass for Parenteral Products: A Surface View Using the Scanning Electron Microscope. *Journal of Pharmaceutical Sciences*, **65**, 22-29.

Rowe T. D., 1992, A technique for the nucleation of ice. In: *Proceedings of International Symposium on Biological Product Freeze-drying and Formulation* (Brown F. and May J. C.). Karger, New York, USA.

Sacha G.A., Saffell-Clemmer W., Abram K. and Akers M.J., 2010, Practical fundamentals of glass, rubber, and plastic sterile packaging systems. *Pharmaceutical Development and Technology*, **15**(1), 6–34.

Saclier M., Peczalski R. and Andrieu J.A., 2010, Theoretical Model for Ice Primary Nucleation Induced by Acoustic Cavitation. *Ultrasonics Sonochemistry*, **17**, 98–105.

Sarciaux J.M., Mansour S., Hageman M.J. and Nail S.L., 1999, Effects of buffer composition and processing conditions on aggregation of bovine IgG during freeze-drying. *Journal of Pharmaceutical Sciences*, **88**(12), 1354-1361.

Schaut R.A., Peanasky J.S., DeMartino S.E. and Schiefelbein S.L., 2014, A new glass option for parenteral packaging. *PDA Journal of Pharmaceutical Science and Technology*, **68**, 527–534.

Schott, PICVD: our unique technology to internally coat hollow bodies. Available at: https://www.schott.com/rd/english/coating/picvd.html. Accessed July 16, 2020.

Schott, TopLyo® Vials Brochure. Available at: https://www.schott.com/d/pharmaceutical_packaging/7f629b7e-e978-4417-a15e-8621f969d225/1.4/schott-datasheet-schott-toplyo-english-14062017.pdf. Accessed May 18, 2020.

Schwartzberg L.S. and Navari M.N., 2018, Safety of Polysorbate 80 in the Oncology Setting. *Advances in Therapy*, **35**(6), 754–767.

Scutellà B., Trelea I.C., Bourlès E. Fonseca F. and Passot S., 2018, Determination of the dried product resistance variability and its influence on the product temperature in pharmaceutical freeze-drying. *European Journal of Pharmaceutics and Biopharmaceutics*, **128**, 379–388.

Searles J.A., Carpenter J.F. and Randolph T.W., 2001a, The ice nucleation temperature determines the primary drying rate of lyophilization for samples frozen on a temperature-controlled shelf. *Journal of Pharmaceutical Sciences*, **90**, 860–871.

Searles J.A., Carpenter J.F. and Randolph T.W., 2001b, Annealing to optimize the primary drying rate, reduce freezing-induced drying rate heterogeneity, and determine T(g)' in pharmaceutical lyophilization. *Journal of Pharmaceutical Sciences*, **90**, 872–887.

Sennhenn B. and Kramer M., *Lyophilization Method*. U.S. Patent US 6684524 B1, February 3, 2004.

Snell G.D., and Cloudman A.M., 1943, The Effect of Rate of Freezing on the Survival of Fourteen Transpantable Tumors of Mice. *Cancer Research*, **3**(6), 396-400.

Stevanato Group, Glass Containers for Pharmaceutical Use Brochure. Available at: https://www.dcvmn.org/IMG/pdf/dcvmn_webinar_d-zuccato_170209.pdf. Accessed May 19, 2020.

Stevanato Group, Sulphate Treated Vials Brochure.

Stoppers Igloo. Available at: https://wheaton.com/13-mm-stopper-igloo-ultra-pure.html. Accessed July 23,2020.

Strambini G.B. and Gabellieri E., 1996, Proteins in frozen solutions: evidence of ice-induced partial unfolding. *Biophysical Journal*, **70**(2), 971-976.

Tang X.C. and Pikal M.J., 2004, Design of Freeze-Drying Processes for Pharmaceuticals: Practical Advice. *Pharmaceutical Research*, **21**(2).

Tang X.C. and Pikal M.J., 2005, The effect of stabilizers and denaturants on the cold denaturation temperatures of proteins and implications for freeze-drying. *Pharmaceutical Research*, **22**, 1167–1175.

Tressler C.J., Zimmerman W.I. and Willits C.O., 1941, Boiling-point Elevation of Sucrose Solutions. *The Journal of Physical Chemistry*, **45**(8), 1242-1245.

Wang W., 2000, Lyophilization and development of solid protein pharmaceuticals. *International Journal of Pharmaceutics*, **203**(1-2), 1-60.

Wang W., 2005, Protein aggregation and its inhibition in biopharmaceutics. *International Journal of Pharmaceutics*, **289**, 1-30.

Webb S.D., Cleland J.L., Carpenter J.F. and Randolph T.W., 2003, Effects of annealing lyophilized and spray-lyophilized formulations of recombinant human interferon-γ. *Journal of Pharmaceutical Sciences*, **92**(4), 715-729.

Weija L., 2012, *Controlled nucleation during freezing step of freeze drying cycle using pressure differential ice fog distribution*. U.S. Patent US 8,839,528 B2, 23 Sept 2014.

Wendorf J.R., Radke C.J. and Blanch H.W., 2004, Reduced protein adsorption at solid interfaces by sugar excipients. *Biotechnology and Bioengineering*, **87**, 565-573.

Weng L., Tessier S.N., Swei A., Stott S.L. and Toner M., 2018, Controlled ice nucleation using freeze-dried Pseudomonas syringae encapsulated in alginate beads. *Cryobiology*, **75**, 1-6.

White F., Koberda M. and Chilamkurti R., 2008, A systematic approach for screening glass containers and elastomeric closures for use with parenteral solutions. *PDA Journal of Pharmaceutical Science and Technology*, **62**(3), 157-176.

Williams N. A., Lee Y., Polli G.P. and Jennings T.A., 1986, The Effects of Cooling Rate on Solid Phase Transitions and Associated Vial Breakage Occurring in Frozen Mannitol Solutions. *Journal of parenteral science and technology*, **40**, 135-141.

Williams N.A. and Dean T., 1991, Vial Breakage by Frozen Mannitol Solutions: Correlation with Thermal Characteristics and Effect of Stereoisomerism, Additives, and Vial Configuration. *Journal of parenteral science and technology*, **45**, 94–100.

Workman E.J. and Reynolds S.E., 1950, Electrical phenomena occurring during the freezing of dilute aqueous solutions and their possible relationship to thunderstorm electricity. *Physical Review*, **78**, 254.

Yu L., Mishra D.S., and Rigsbee D.R., 1998, Determination of the glass properties of D-mannitol using sorbitol as an impurity. *Journal of Pharmaceutical Sciences*, **87**, 774-777.

Zhang X., Inada T. and Tezuka A., 2003, Ultrasonic-Induced Nucleation of Ice in Water Containing Air Bubbles. *Ultrasonics Sonochemistry*, **10**, 71–76.

Zhou Y., Gasteyer T.H., Grinter N.J., Cheng A.T, Ho S. Y.-C. and Sever R.R., 2014, *Method and system for nucleation control in a controlled rate freezer (CRF)*. U.S. Patent US 8,794,013 B2, 5 Aug 2014.

Acknowledgements

Carrying out my master's degree project in Belgium in the GSK R&D department was an experience that, in addition to being challenging and fascinating, taught me a lot making me face with the research world. I am grateful to my professor Roberto Pisano and my academic supervisor Bernadette Scutellà who both made this happen. I am appreciative for the whole team I worked with in Belgium, especially to Erwan Bourlès, Vincent Ronsse and Alain Philippart, who shared their deep knowledge with me and made me feel part of a family.

The coronavirus did not simplify my work, and indeed forced me to spend practically two months alone in homeworking, making the path very difficult even from a mental point of view. During this experience, as in all these five years of university, my friends have confirmed themselves as fantastic people capable of being close to me, supporting me and cheering up the path. For this a big thank you goes to them.

A special thanks goes to the ever-present Martina who, besides tolerating me more than anyone else and supporting me in every choice, has made me grow a lot as a person which is the most important thing.

Finally, I would like to thank my parents who gave me the opportunity to go to university and focus only on that in the best possible conditions. I know they are my first supporters and I have done everything possible to make them proud of me.